Appendix A.34:

Dunarnan St – CPT 24039

Table 1: Site Description for Dunarnan St (CC LIQ 25 – CPT 24039).

Attribute	Yes/No			Description/Date	Symbol in Figure 1
	10-m Buffer	20-m Buffer	50-m Buffer		
Near a body of surface water or other free face features?	No	No	No	The center of the site is ~160 m to the SE from the Avon River. The height of the free face is ~1.5 m.	NA
Lateral spreading observed during the CES?	No	No	No	No lateral spreading was observed by the mapping team.[1]	NA
Nearby buildings or structures?	No	Yes	Yes	Building coverage of the 20-m and 50-m buffer is 9% and 22%, respectively. The buildings cover the NW and NE quadrants of the 20-m buffer and all quadrants of the 50-m buffer.	White Fill + Brown Outline
Sloping land?	No	No	No	Flat land, residential area	NA
Step changes in the ground surface?	No	No	No	NA	NA
Retaining walls?	No	No	No	NA	NA
Vegetation?	Yes	Yes	Yes	Trees and bushes cover 17, 23, and 15% of the 10-, 20-, and 50-m buffers, respectively. They are in all quadrants of the buffers.	White Fill + Green Outline
Anthropogenic changes to the site between the LiDAR surveys?	Yes	Yes	Yes	Addition of pavement in the SW quadrant of the 50-m buffer and possible vegetation removal in the N portion of the 20- and 50-m buffers between Feb 2006 and Jun 2009. Road construction in all quadrants of all buffers, landscaping (vegetation addition) in the SE and SW quadrants of the 50-m buffer, tree removal in the E portion of all quadrants, and tree removal in the SW quadrant of the 50-m buffer between Jun 2009 and Oct 2009. Building removal in the SE quadrant of the 50-m buffer between Mar 2011 and Apr 2012. A house was added at the same property between Aug 2013 and Feb 2014. Removal of two buildings in the NW and SW quadrants of the 50-m buffer between Jan 2015 and July 2015.	Vegetation Removal/ Addition: Green Outline; Pavement Addition: Orange Outline; Building Removal: Orange Crossline
Other important factors?	Yes	Yes	Yes	Low-motor-vehicle-volume, two-way roadway (Dunarnan St) occupies 45, 23, and 9, respectively of the 10-, 20-, and 50-m buffers, respectively. It stretches in the E-W direction and is in all quadrants (primarily in the SW and SE quadrants) of all buffers.	Road: Gray Fill + Red Outline

Note: Buffer is the area within a circle of a specified radius with CPT investigations done at its center (172.675985°, -43.522271°).

[1] Canterbury Geotechnical Database. (2012). "Observed Ground Crack Locations", Map Layer CGD0400 - 23 July 2012, retrieved July 09, 2018 from https://canterburygeotechnicaldatabase.projectorbit.com/

Figure 1: Site plan with areas where ejecta-induced settlement is considered.

Note 1: Two patches (outlined in red) in the free field were selected for settlement assessment as areas free of vegetation and structures. Other important factors considered in the patch selection process were its proximity to a CPT, a property subjected to addition and/or demolition of a structure, front yard/backyard alterations (e.g., ploughing, rubble, scrap), and aerial distribution of sediment ejecta. In addition, the entire portion of the road within the 50-m buffer was considered for the settlement assessment. Roads as hard, relatively flat surfaces provide many ground-classified points. Finally, the LiDAR-based settlement analyses for the Sep-10 EQ were not conducted due to the evident absence of ejecta from Patches A and B and Road. The Oct 2015 LiDAR survey was not considered for Patch B due to the building removal between Jan 2015 and July 2015.

Table 2: LiDAR flight error adjustments, global adjustments for the difference between average LiDAR point elevations and benchmark survey elevations, and vertical tectonic movement adjustments.

	Adjustments (mm)		
Earthquake Event(s)	LiDAR Flight Error	Global Offset[2]	Tectonic Vertical Movement
Sep-10	-100	-3	0
Feb-11	+100	16	-50
Jun-11	0	38	-50
Dec-11	0	-65	+10
CES	0	-14	-90
Any LiDAR survey affected by ejecta?			No

Note: The negative sign indicates the subtraction from the ground surface subsidence, while the positive sign indicates the addition to the ground surface subsidence.

Table 3a: LiDAR Measurement Error for Patch A.

Surveys	Buffer	Area Averaged Difference Indicating Repeat Measurement Error (mm)	б*$_{individual}$ LiDAR points (mm)	%Reduction in б due to Area Averaging of LiDAR Points
Post Feb 2011: Mar 2011 and May 2011	10-m	ND	59	[46,46]
	20-m	27		
	50-m	27		
Post Dec 2011: Feb 2012 and Oct 2015	10-m	ND	70	[97,97]
	20-m	68		
	50-m	68		

*Standard deviation.

[2] Russell, J., & van Ballegooy, S. (2015). *Canterbury Earthquake Sequence: Increased liquefaction vulnerability assessment methodology*. New Zealand: Tonkin & Taylor Ltd.

Table 3b: LiDAR Measurement Error for Patch B.

Surveys	Buffer	Area Averaged Difference Indicating Repeat Measurement Error (mm)	$\sigma^*_{\text{individual LiDAR points}}$ (mm)	%Reduction in σ due to Area Averaging of LiDAR Points
Post Feb 2011: Mar 2011 and May 2011	10-m	NA	59	[7,7]
	20-m	NA		
	50-m	4		
Post Dec 2011: Feb 2012 and Oct 2015	10-m	ND	70	[ND,ND]
	20-m	ND		
	50-m	ND		

*Standard deviation; NA = Not available; ND = Not determined.

Table 3c: LiDAR Measurement Error for Road.

Surveys	Buffer	Area Averaged Difference Indicating Repeat Measurement Error (mm)	$\sigma^*_{\text{individual LiDAR points}}$ (mm)	%Reduction in σ due to Area Averaging of LiDAR Points
Post Feb 2011: Mar 2011 and May 2011	10-m	12	59	[20,36]
	20-m	15		
	50-m	21		
Post Dec 2011: Feb 2012 and Oct 2015	10-m	12	70	[13,99]
	20-m	9		
	50-m	69		

*Standard deviation.

Table 4a: Ground surface subsidence adjustments due to LiDAR measurement error for Patch A.

Earthquake Event(s)	$\sigma_{\text{pre-EQ LiDAR survey}}$ (mm)	$\sigma_{\text{post-EQ LiDAR survey}}$ (mm)	σ_{total} (mm)	Area Average Adjusted σ (mm) **
Sep-10	158	56	134	$\pm$130
Feb-11	56	59	59	$\pm$57
Jun-11	59	61	62	$\pm$60
Dec-11	61	70	87	$\pm$84
CES	158	70	124	$\pm$121

**Based on the highest %Reduction in Table 3a.

Table 4b: Ground surface subsidence adjustments due to LiDAR measurement error for Patch B.

Earthquake Event(s)	$\sigma_{\text{pre-EQ LiDAR survey}}$ (mm)	$\sigma_{\text{post-EQ LiDAR survey}}$ (mm)	σ_{total} (mm)	Area Average Adjusted σ (mm) **
Sep-10	158	56	134	±9
Feb-11	56	59	59	±4
Jun-11	59	61	62	±4
Dec-11	61	70	87	±6
CES	158	70	124	±8

**Based on the highest %Reduction in Table 3b.

Table 4c: Ground surface subsidence adjustments due to LiDAR measurement error for Road.

Earthquake Event(s)	$\sigma_{\text{pre-EQ LiDAR survey}}$ (mm)	$\sigma_{\text{post-EQ LiDAR survey}}$ (mm)	σ_{total} (mm)	Area Average Adjusted σ (mm) **
Sep-10	158	56	134	±132
Feb-11	56	59	59	±58
Jun-11	59	61	62	±61
Dec-11	61	70	87	±85
CES	158	70	124	±123

**Based on the highest %Reduction in Table 3c.

Table 5a: Raw liquefaction-related ground surface subsidence using original LiDAR points for Patch A.

	Average Ground Surface Subsidence (mm)		
Earthquake Event(s)	10-m Buffer	20-m Buffer	50-m Buffer
Sep-10	ND	ND	ND
Feb-11	ND	52	52
Jun-11	ND	115	115
Dec-11	ND	3	3
CES	ND	ND	ND

ND = Not determined.

Table 5b: Raw liquefaction-related ground surface subsidence using original LiDAR points for Patch B.

	Average Ground Surface Subsidence (mm)		
Earthquake Event(s)	10-m Buffer	20-m Buffer	50-m Buffer
Sep-10	NA	NA	ND
Feb-11	NA	NA	95
Jun-11	NA	NA	68
Dec-11	NA	NA	48
CES	NA	NA	ND

Table 5c: Raw liquefaction-related ground surface subsidence using original LiDAR points for Road.

	Average Ground Surface Subsidence (mm)		
Earthquake Event(s)	10-m Buffer	20-m Buffer	50-m Buffer
Sep-10	ND	ND	ND
Feb-11	5	16	11
Jun-11	85	84	91
Dec-11	59	59	31
CES	ND	ND	ND

ND = Not determined.

Table 6a: Corrected liquefaction-related ground surface subsidence using original LiDAR points for Patch A with the calculated adjustments in Table 2.

	Average Calculated Ground Surface Subsidence (mm)		
Earthquake Event(s)	10-m Buffer	20-m Buffer	50-m Buffer
Sep-10	ND	ND	ND
Feb-11	ND	119±50	119±50
Jun-11	ND	103±50	103±50
Dec-11	ND	-52±75	-52±75
CES	ND	ND	ND

Notes: Plus/minus values are same as those in Table 4a, but rounded to the nearest 25 mm; Positive overall values indicate ground surface subsidence, while negative overall values indicate ground surface uplift; ND = Not determined.

Table 6b: Corrected liquefaction-related ground surface subsidence using original LiDAR points for Patch B with the calculated adjustments in Table 2.

	Average Calculated Ground Surface Subsidence (mm)		
Earthquake Event(s)	10-m Buffer	20-m Buffer	50-m Buffer
Sep-10	NA	NA	ND
Feb-11	NA	NA	161±25
Jun-11	NA	NA	56±25
Dec-11	NA	NA	-7±25
CES	NA	NA	ND

Notes: Plus/minus values are same as those in Table 4b, but rounded to the nearest 25 mm; Positive overall values indicate ground surface subsidence, while negative overall values indicate ground surface uplift.

Table 6c: Corrected liquefaction-related ground surface subsidence using original LiDAR points for Road with the calculated adjustments in Table 2.

	Average Calculated Ground Surface Subsidence (mm)		
Earthquake Event(s)	10-m Buffer	20-m Buffer	50-m Buffer
Sep-10	ND	ND	ND
Feb-11	71±50	82±50	77±50
Jun-11	73±50	72±50	79±50
Dec-11	4±75	4±75	-25±75
CES	ND	ND	ND

Notes: Plus/minus values are same as those in Table 4c, but rounded to the nearest 25 mm; Positive overall values indicate ground surface subsidence, while negative overall values indicate ground surface uplift; ND = Not determined.

Table 7a: Corrected liquefaction-related ground surface subsidence for Patch A using LiDAR DEMs.

	Estimated Ground Surface Subsidence (mm)								
	10-m Buffer			20-m Buffer			50-m Buffer		
Earthquake Event(s)	16th %ile	50th %ile	84th %ile	16th %ile	50th %ile	84th %ile	16th %ile	50th %ile	84th %ile
Sep-10	ND	ND	ND	ND	ND	ND	ND	ND	ND
Feb-11	100	100	150	100	100	150	100	100	150
Jun-11	<50	50	100	<50	50	100	<50	50	100
Dec-11	<50	<50	<50	<50	<50	<50	<50	<50	<50
CES	ND	ND	ND	ND	ND	ND	ND	ND	ND

Note: These percentiles are not the exact statistical measures; they indicate the spatial variability of ground surface subsidence; ND = Not determined due to the anthropogenic changes.

Table 7b: Corrected liquefaction-related ground surface subsidence for Patch B using LiDAR DEMs.

	Estimated Ground Surface Subsidence (mm)								
	10-m Buffer			20-m Buffer			50-m Buffer		
Earthquake Event(s)	16th %ile	50th %ile	84th %ile	16th %ile	50th %ile	84th %ile	16th %ile	50th %ile	84th %ile
Sep-10	NA	NA	NA	NA	NA	NA	<50	<50	<50
Feb-11	NA	NA	NA	NA	NA	NA	100	150	200
Jun-11	NA	NA	NA	NA	NA	NA	150	150	150
Dec-11	NA	NA	NA	NA	NA	NA	<50	<50	<50
CES	NA	NA	NA	NA	NA	NA	250	350	350

Note: These percentiles are not the exact statistical measures; they indicate the spatial variability of ground surface subsidence.

Table 7c: Corrected liquefaction-related ground surface subsidence for Road using LiDAR DEMs.

	Estimated Ground Surface Subsidence (mm)								
	10-m Buffer			20-m Buffer			50-m Buffer		
Earthquake Event(s)	16th %ile	50th %ile	84th %ile	16th %ile	50th %ile	84th %ile	16th %ile	50th %ile	84th %ile
Sep-10	ND	ND	ND	ND	ND	ND	ND	ND	ND
Feb-11	100	100	150	100	100	150	100	100	150
Jun-11	<50	50	50	<50	50	50	<50	50	50
Dec-11	50	100	150	50	100	150	50	50	100
CES	ND	ND	ND	ND	ND	ND	ND	ND	ND

Note: These percentiles are not the exact statistical measures; they indicate the spatial variability of ground surface subsidence; ND = Not determined due to the anthropogenic changes.

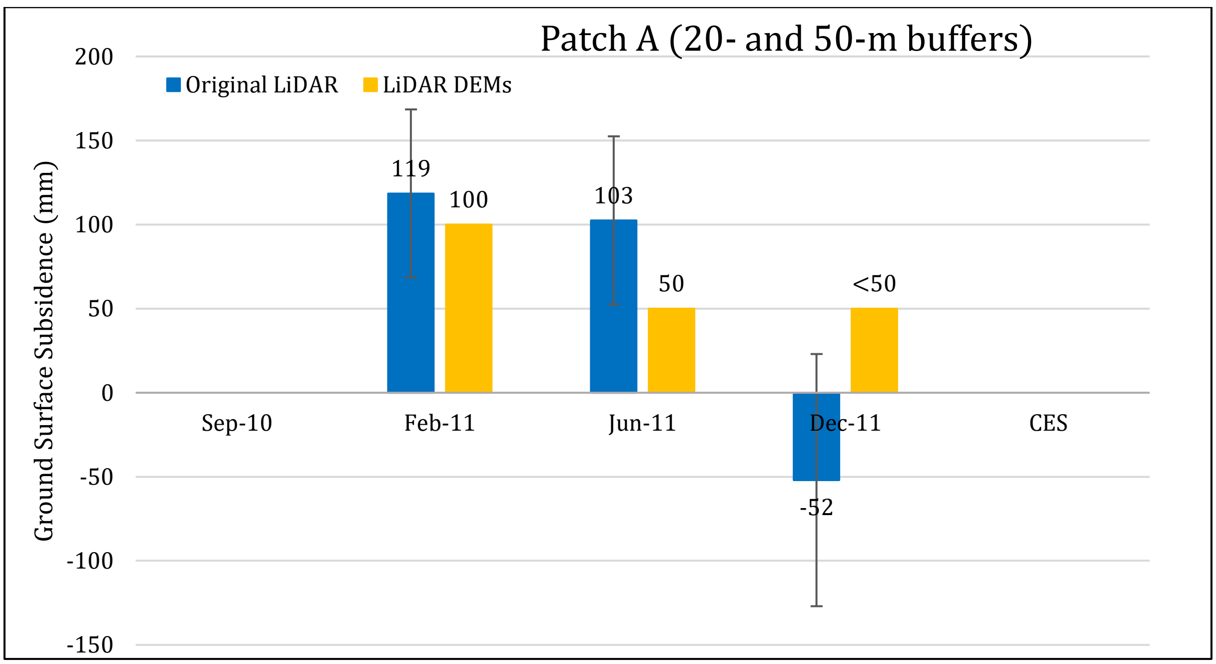

Figure 2: Comparison between ground surface subsidence determined from original LiDAR survey points and ground surface subsidence (50th %ile) estimated using LiDAR DEMs for Patch A (20-m and 50-m buffers).

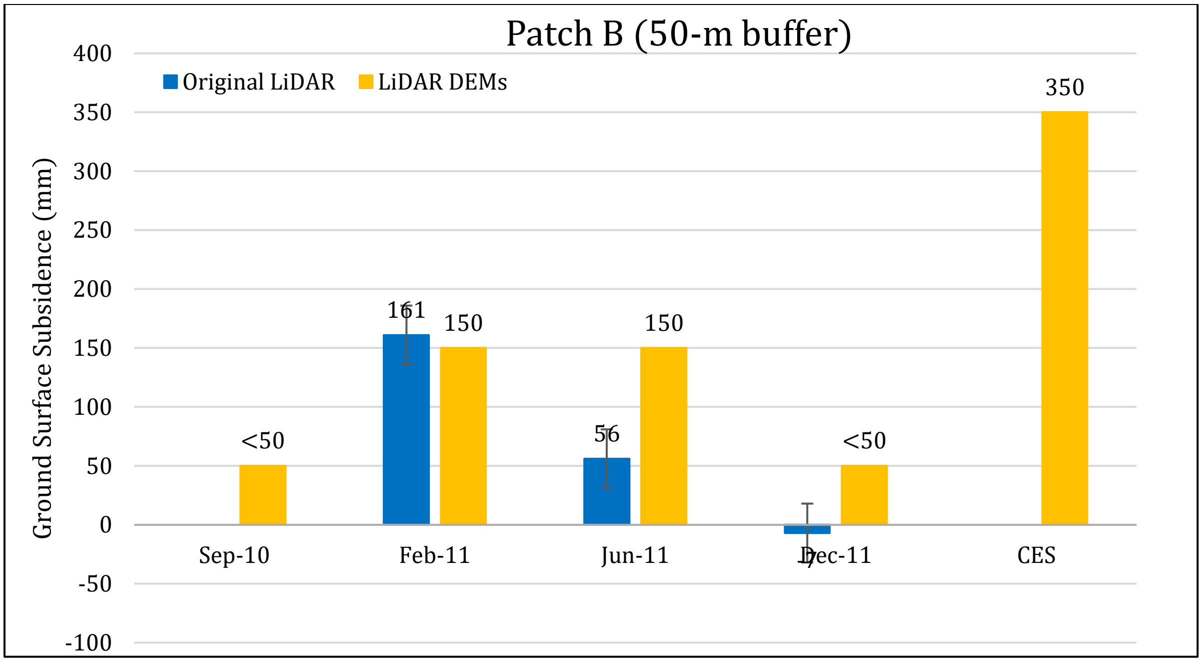

Figure 3: Comparison between ground surface subsidence determined from original LiDAR survey points and ground surface subsidence (50th %ile) estimated using LiDAR DEMs for Patch B (50-m buffer).

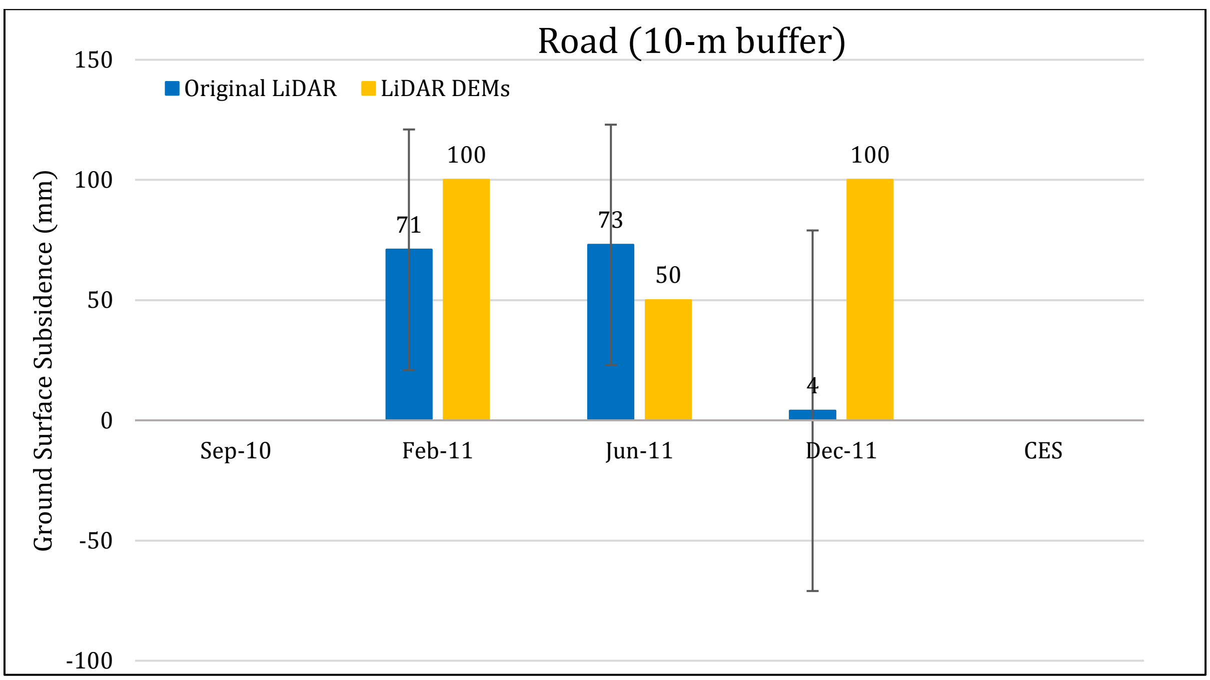

Figure 4: Comparison between ground surface subsidence determined from original LiDAR survey points and ground surface subsidence (50th %ile) estimated using LiDAR DEMs for Road (10-m buffer).

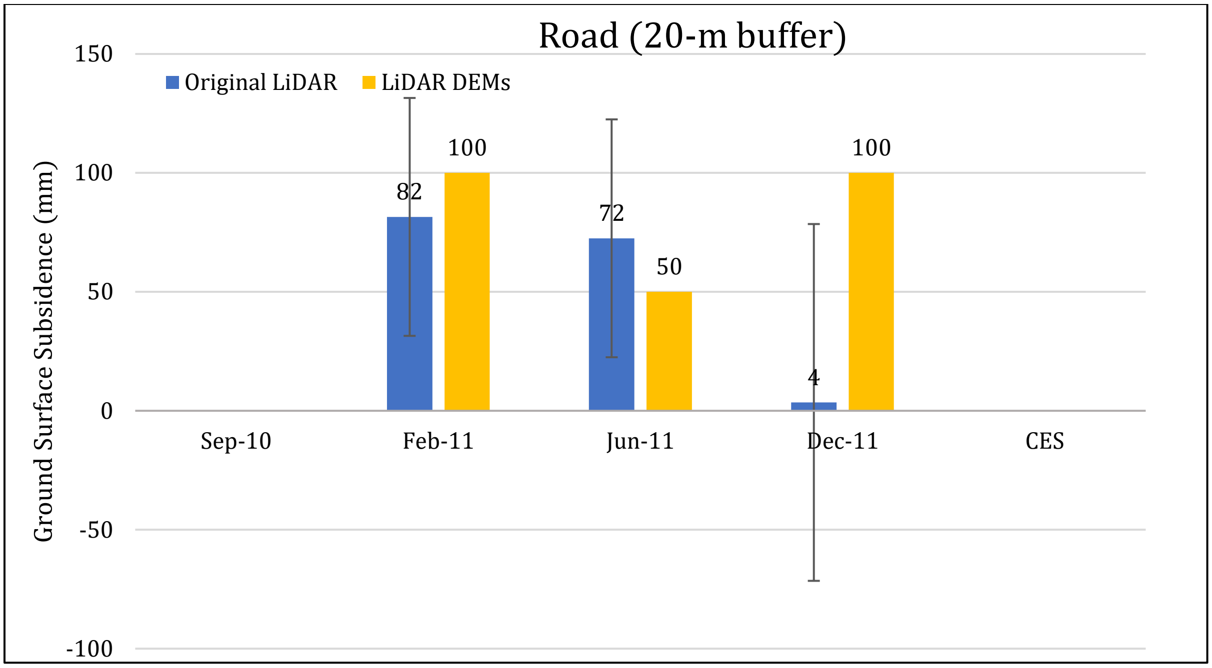

Figure 5: Comparison between ground surface subsidence determined from original LiDAR survey points and ground surface subsidence (50th %ile) estimated using LiDAR DEMs for Road (20-m buffer).

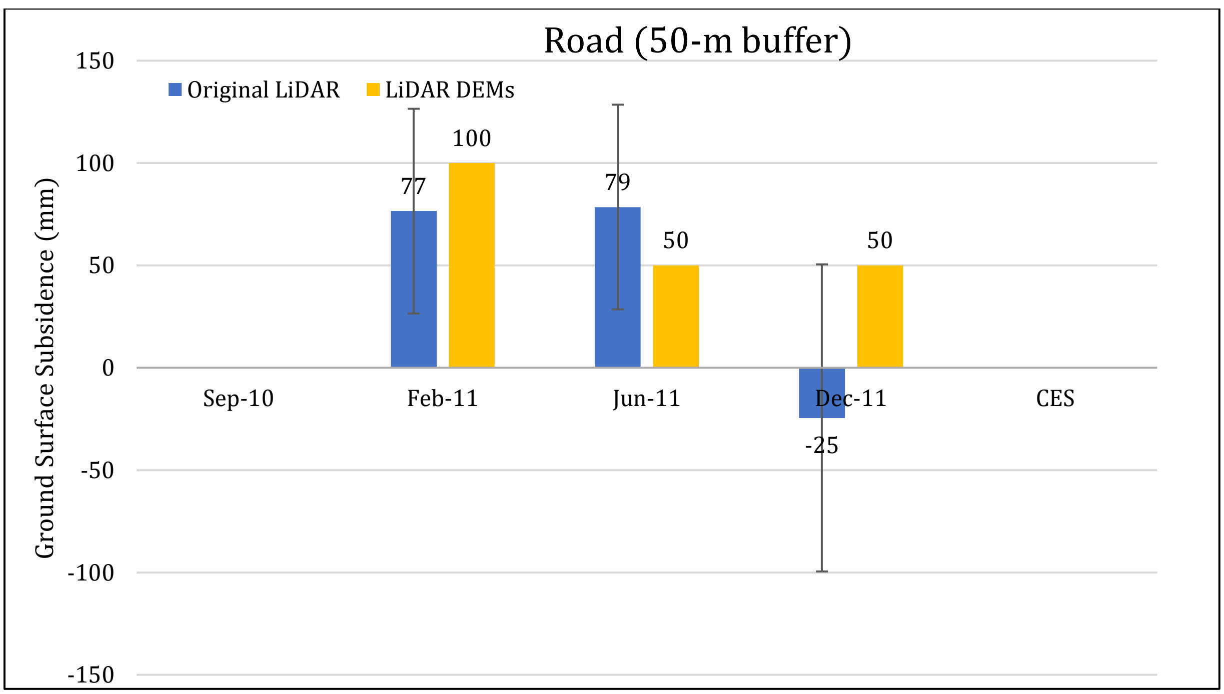

Figure 6: Comparison between ground surface subsidence determined from original LiDAR survey points and ground surface subsidence (50th %ile) estimated using LiDAR DEMs for Road (50-m buffer).

Note 2: The ground surface subsidence values determined from the original LiDAR survey points are similar to the ground surface subsidence values estimated using LiDAR DEMs for all earthquake events.

Table 8a: Ejecta-Induced settlement for the top 20 m of the soil profile for Patch A (20- and 50-m buffers) for the 50th %ile PGA, P_L=50%, and C_{FC}=0.13 using BI-2014, ZRB-2002, and I_C cutoff of 2.6.

Earthquake Event(s)	M_W	PGA (g)	Depth to Groundwater (m)	S_T (mm)	S_{V1D} (mm)	$S_{E,L}$ (mm)
Sep-10	7.1	0.21	2.0	ND	4±20	ND
Feb-11	6.2	0.53	2.0	119±50	54±50	65±71
Jun-11	6.2	0.31	1.8	103±50	18±25	85±56
Dec-11	6.1	0.27	2.0	-52±75	7±50	-59±90

Notes: S_T = Total settlement (Table 6); S_{V1D} = Average vertical settlement due to volumetric compression using Boulanger and Idriss (2014) (BI-2014), Zhang et al. (2002) (ZRB-2002) procedures and de Greef and Lengkeek (2018) thin-layer correction; $S_{E,L}$ = Ejecta-induced settlement as the difference between the LiDAR-based S_T and S_{V1D}; ND = Not determined due to the anthropogenic changes.

Table 8b: Ejecta-Induced settlement for the top 20 m of the soil profile for Patch B (50-m buffer) for the 50th %ile PGA, P_L=50%, and C_{FC}=0.13 using BI-2014, ZRB-2002, and I_C cutoff of 2.6.

Earthquake Event(s)	M_W	PGA (g)	Depth to Groundwater (m)	S_T (mm)	S_{V1D} (mm)	$S_{E,L}$ (mm)
Sep-10	7.1	0.21	2.0	ND	12±20	ND
Feb-11	6.2	0.53	2.0	161±25	76±50	85±56
Jun-11	6.2	0.31	1.8	56±25	36±25	20±35
Dec-11	6.1	0.27	2.0	-7±25	18±50	-25±56

Notes: S_T = Total settlement (Table 6); S_{V1D} = Average vertical settlement due to volumetric compression using Boulanger and Idriss (2014) (BI-2014), Zhang et al. (2002) (ZRB-2002) procedures and de Greef and Lengkeek (2018) thin-layer correction; $S_{E,L}$ = Ejecta-induced settlement as the difference between the LiDAR-based S_T and S_{V1D}; ND = Not determined due to the anthropogenic changes.

Table 8c: Ejecta-Induced settlement for the top 20 m of the soil profile for Road (10-m buffer) for the 50th %ile PGA, P_L=50%, and C_{FC}=0.13 using BI-2014, ZRB-2002, and I_C cutoff of 2.6.

Earthquake Event(s)	M_W	PGA (g)	Depth to Groundwater (m)	S_T (mm)	S_{V1D} (mm)	$S_{E,L}$ (mm)
Sep-10	7.1	0.21	2.0	ND	4±20	ND
Feb-11	6.2	0.53	2.0	71±50	54±50	17±71
Jun-11	6.2	0.31	1.8	73±50	18±25	55±56
Dec-11	6.1	0.27	2.0	4±75	7±50	-3±90

Notes: S_T = Total settlement (Table 6); S_{V1D} = Average vertical settlement due to volumetric compression using Boulanger and Idriss (2014) (BI-2014), Zhang et al. (2002) (ZRB-2002) procedures and de Greef and Lengkeek (2018) thin-layer correction; $S_{E,L}$ = Ejecta-induced settlement as the difference between the LiDAR-based S_T and S_{V1D}; ND = Not determined due to the anthropogenic changes.

Table 8d: Ejecta-Induced settlement for the top 20 m of the soil profile for Road (20-m buffer) for the 50th %ile PGA, P_L=50%, and C_{FC}=0.13 using BI-2014, ZRB-2002, and I_C cutoff of 2.6.

Earthquake Event(s)	M_W	PGA (g)	Depth to Groundwater (m)	S_T (mm)	S_{V1D} (mm)	$S_{E,L}$ (mm)
Sep-10	7.1	0.21	2.0	ND	4±20	ND
Feb-11	6.2	0.53	2.0	82±50	54±50	28±71
Jun-11	6.2	0.31	1.8	72±50	18±25	54±56
Dec-11	6.1	0.27	2.0	4±75	7±50	-3±90

Notes: S_T = Total settlement (Table 6); S_{V1D} = Average vertical settlement due to volumetric compression using Boulanger and Idriss (2014) (BI-2014), Zhang et al. (2002) (ZRB-2002) procedures and de Greef and Lengkeek (2018) thin-layer correction; $S_{E,L}$ = Ejecta-induced settlement as the difference between the LiDAR-based S_T and S_{V1D}; ND = Not determined due to the anthropogenic changes.

Table 8e: Ejecta-Induced settlement for the top 20 m of the soil profile for Road (50-m buffer) for the 50th %ile PGA, P_L=50%, and C_{FC}=0.13 using BI-2014, ZRB-2002, and I_C cutoff of 2.6.

Earthquake Event(s)	M_W	PGA (g)	Depth to Groundwater (m)	S_T (mm)	S_{V1D} (mm)	$S_{E,L}$ (mm)
Sep-10	7.1	0.21	2.0	ND	10±20	ND
Feb-11	6.2	0.53	2.0	77±50	63±50	14±71
Jun-11	6.2	0.31	1.8	79±50	28±25	51±56
Dec-11	6.1	0.27	2.0	-25±75	15±50	-40±90

Notes: S_T = Total settlement (Table 6); S_{V1D} = Average vertical settlement due to volumetric compression using Boulanger and Idriss (2014) (BI-2014), Zhang et al. (2002) (ZRB-2002) procedures and de Greef and Lengkeek (2018) thin-layer correction; $S_{E,L}$ = Ejecta-induced settlement as the difference between the LiDAR-based S_T and S_{V1D}; ND = Not determined due to the anthropogenic changes.

Note 3: The uncertainty for volumetric settlement was derived based on the sensitivity of volumetric settlement to PGA, C_{FC}, and P_L for each earthquake event for VsVp 57203 *Shirley Intermediate School* and CC LIQ 1 – CPT 5586 – *Vivian St* sites. Taking the 50th percentile as the baseline case, the minimum and maximum values corresponding to the difference between the 25th percentile and the 50th percentile and the 75th percentile and the 50th percentile were determined. The arithmetic mean of the range of the minimum and maximum difference was evaluated for each patch at the two sites. The maximum arithmetic mean for each earthquake event was rounded to the nearest five and used as the uncertainty value. Accordingly, the 1-D volumetric settlement uncertainties of $\pm$20, $\pm$50, $\pm$25, and $\pm$50 mm for the Sep-10, Feb-11, Jun-11, and Dec-11 earthquake events, respectively, were used for all sites in this study.

Table 9a: Coverage area and height of ejecta estimates for Patch A (20- and 50-m buffers) using photographs.

Earthquake Event	$H_{E,thick1}$ (mm)	$A_{E,thick1}$ (m^2)	$H_{E,thick2}$ (mm)	$A_{E,thick2}$ (m^2)	$H_{E,thin}$ (mm)	$A_{E,thin}$ (m^2)	A_T (m^2)
Sep-10	0	0	0	0	0	0	37.5
Feb-11	60-80	6.2	40-60	6.0	30-50	6.6	35.1*
Jun-11	NA	NA	NA	NA	NA	NA	37.5
Dec-11	0	0	30-50	6.0	40-60	0.7	37.5

Notes: $A_{E,thick/thin}$ = Coverage area of thick/thin ejecta layers; $H_{E,thick/thin}$ = Lower-upper estimate of height of thick/thin ejecta layers; Thin and thick layers correspond to light gray and dark gray colors of ejecta observed in aerial photographs; A_T = Total assessment area of a buffer being considered; * indicates reduction in A_T due to the presence of the tree (unable to see below the tree crown).

Table 9b: Coverage area and height of ejecta estimates for Patch B (50-m buffer) using photographs.

Earthquake Event	$A_{E,thick}$ (m^2)	$H_{E,thick}$ (m)	$A_{E,thin}$ (m^2)	$H_{E,thin}$ (m)	A_T (m^2)
Sep-10	0	0	0	0	27.9
Feb-11	18.9	80-120	8.0	30-50	27.9
Jun-11	6.8	40-60	7.4	20-40	27.9
Dec-11	4.3	30-50	0	0	27.9

Notes: $A_{E,thick/thin}$ =Coverage area of thick/thin ejecta layers; $H_{E,thick/thin}$ = Lower-upper estimate of height of thick/thin ejecta layers; A_T= Total assessment area of a buffer being considered; Thin and thick layers correspond to light gray and dark gray colors of ejecta observed in aerial photographs.

Table 9c: Coverage area and height of ejecta estimates for Road (10-m buffer) using photographs.

EQ Event	$H_{E,prism/pyr}$ (mm)	$V_{E,prism+pyr}$ (m^3)	$H_{E,cc}$ (mm)	$V_{E,cc}$ (m^3)	$H_{E,thick}$ (mm)	$A_{E,thick}$ (m^2)	$H_{E,thin}$ (mm)	$A_{E,thin}$ (m^2)	A_T (m^2)
Sep-10	0	0	0	0	0	0	0	0	149
Feb-11	10-20	0.023-0.046	370	0.16	20-40	1.1	5-10	85.3	149
Jun-11	35-150	2.37-4.75	0	0	10-30	9.4	0	0	149
Dec-11	12-24	0.003-0.006	0	0	0	0	5-10	13.4	148

Notes: $H_{E,cc}$ = Lower-upper estimate of height of conically shaped ejecta pile components (based on the repose angle of 30°); $V_{E,cc}$ = Volume of conically shaped ejecta pile components; $H_{E,prism/pyr}$ = Lower-upper estimate of ejecta height near the curb based on 2-4% cross slope of normal crown; $V_{E,prism+pyr}$ = Lower-upper estimate of total volume of prismatic- and pyramidal-shape ejecta; $A_{E,thin/thick}$ =Coverage area of thin/thick ejecta layers; $H_{E,thin/thick}$ = Lower-upper estimate of height of thin/thick ejecta layers; A_T= Total assessment area of a buffer being considered.

Table 9d: Coverage area and height of ejecta estimates for Road (20-m buffer) using photographs.

EQ Event	$H_{E,prism/pyr}$ (mm)	$V_{E,prism+pyr}$ (m^3)	$H_{E,cc}$ (mm)	$V_{E,cc}$ (m^3)	$H_{E,thick}$ (mm)	$A_{E,thick}$ (m^2)	$H_{E,thin}$ (mm)	$A_{E,thin}$ (m^2)	A_T (m^2)
Sep-10	0	0	0	0	0	0	0	0	298
Feb-11	10-48	0.13-0.26	370	0.16	20-40	13.1	5-10	178	298
Jun-11	12-150	5.80-11.3	0	0	10-30	10.4	0	0	297
Dec-11	9-36	0.03-0.06	0	0	0	0	5-10	30.4	297

Notes: $H_{E,cc}$ = Lower-upper estimate of height of conically shaped ejecta pile components (based on the repose angle of 30°); $V_{E,cc}$ = Volume of conically shaped ejecta pile components; $H_{E,prism/pyr}$ = Lower-upper estimate of ejecta height near the curb based on 2-4% cross slope of normal crown; $V_{E,prism+pyr}$ = Lower-upper estimate of total volume of prismatic- and pyramidal-shape ejecta; $A_{E,thin/thick}$ =Coverage area of thin/thick ejecta layers; $H_{E,thin/thick}$ = Lower-upper estimate of height of thin/thick ejecta layers; A_T= Total assessment area of a buffer being considered.

Table 9e: Coverage area and height of ejecta estimates for Road (50-m buffer) using photographs.

EQ Event	$H_{E,prism/pyr}$ (mm)	$V_{E,prism+pyr}$ (m^3)	$H_{E,cc}$ (mm)	$V_{E,cc}$ (m^3)	$H_{E,thick}$ (mm)	$A_{E,thick}$ (m^2)	$H_{E,thin}$ (mm)	$A_{E,thin}$ (m^2)	A_T (m^2)
Sep-10	0	0	0	0	0	0	0	0	750
Feb-11	10-150	2.49-4.90	219-456	0.88	20-40	13.1	5-10	360	750
Jun-11	11-150	10.5-20.7	0	0	10-30	10.4	0	0	750
Dec-11	10-55	0.29-0.58	0	0	0	0	5-10	73.4	750

Notes: $H_{E,cc}$ = Lower-upper estimate of height of conically shaped ejecta pile components (based on the repose angle of 30°); $V_{E,cc}$ = Volume of conically shaped ejecta pile components; $H_{E,prism/pyr}$ = Lower-upper estimate of ejecta height near the curb based on 2-4% cross slope of normal crown; $V_{E,prism+pyr}$ = Lower-upper estimate of total volume of prismatic- and pyramidal-shape ejecta; $A_{E,thin/thick}$ =Coverage area of thin/thick ejecta layers; $H_{E,thin/thick}$ = Lower-upper estimate of height of thin/thick ejecta layers; A_T= Total assessment area of a buffer being considered.

Note 4: The values in Table 9 correspond to the coverage area of ejecta outlined in aerial photographs (Figures 29, 31, and 84-86) and the lower and upper estimates of ejecta height based on geometrical approximations, ground photographs (Figure 87), and EQC LDAT property inspection reports. The ejecta-induced settlement using photographs and engineering judgment, $S_{E,P}$, is estimated as

$$S_{E,P} = \frac{\sum_{i=1}^{a} A_{E,thick,i} * H_{E,thick,i} + \sum_{j=1}^{b} A_{E,thin,j} * H_{E,thin,j} + \frac{1}{3}\sum_{k=1}^{c} A_{E,pile,k} * R_{E,pile,k} * tan30°}{A_T} + \frac{\frac{1}{2}\sum_{n=1}^{f} W_{E,prism,n} * H_{E,prism,n} * L_{E,prism,n} + \frac{1}{6}\sum_{p=1}^{g} W_{E,pyramid,p} * H_{E,pyramid} * L_{E,pyramid}}{A_T}$$

$$= \frac{\sum_{i=1}^{a} V_{E,thick,i} + \sum_{j=1}^{b} V_{E,thin,j} + \sum_{k=1}^{c} V_{E,conical\ component,k} + \sum_{n=1}^{f} V_{E,prism,n} + \sum_{p=1}^{g} V_{E,pyramid,p}}{A_T}$$

where

- $A_{E,thick,i}$ and $H_{E,thick,i}$ are the area and the height, respectively, of a thick ejecta layer;
- $A_{E,thin,j}$ and $H_{E,thin,j}$ are the area and the height, respectively, of a thin ejecta layer;
- $A_{E,pile,k}$ and $R_{E,pile,k}$ are the area and the radius, respectively, of an ejecta pile component shaped as a cone with the repose angle of 30°;
- $W_{E,prism,n}$ and $L_{E,prism,n}$ are the width and the length, respectively, of the coverage area of a prismatically shaped ejecta layer and $H_{E,prism,n}$ is the height of a prism-like ejecta layer;
- $W_{E,pyr,p}$ and $L_{E,pyr,p}$ are the width and the length, respectively, of the coverage area of a pyramid-like ejecta layer and $H_{E,pyr,p}$ is the height of a pyramid-like ejecta layer;
- A_T is the total assessment area for a buffer being considered (Figure 1).

Table 10a: Ejecta-induced settlement estimates for Patches A and B based on photographs.

Earthquake Event	Patch A (20- and 50-m buffers)		Patch B (50-m buffer)	
	$S_{E,P,lower}$ (mm)	$S_{E,P,upper}$ (mm)	$S_{E,P,lower}$ (mm)	$S_{E,P,upper}$ (mm)
Sep-10	0	0	0	0
Feb-11	23	34	63	96
Jun-11	NA	NA	15	25
Dec-11	6	9	5	8

Note: $S_{E,P,lower}$ and $S_{E,P,upper}$ correspond to lower and upper estimates of $S_{E,P}$, respectively.

Table 10b: Ejecta-induced settlement estimates for Road based on photographs.

Earthquake Event	Road (10-m buffer)		Road (20-m buffer)		Road (50-m buffer)	
	$S_{E,P,lower}$ (mm)	$S_{E,P,upper}$ (mm)	$S_{E,P,lower}$ (mm)	$S_{E,P,upper}$ (mm)	$S_{E,P,lower}$ (mm)	$S_{E,P,upper}$ (mm)
Sep-10	0	0	0	0	0	0
Feb-11	4	7	5	9	7	13
Jun-11	17	34	20	39	14	28
Dec-11	≈0	1	≈0	1	1	2

Note: $S_{E,P,lower}$ and $S_{E,P,upper}$ correspond to lower and upper estimates of $S_{E,P}$, respectively.

Table 11a: Best final estimates of ejecta-induced settlement for Patches A and B.

Earthquake Event	Patch A (20- and 50-m buffers)			Patch B (50-m buffer)		
	$S_{E,L}$ (mm)	$S_{E,P}$ (mm)	$S_{E,final}$ (mm)	$S_{E,L}$ (mm)	$S_{E,P}$ (mm)	$S_{E,final}$ (mm)
Sep-10	ND	0	0	ND	0	0
Feb-11	65±71	29±5	40±25	85±56	79±17	80±20
Jun-11	85±56	NA	ND*	20±35	20±5	20±20
Dec-11	-59±90	7.5±1.5	10±5	-25±56	6.5±1.5	5±5

Notes: $S_{E,L}$ = Ejecta-induced settlement based on LiDAR data reported in Table 8; $S_{E,P}$ = Median ejecta-induced settlement for the range of values reported in Table 10; $S_{E,final}$ = Best final estimate of ejecta-induced settlement rounded to the nearest 5 mm; Final plus/minus values are also rounded to the nearest 5 mm; ND = Not determined; * indicates that $S_{E,final}$ was not estimated because the $S_{E,L}$ value appears to be too high and there is no available $S_{E,P}$.

Table 11b: Best final estimates of ejecta-induced settlement for Road.

EQ Event	Road (10-m buffer)			Road (20-m buffer)			Road (50-m buffer)		
	$S_{E,L}$ (mm)	$S_{E,P}$ (mm)	$S_{E,final}$ (mm)	$S_{E,L}$ (mm)	$S_{E,P}$ (mm)	$S_{E,final}$ (mm)	$S_{E,L}$ (mm)	$S_{E,P}$ (mm)	$S_{E,final}$ (mm)
Sep-10	ND	0	0	ND	0	0	ND	0	0
Feb-11	17±71	5.5±1.5	10±25	28±71	7±2	15±25	14±71	10±3	10±25
Jun-11	55±56	26±8	40±30	54±56	30±9	40±30	51±56	21±7	35±30
Dec-11	-3±90	0.5±0.5	<5	-3±90	0.5±0.5	<5	-40±90	1.5±0.5	<5

Notes: $S_{E,L}$ = Ejecta-induced settlement based on LiDAR data reported in Table 8; $S_{E,P}$ = Median ejecta-induced settlement for the range of values reported in Table 10; $S_{E,final}$ = Best final estimate of ejecta-induced settlement rounded to the nearest 5; Final plus/minus values are also rounded to the nearest 5; ND = Not determined.

Note 5:

- $S_{E,final}$ for the Sep-10 and Dec-11 EQs is based solely on $S_{E,P}$ due to the evident absence of ejecta for the Sep-10 EQ and the negative $S_{E,L}$ values for the Dec-11 EQ. $S_{E,final}$ for the Feb-11 EQ is a weighted average of $S_{E,L}$ and $S_{E,P}$ with weights of 1/3 and 2/3, respectively, while $S_{E,final}$ for the Jun-11 EQ is a weighted average of $S_{E,L}$ and $S_{E,P}$ with weights of 1/2 and 1/2, respectively. The uncertainty associated with $S_{E,final}$ is also the weighted average of uncertainties associated with $S_{E,L}$ and $S_{E,P}$ with the same respective weights of 1/3 and 2/3 for the Feb-11 EQ and 1/2 and 1/2 for the Jun-11 EQ.

- The weight coefficients are based on the LiDAR error bands, LPI prediction error (Maurer et al. 2014[3]), presence of ejecta at the time of LiDAR surveys, and completeness of visual evidence (i.e., ground and aerial photographs and EQC LDAT property inspection reports for the site). The Dunarnan St site is in the apparent zone of higher ground surface subsidence for the Sep-10 EQ and the apparent zone of lower ground surface subsidence for the Feb-11 EQ (i.e., the underestimate of the ground surface elevation by the Sep-10 LiDAR survey). The site is in the zone of accurate LPI prediction of liquefaction severity for the Sep-10 EQ and slight LPI overprediction of liquefaction severity for the Feb-11 EQ. The LDAT property inspection reports and ground photographs are available for all properties within the 50-m buffer. The ejecta height was measured as 200 mm at one property (no other measurements are available). No ground photographs of the road are available.

<u>Summary 1</u>:

- **The best estimate of the ejecta-induced free-field ground settlement at the Dunarnan St site for the SEP 2010, FEB 2011, JUN 2011, and DEC 2011 earthquake is 0 mm, 40±25 mm, 20±20 mm, and 10±5 mm, respectively. For the FEB 2011 earthquake, about 20% of the site had 80±20 mm of the ejecta-induced free-field ground settlement.**
- **The best estimate of the ejecta-induced free-field ground settlement of the road at the Dunarnan St site for the SEP 2010, FEB 2011, JUN 2011, and DEC 2011 earthquake is 0 mm, 10±25 mm, 35±30 mm, and <5 mm, respectively.**

Note 6: The site was initially labeled as CPT 17908, but was later renamed as CPT 24039. The original CPT 17908 label appears in all figures below.

[3] Maurer, B. W., Green, R. A., Cubrinovski, M., & Bradley, B. A. (2014). Evaluation of the Liquefaction Potential Index for Assessing Liquefaction Hazard in Christchurch, New Zealand. *Journal of Geotechnical and Geoenvironmental Engineering*, 140(7), 04014032-1-11. doi:10.1061/(asce)gt.1943-5606.0001117

Figure 8: Location of the site.

Figure 9: Position of the site relative to nearby buildings, vegetation, and free-face features.

Figure 10: Street view of the flat land.

Figure 11: Satellite image of the site taken in Dec 2004.

Figure 12: Satellite image of the site taken in Feb 2006.

Figure 13: Satellite image of the site taken in Mar 2009.

Figure 14: Satellite image of the site taken in Jun 2009.

Figure 15: Satellite image of the site taken in Oct 2009.

Figure 16: Satellite image of the site taken on Sep 3, 2010.

Figure 17: Satellite image of the site taken on Sep 5, 2010.

Figure 18: Satellite image of the site taken on Feb 7, 2011.

Figure 19: Satellite image of the site taken on Feb 23, 2011.

Figure 20: Satellite image of the site taken on Feb 26, 2011.

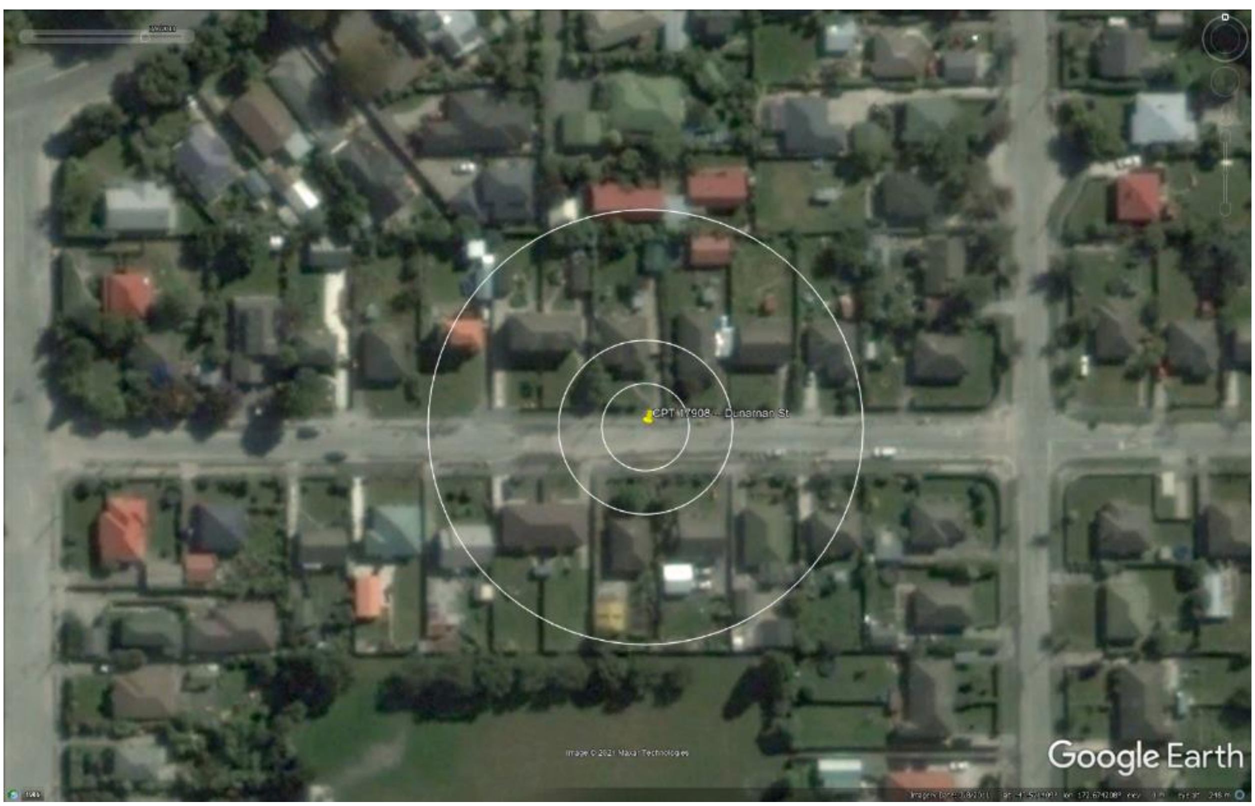

Figure 21: Satellite image of the site taken on Mar 8, 2011.

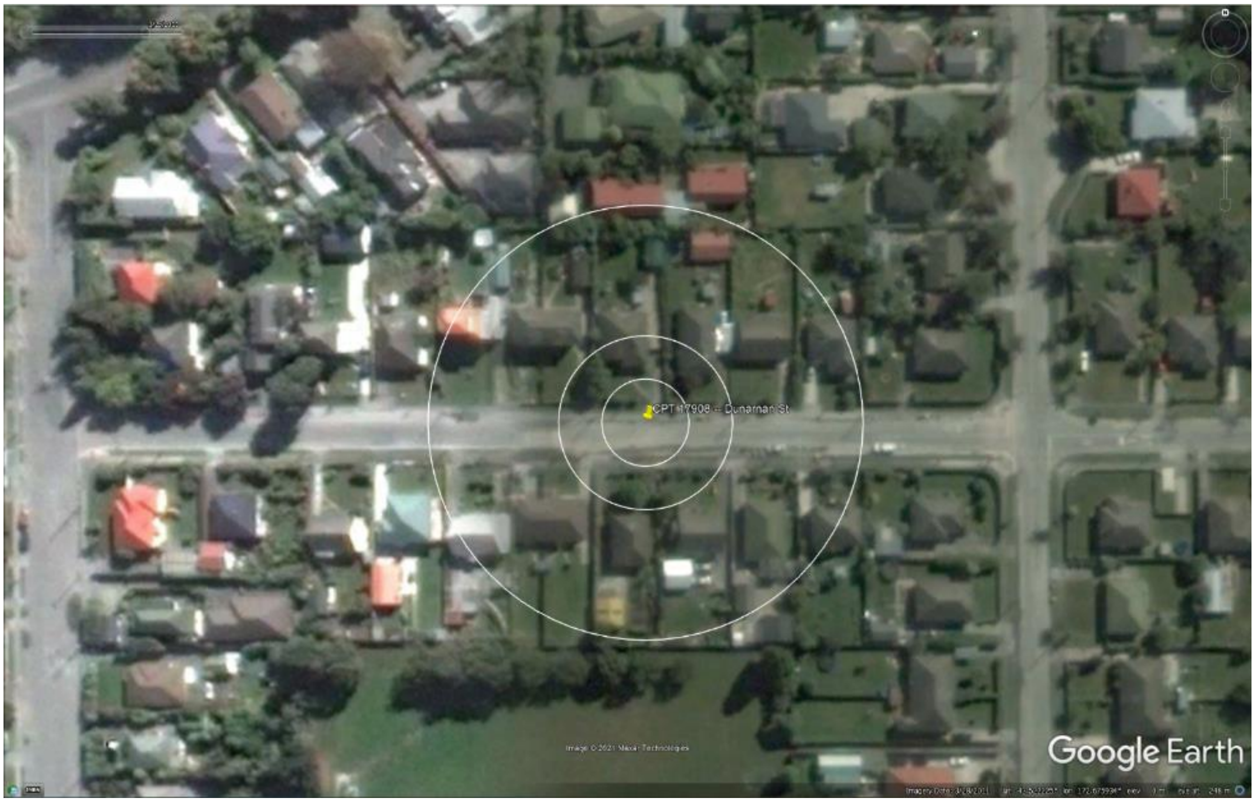

Figure 22: Satellite image of the site taken on Mar 28, 2011 (only the left portion of the image; the right portion of the image was acquired on Mar 8, 2011).

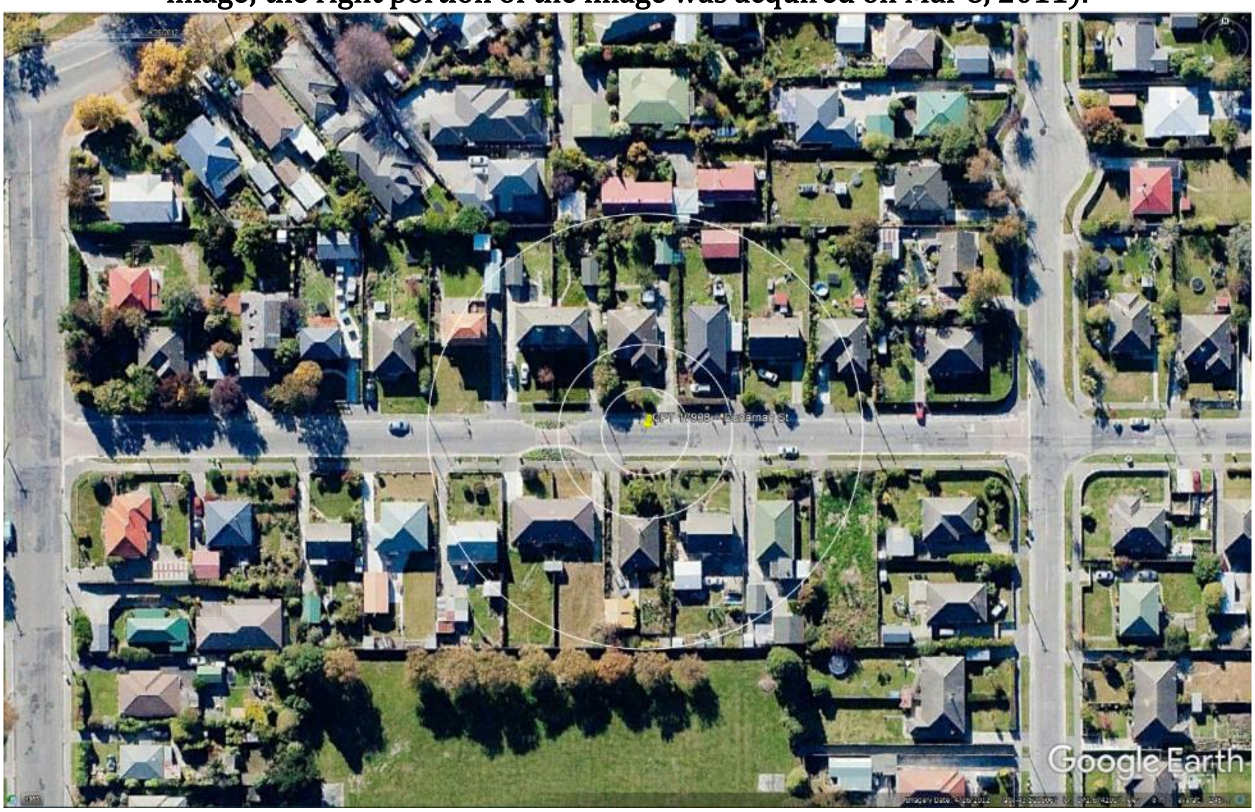

Figure 23: Satellite image of the site taken in Apr 2012.

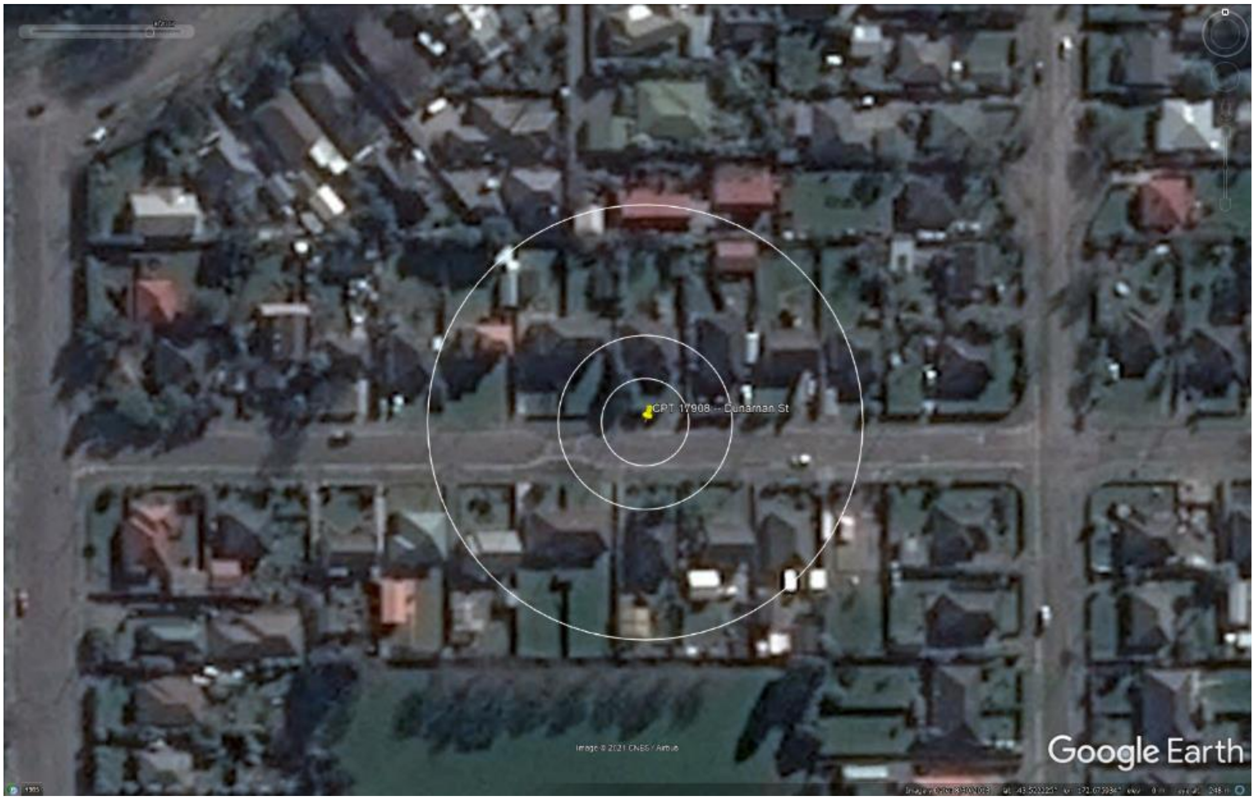

Figure 24: Satellite image of the site taken in Aug 2013.

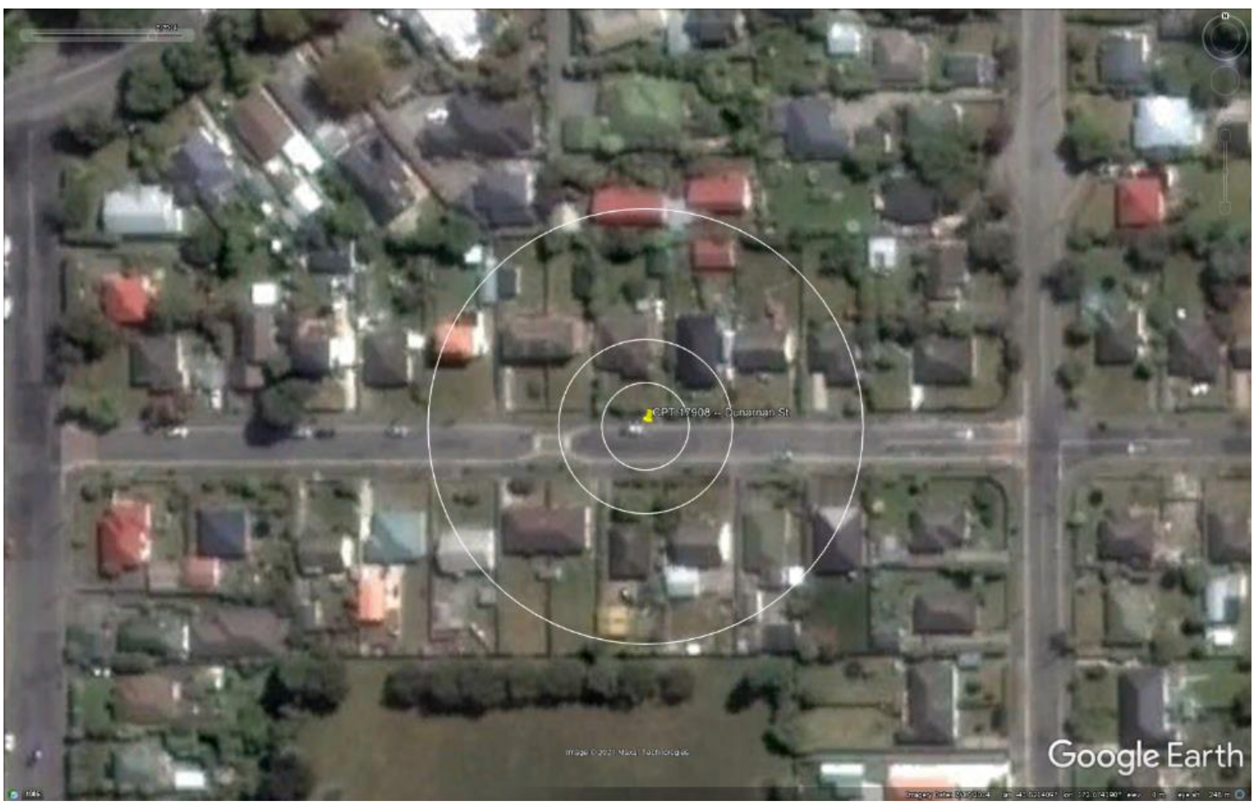

Figure 25: Satellite image of the site taken in Feb 2014.

Figure 26: Satellite image of the site taken in Jan 2015.

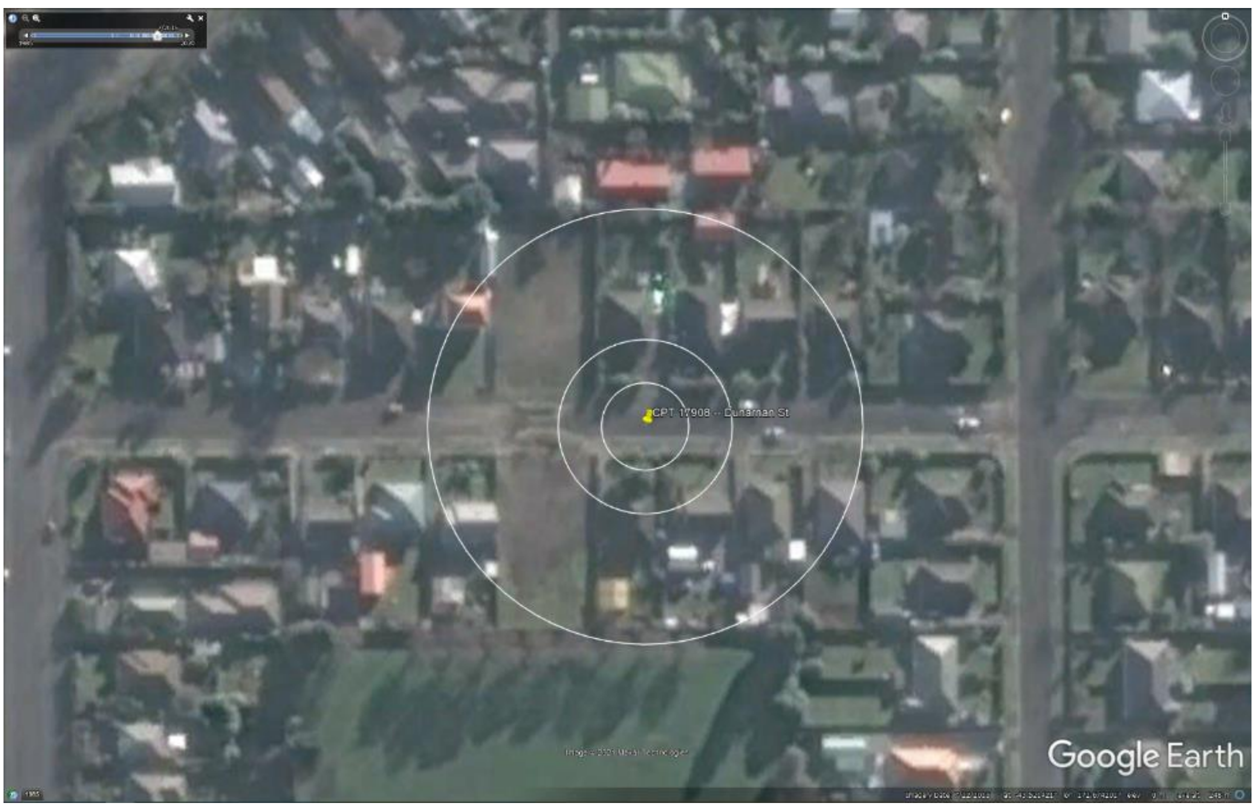

Figure 27: Satellite image of the site taken in Jul 2015.

Figure 28: Satellite image of the site taken in Nov 2015.

Figure 29: Aerial photograph of the site taken on Sep 4, 2010.

Figure 30: Aerial photograph of the site taken on Feb 24, 2011.

Figure 31: Aerial photograph of the site taken on June 14-15, 2011.

Figure 32: Aerial photograph of the site taken on June 16, 2011.

Figure 33: Aerial photograph of the site taken on Dec 24, 2011.

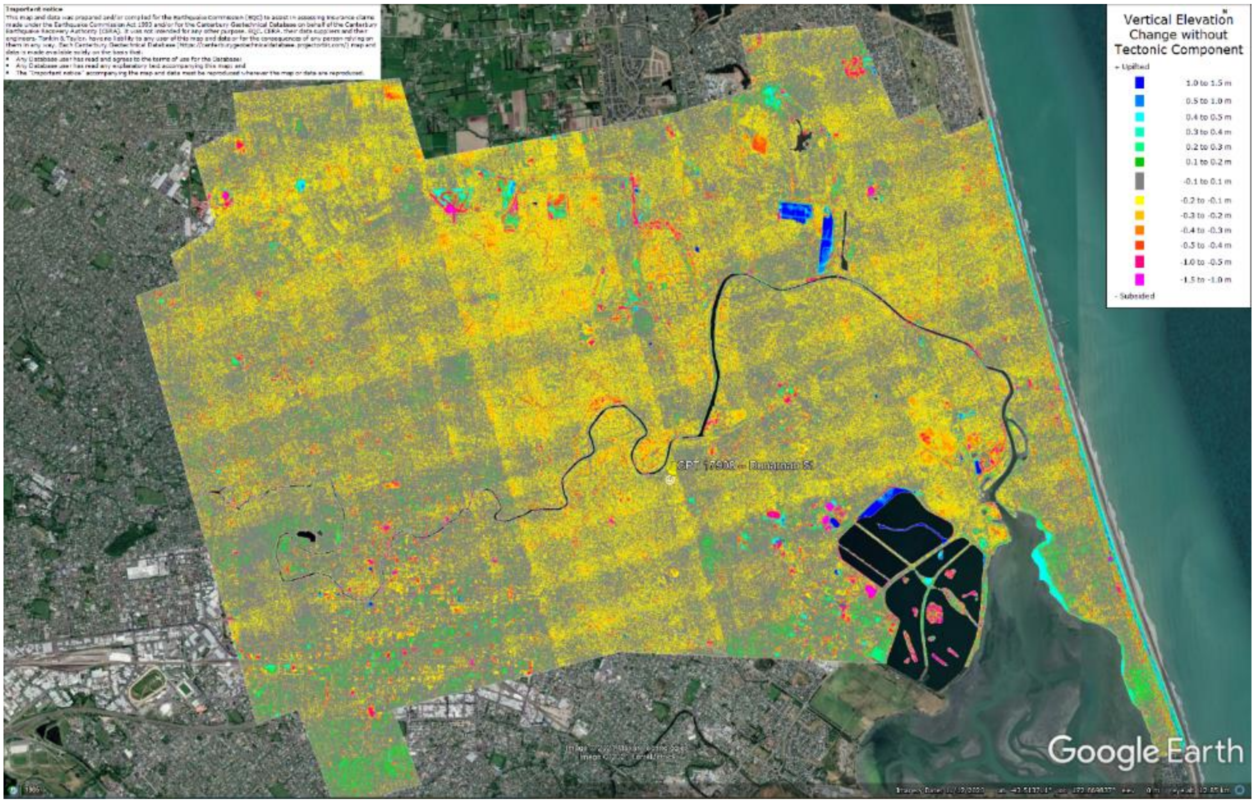

Figure 34: Vertical Ground Movements (Surface – Tectonic) for Sep 2010 Earthquake – the site is in the apparent zone of overestimated ground surface subsidence (i.e., flight error band for Sep 2010).

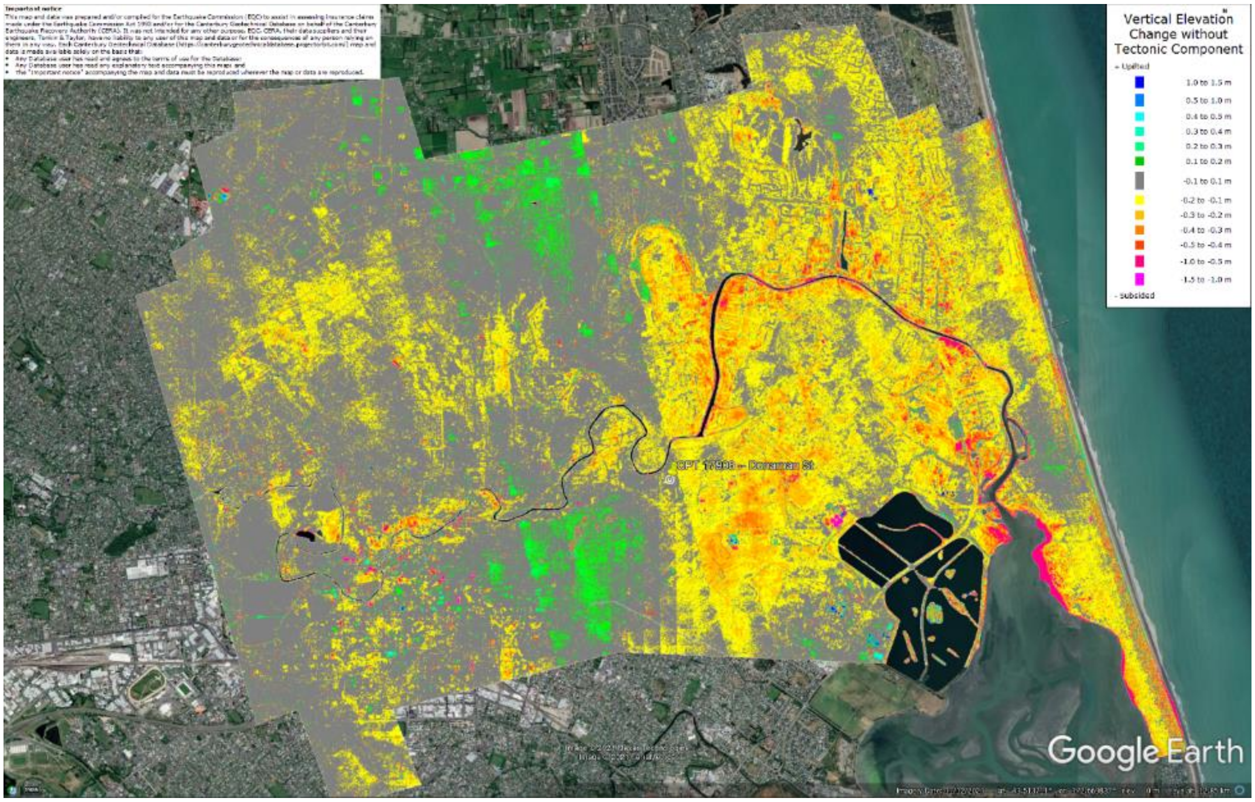

Figure 35: Vertical Ground Movements (Surface – Tectonic) for Feb 2011 Earthquake – the site is in the apparent zone of underestimated ground surface subsidence (i.e., flight error band for Sep 2010).

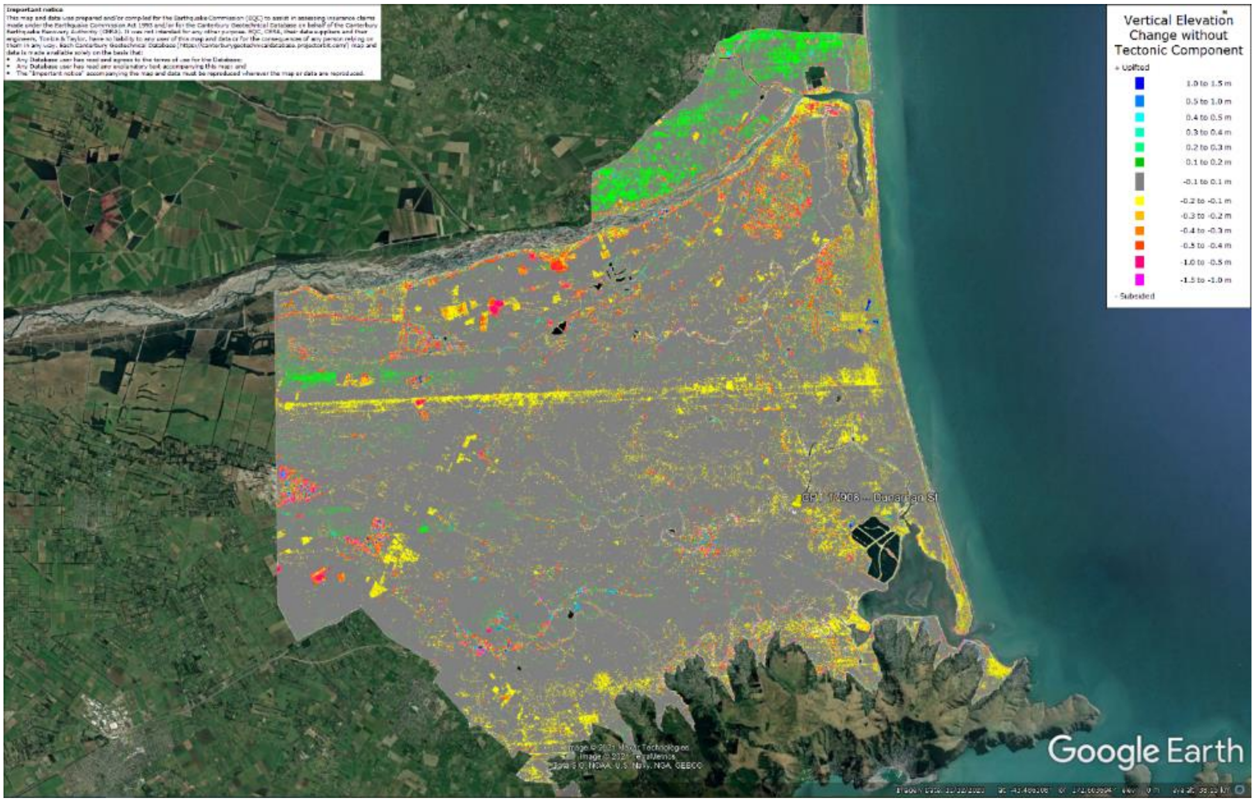

Figure 36: Vertical Ground Movements (Surface – Tectonic) for June 2011 Earthquake – the site is not in the apparent zone of overestimated or underestimated ground surface subsidence.

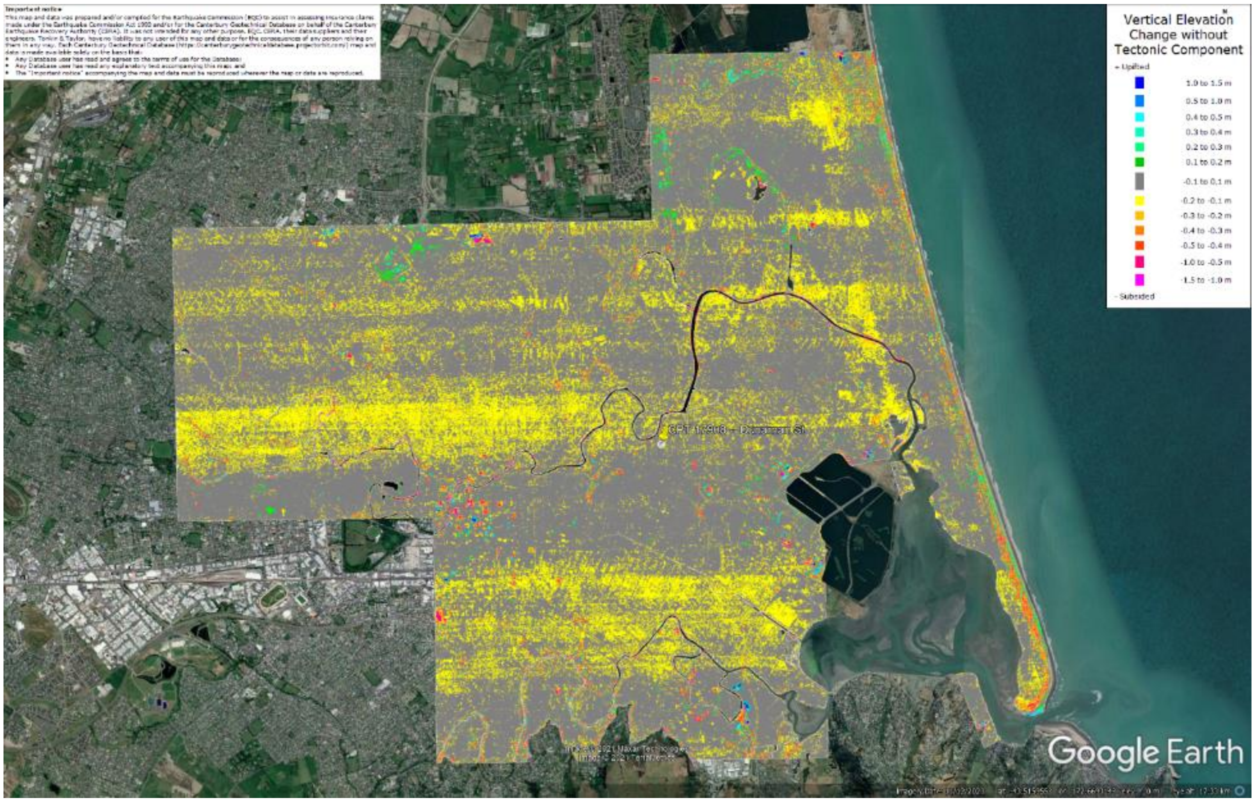

Figure 37: Vertical Ground Movements (Surface – Tectonic) for Dec 2011 Earthquake – the site is not in the apparent zone of overestimated or underestimated ground surface subsidence.

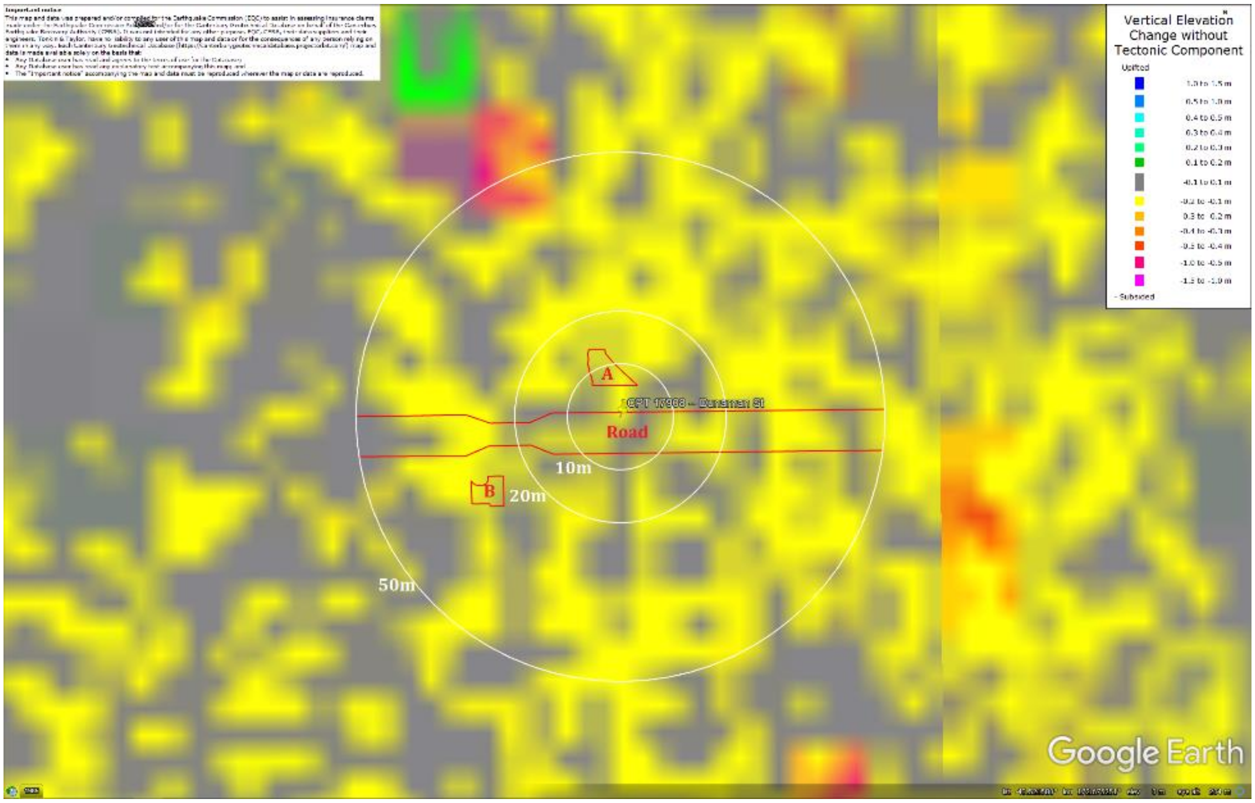

Figure 38: Ground surface subsidence without tectonic component for Sep 2010 Earthquake according to the LiDAR DEM.

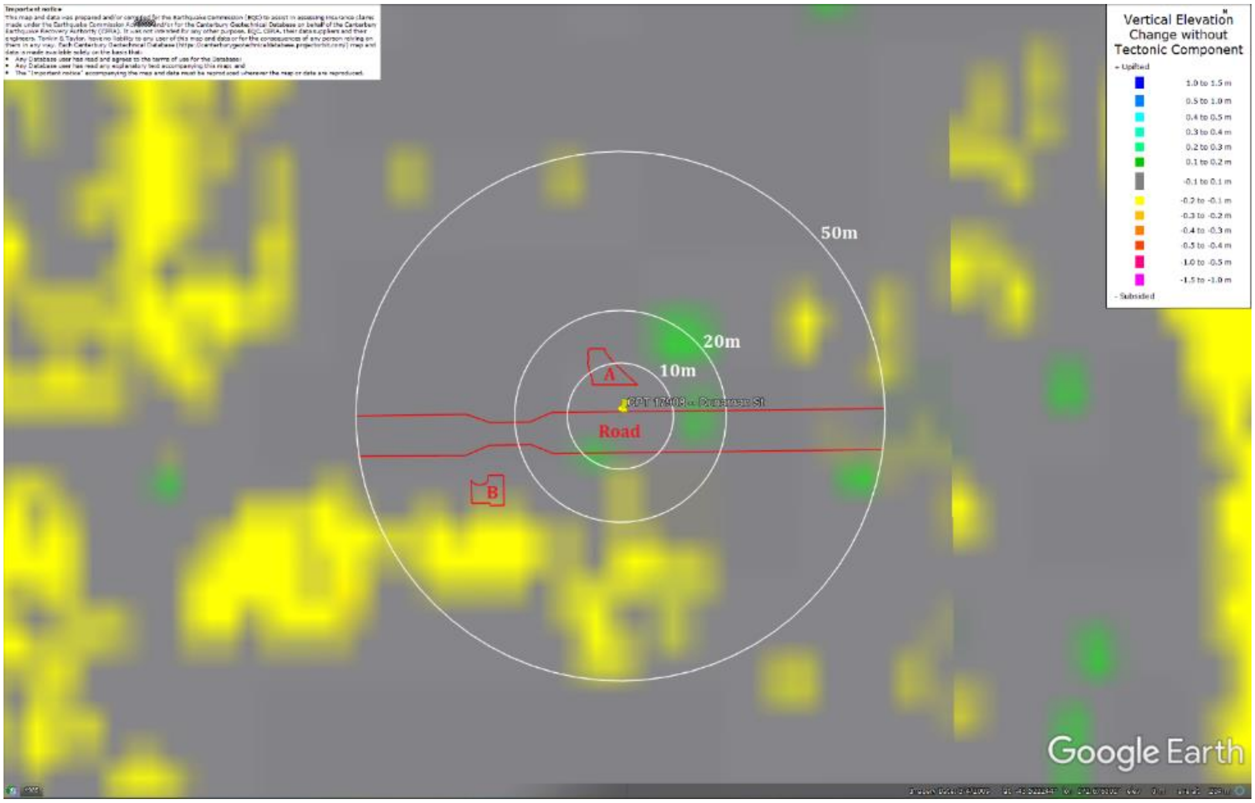

Figure 39: Ground surface subsidence without tectonic component for Feb 2011 Earthquake according to the LiDAR DEM.

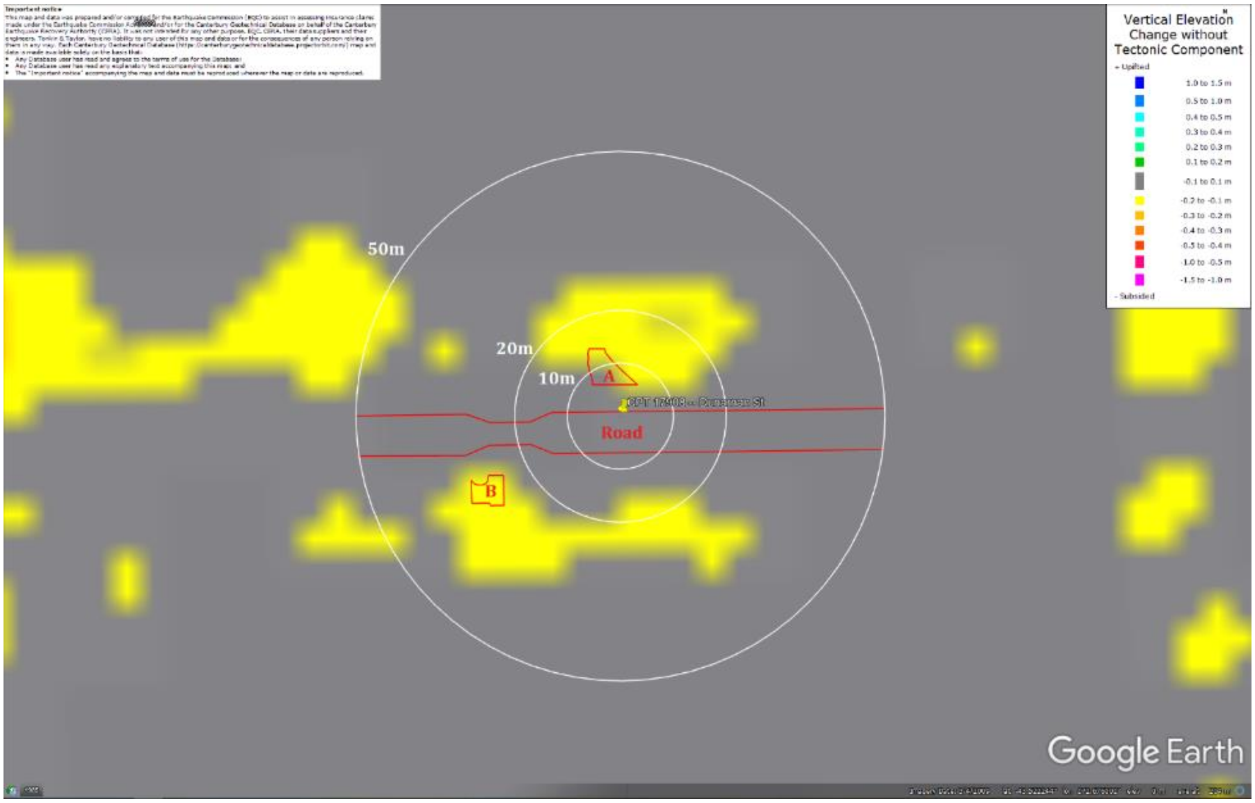

Figure 40: Ground surface subsidence without tectonic component for June 2011 Earthquake according to the LiDAR DEM.

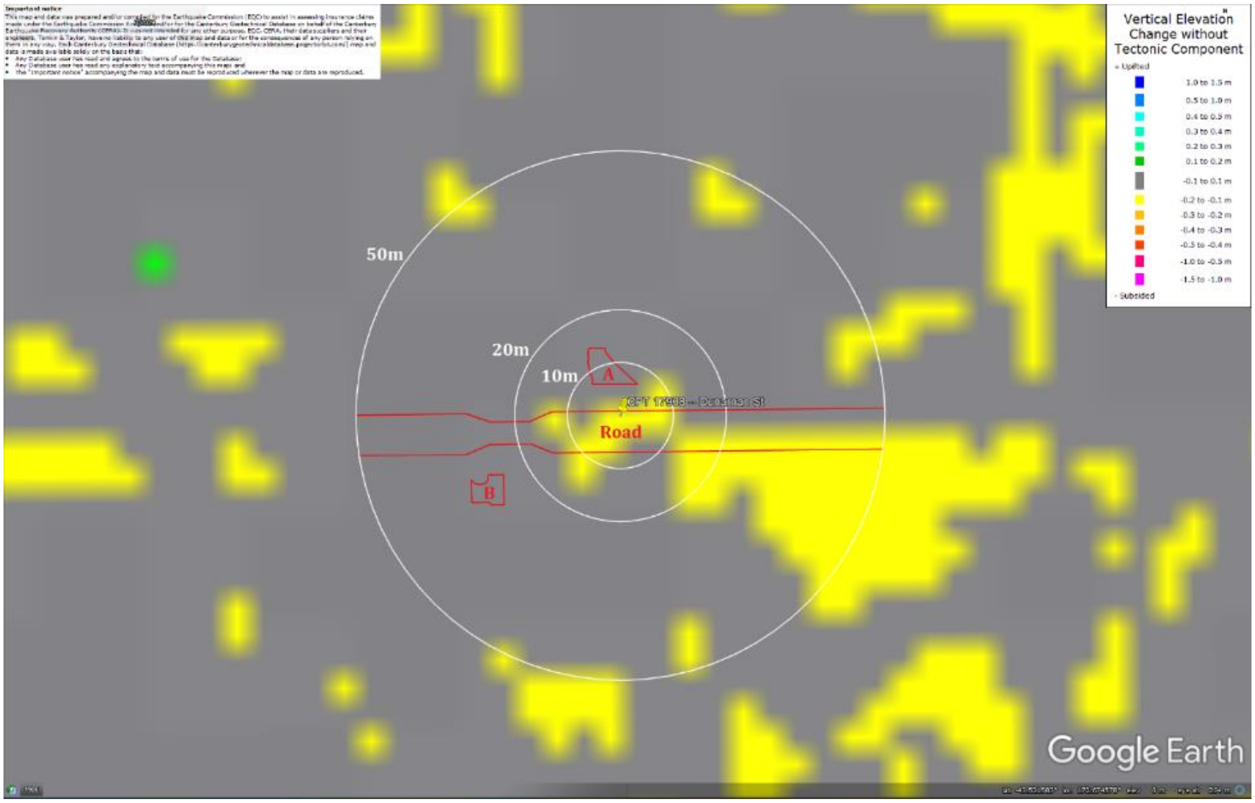

Figure 41: Ground surface subsidence without tectonic component for Dec 2011 Earthquake according to the LiDAR DEM.

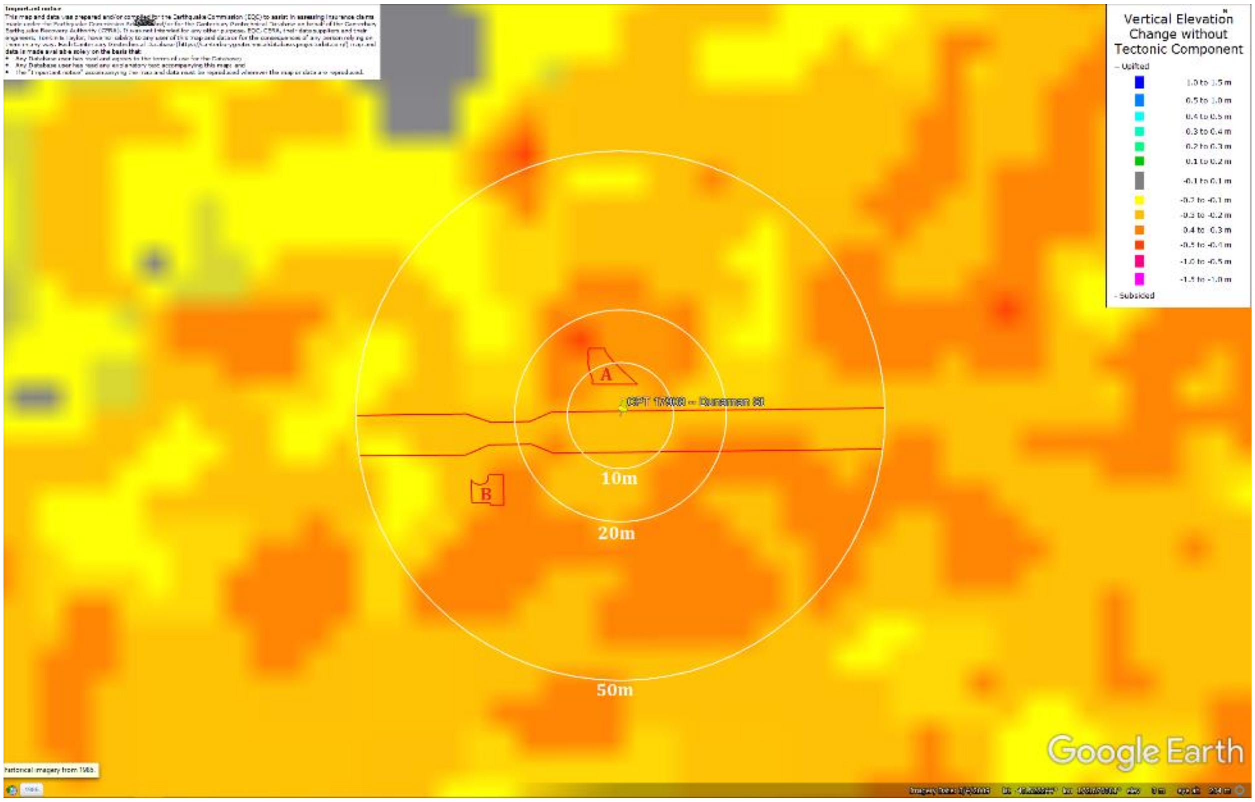

Figure 42: Ground surface subsidence without tectonic component for Canterbury Earthquake Sequence according to the LiDAR DEM.

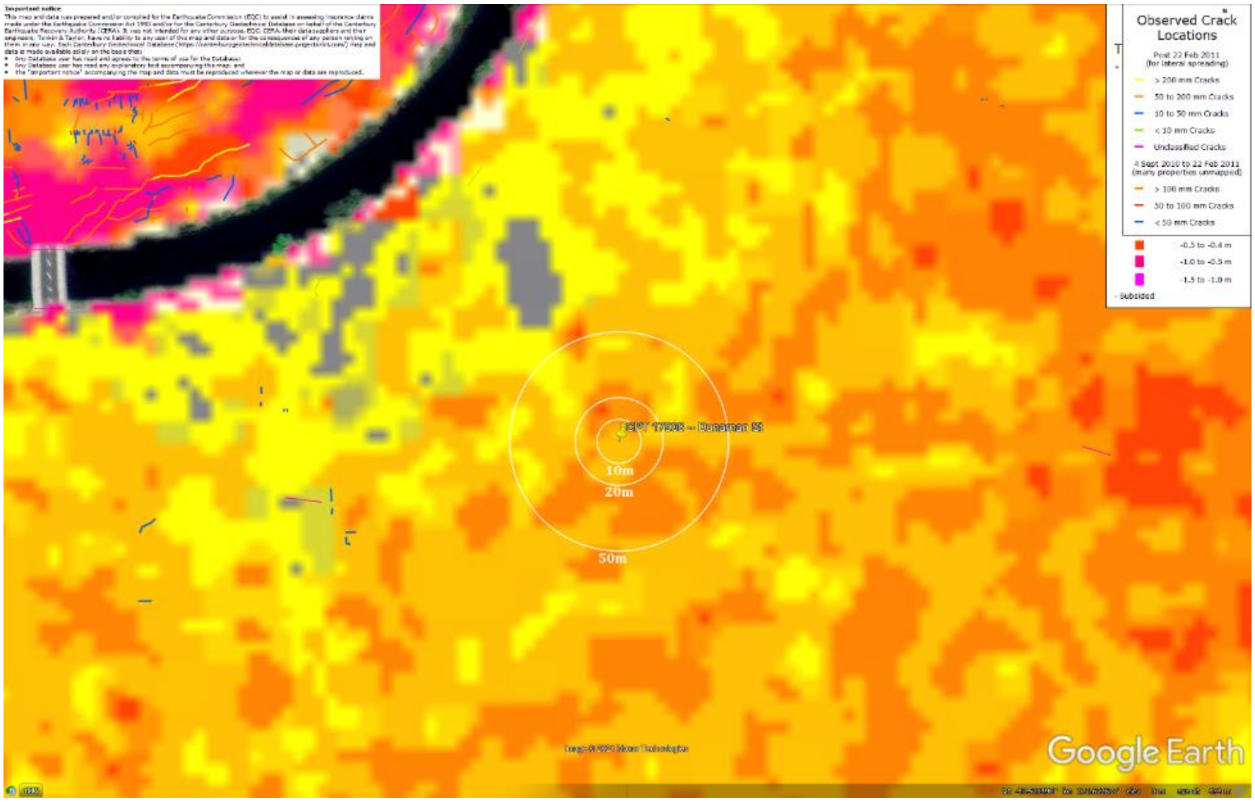

Figure 43: No lateral spreading for Canterbury Earthquake Sequence.

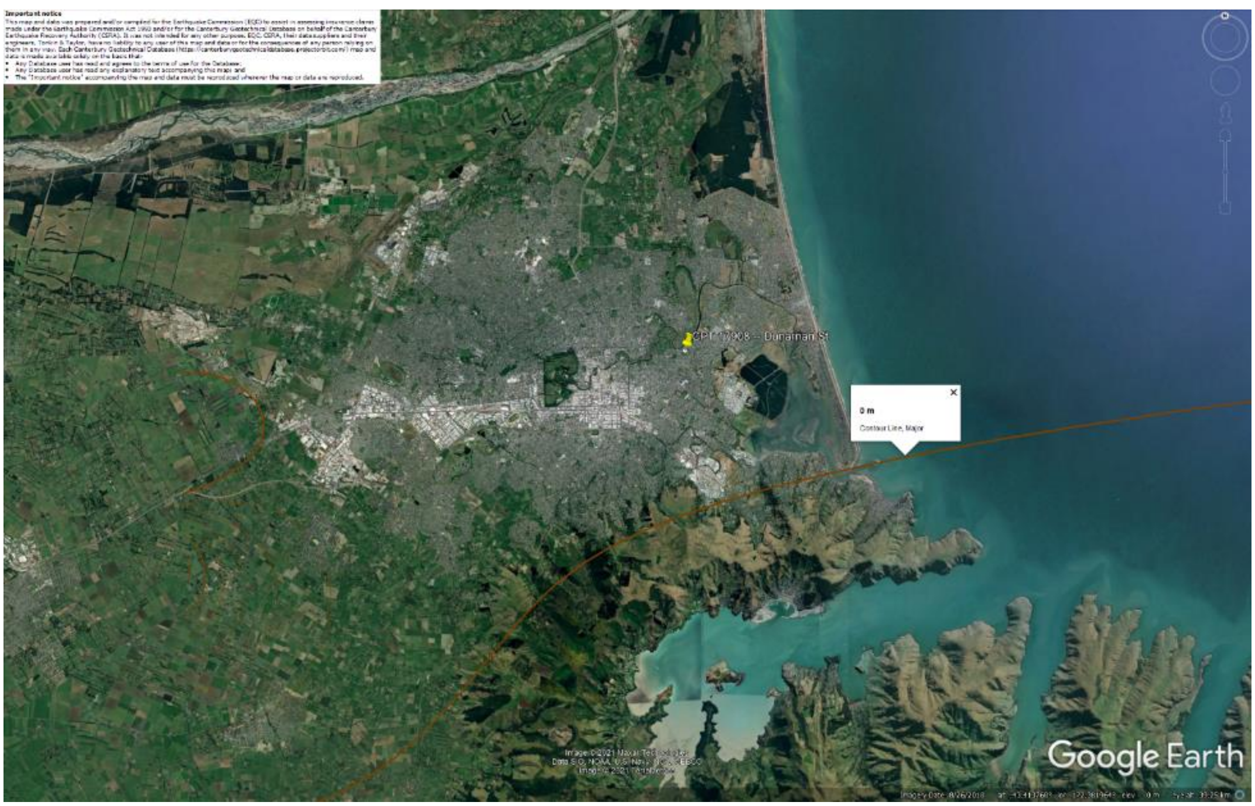

Figure 44: Vertical tectonic movements for Sep 2010 Earthquake.

Figure 45: Vertical tectonic movements for Feb 2011 Earthquake.

Figure 46: Vertical tectonic movements for June 2011 Earthquake.

Figure 47: Vertical tectonic movements for Dec 2011 Earthquake.

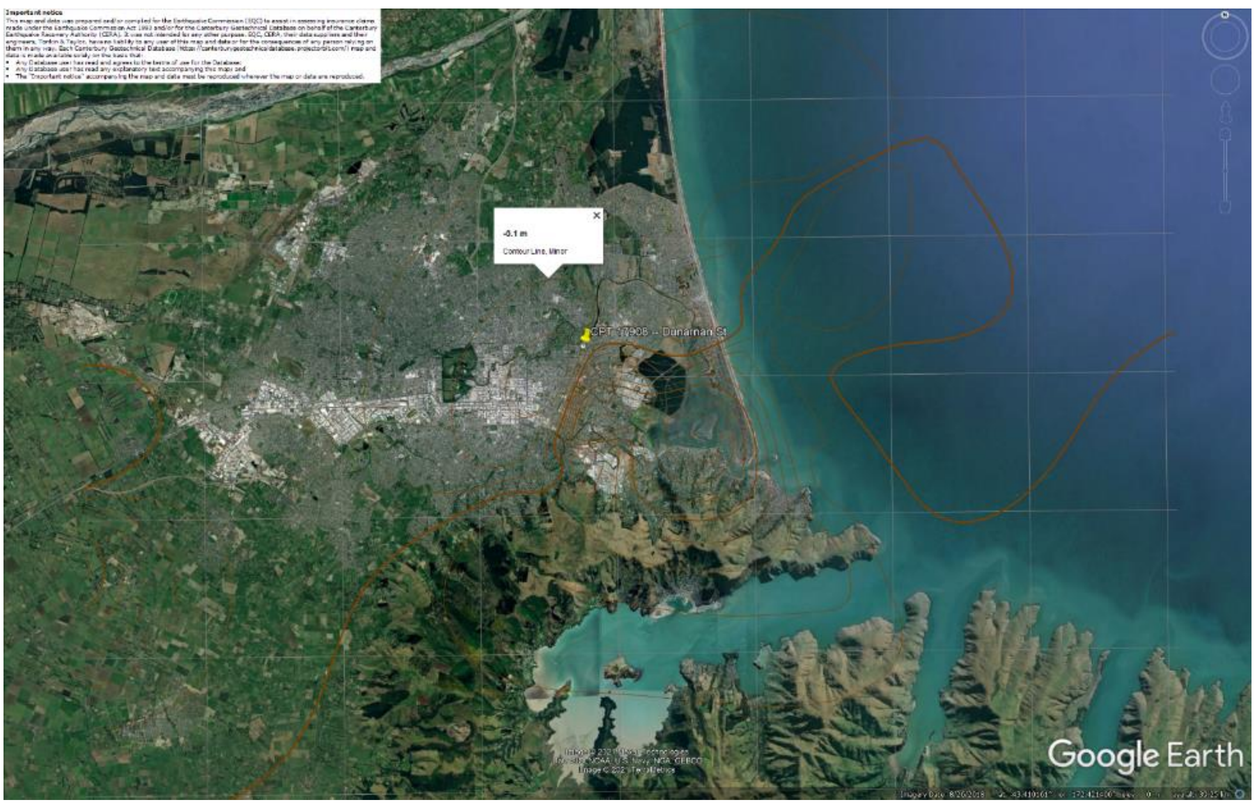

Figure 48: Vertical tectonic movements for Canterbury Earthquake Sequence.

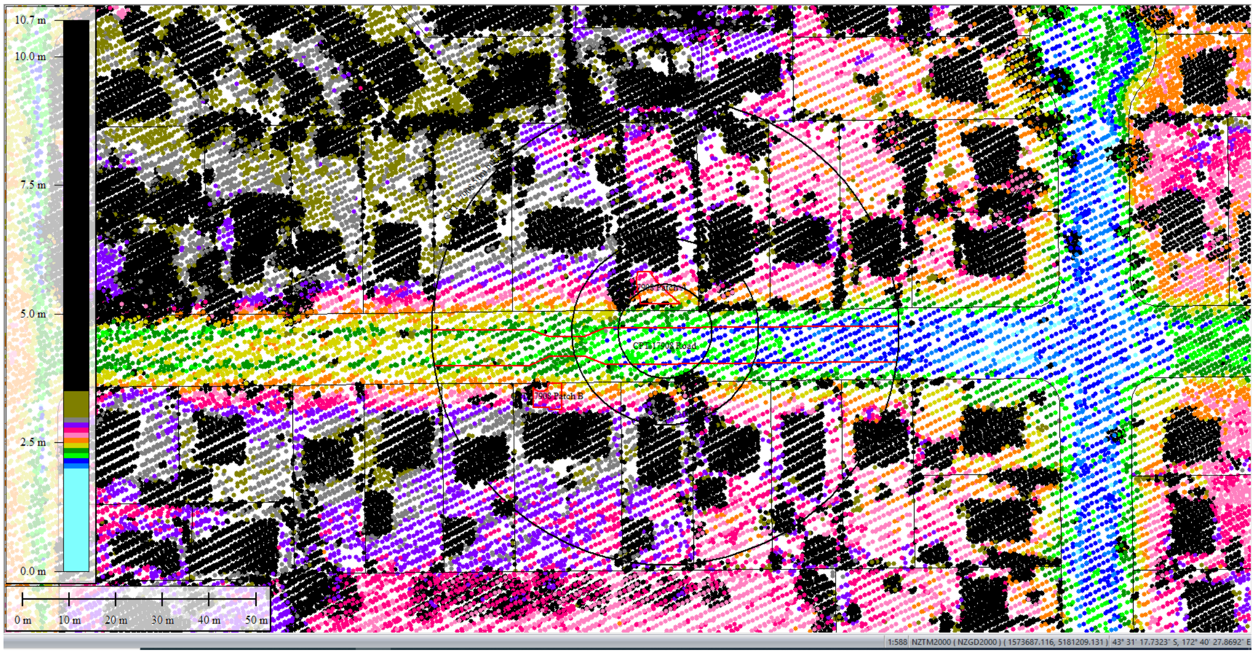

Figure 49: Sep 5, 2010 LiDAR survey.

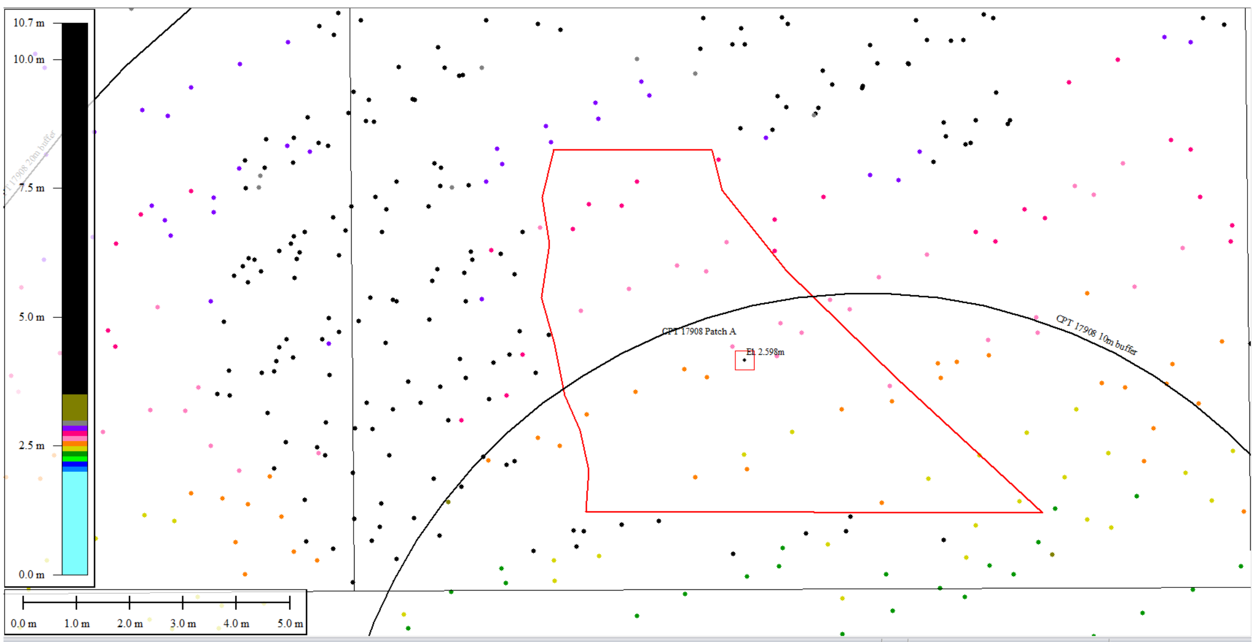

Figure 50: Ground surface elevation averaged over 20-m and 50-m buffers for Patch A for Sep 5, 2010 LiDAR survey.

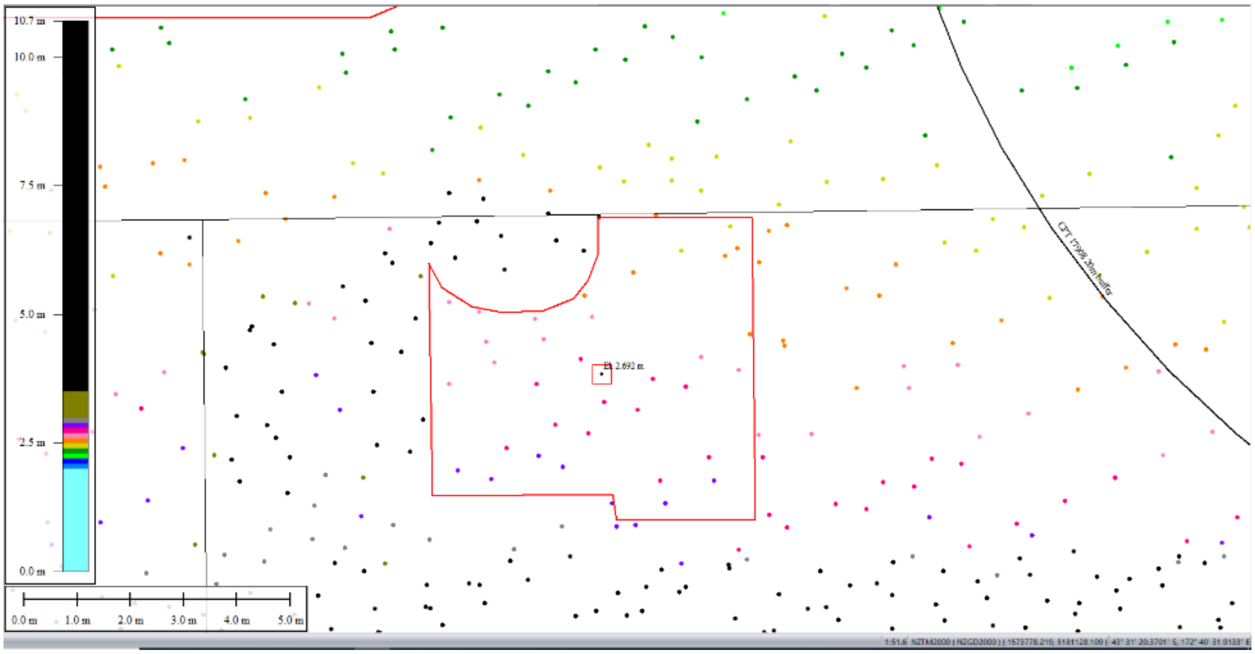

Figure 51: Ground surface elevation averaged over 50-m buffer for Patch B for Sep 5, 2010 LiDAR survey.

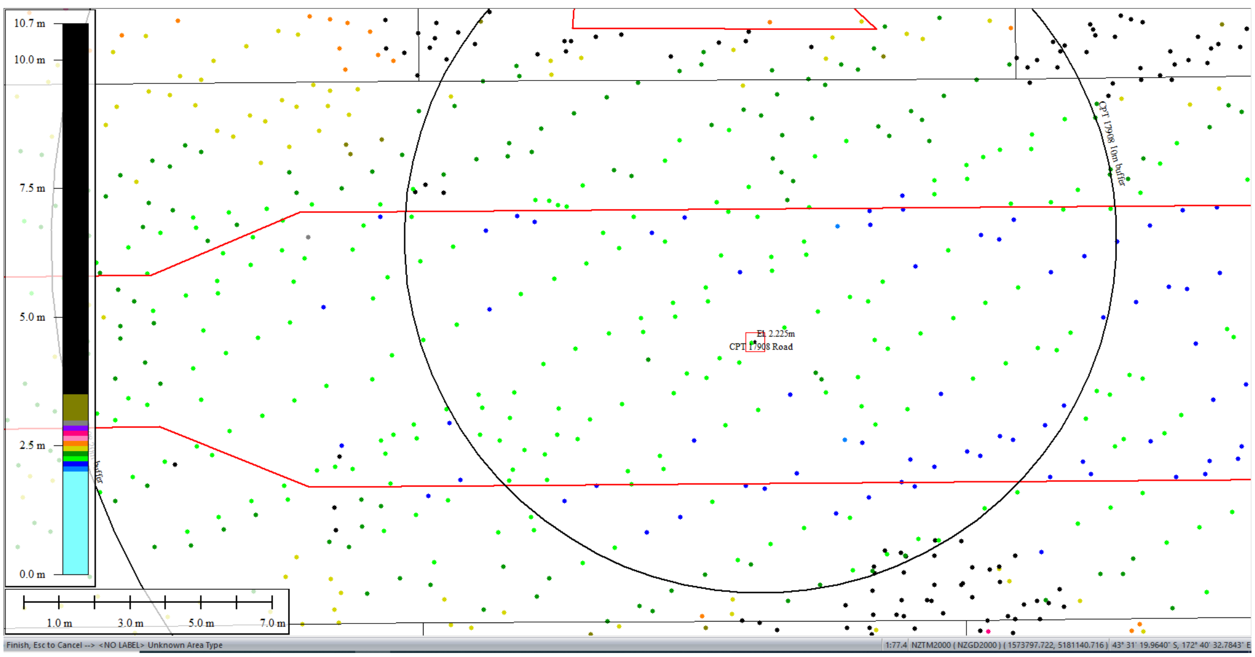

Figure 52: Ground surface elevation averaged over 10-m buffer for Road for Sep 5, 2010 LiDAR survey.

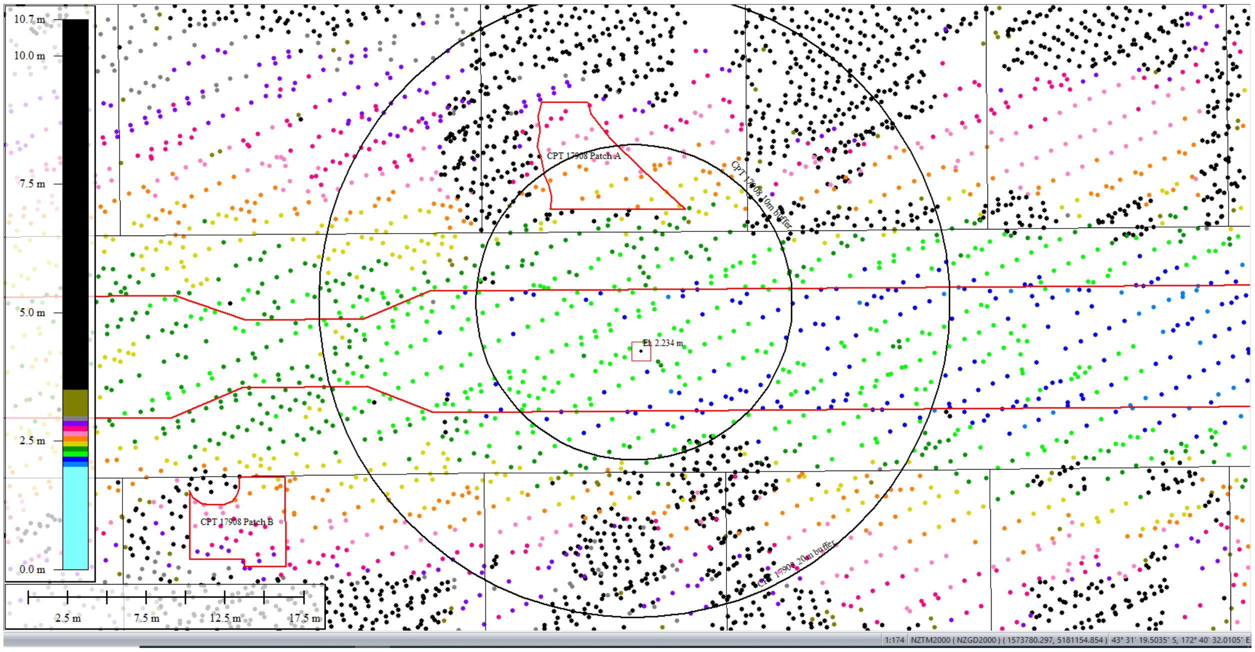

Figure 53: Ground surface elevation averaged over 20-m buffer for Road for Sep 5, 2010 LiDAR survey.

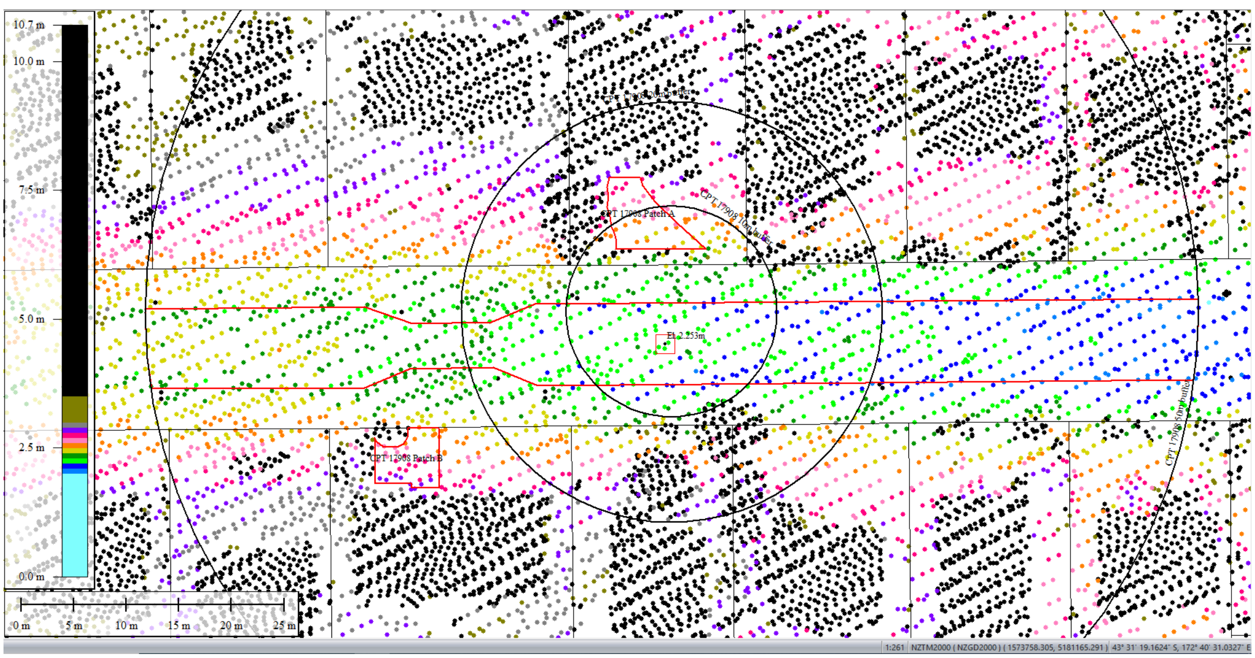

Figure 54: Ground surface elevation averaged over 50-m buffer for Road for Sep 5, 2010 LiDAR survey.

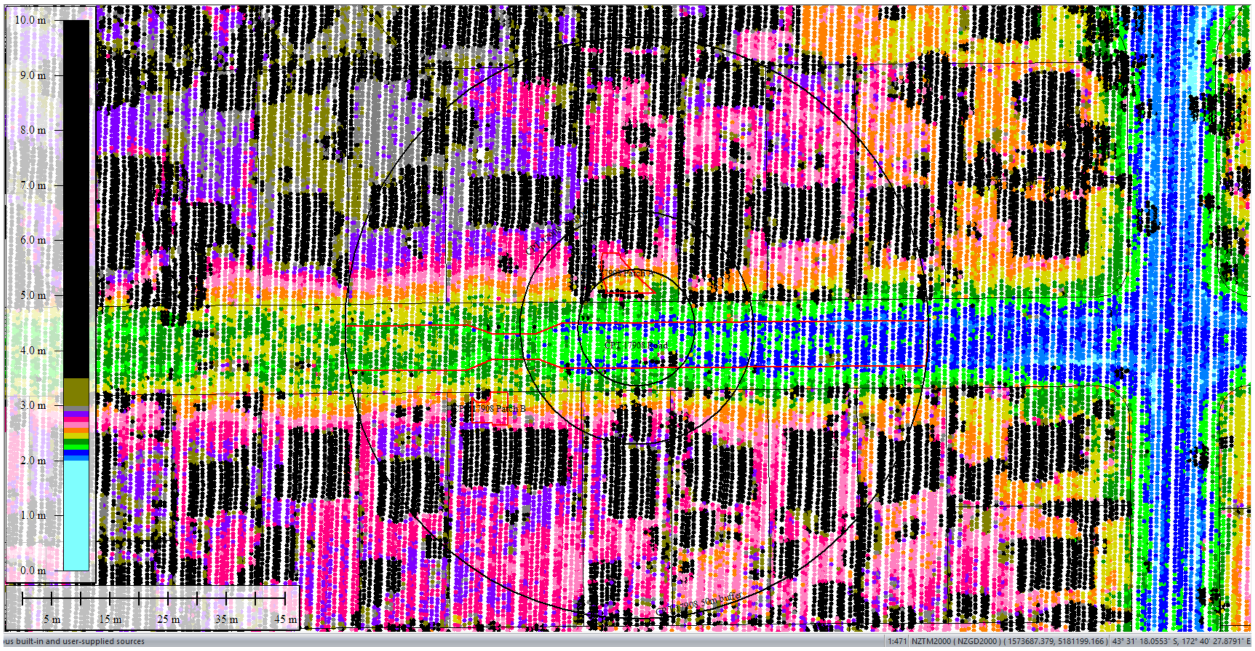

Figure 55: Mar 2011 LiDAR survey.

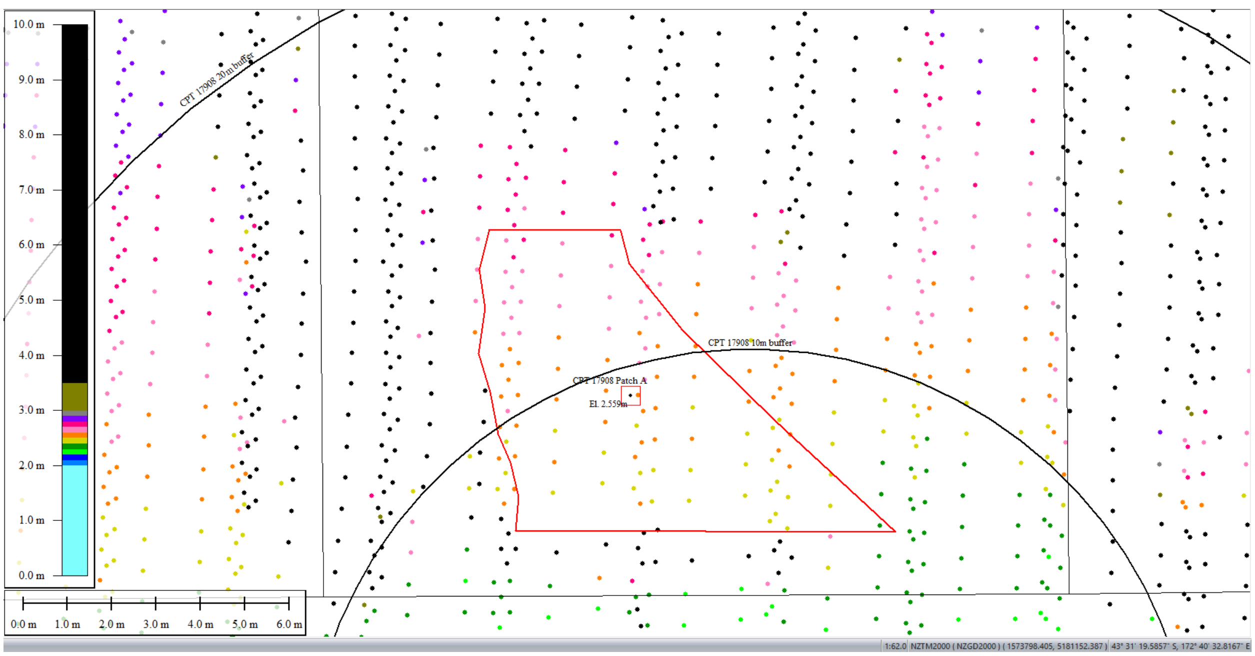

Figure 56: Ground surface elevation averaged over 20-m and 50-m buffers for Patch A for Mar 2011 LiDAR survey.

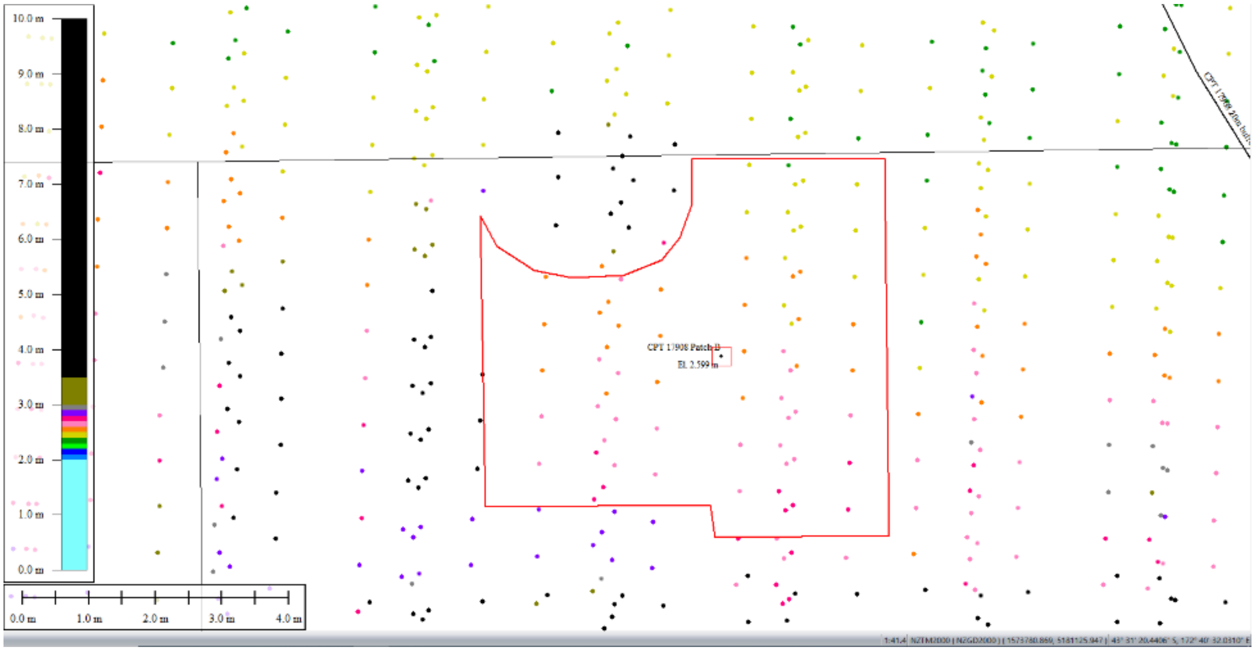

Figure 57: Ground surface elevation averaged over 50-m buffer for Patch B for Mar 2011 LiDAR survey.

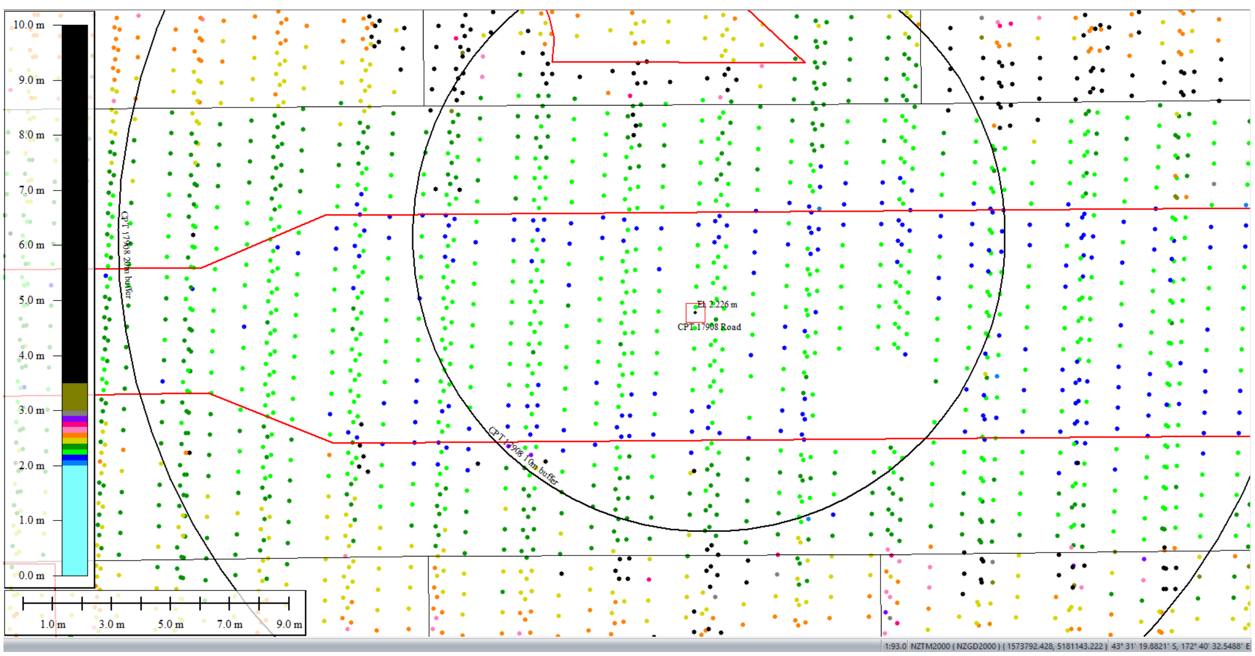

Figure 58: Ground surface elevation averaged over 10-m buffer for Road for Mar 2011 LiDAR survey.

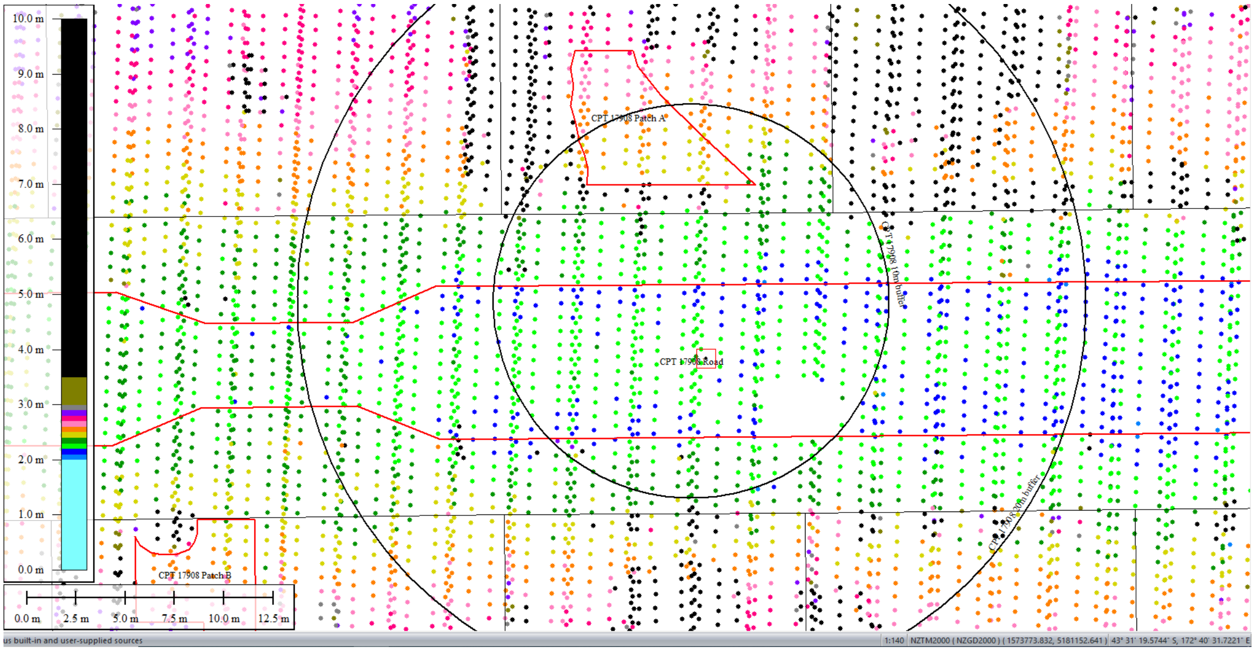

Figure 59: Ground surface elevation averaged over 20-m buffer for Road for Mar 2011 LiDAR survey (el. 2.226m).

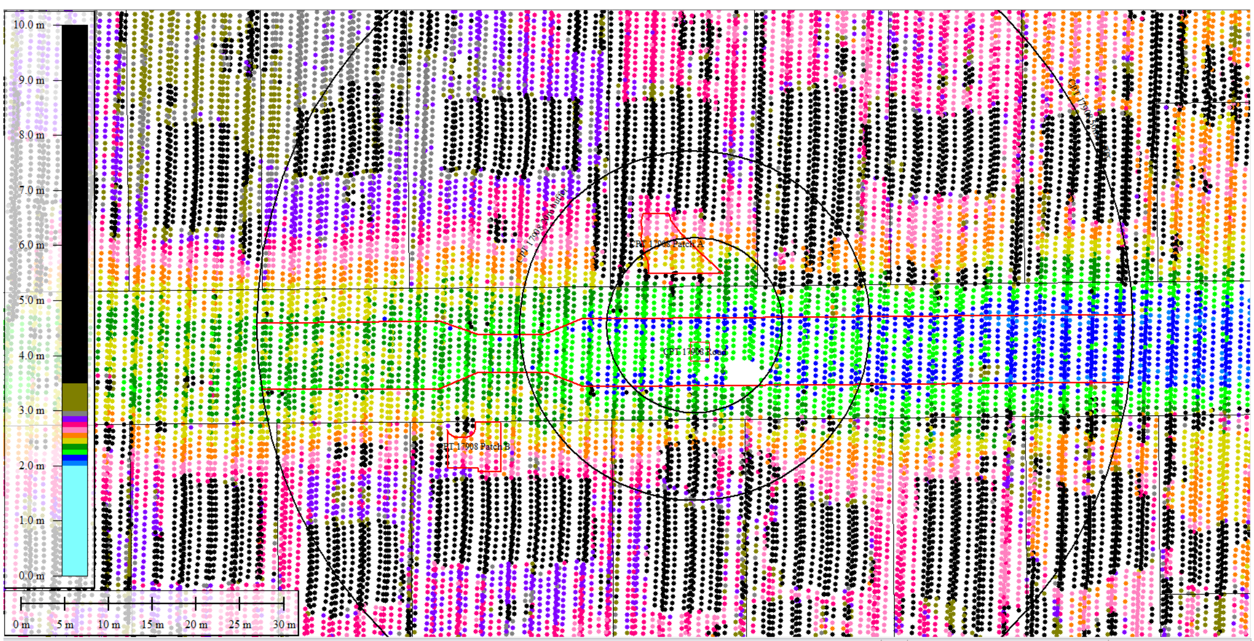

Figure 60: Ground surface elevation averaged over 50-m buffer for Road for Mar 2011 LiDAR survey (el. 2.253m).

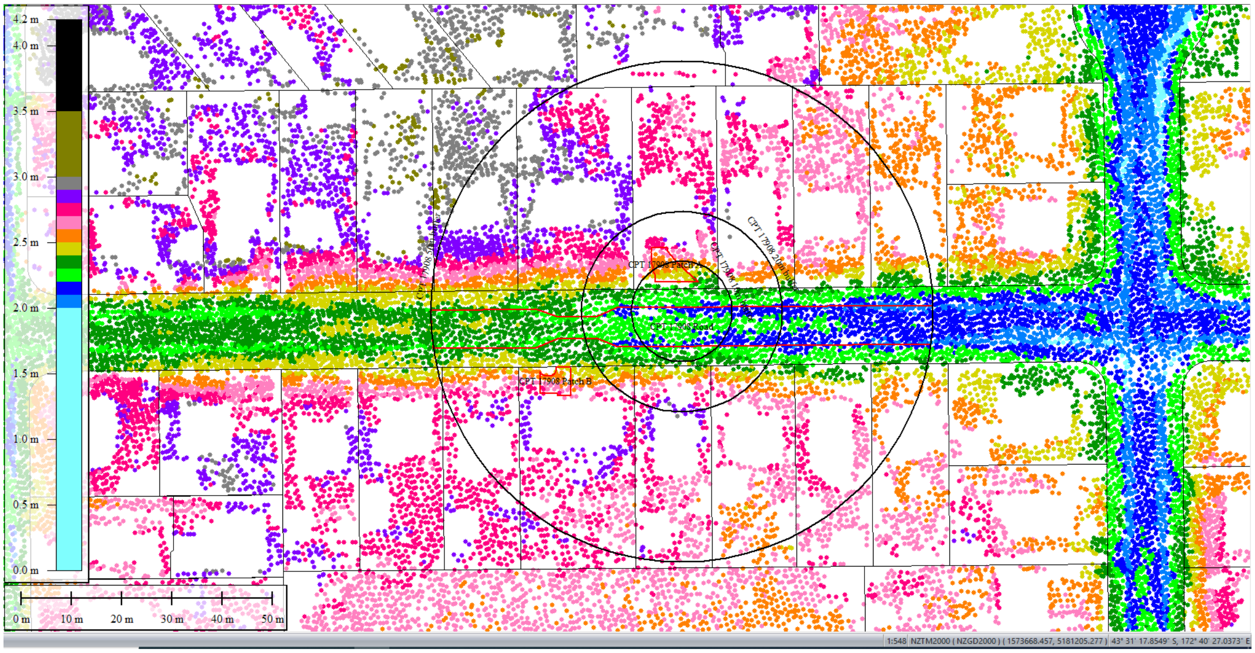

Figure 61: May 2011 LiDAR survey.

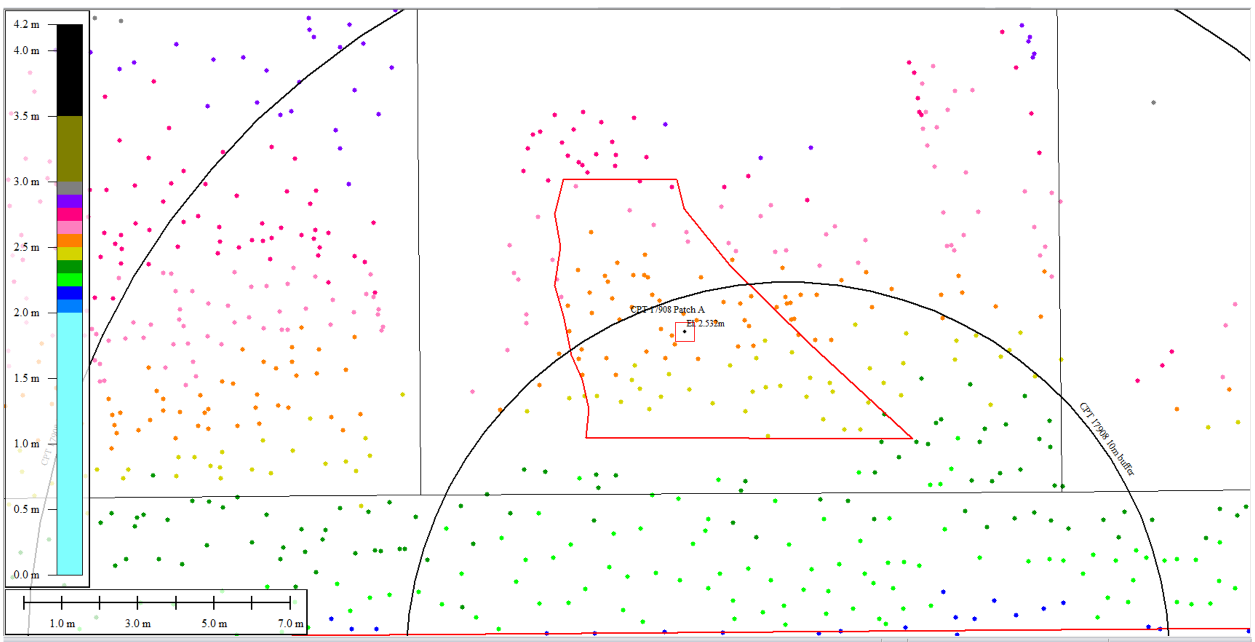

Figure 62: Ground surface elevation averaged over 20-m and 50-m buffers for Patch A for May 2011 LiDAR survey.

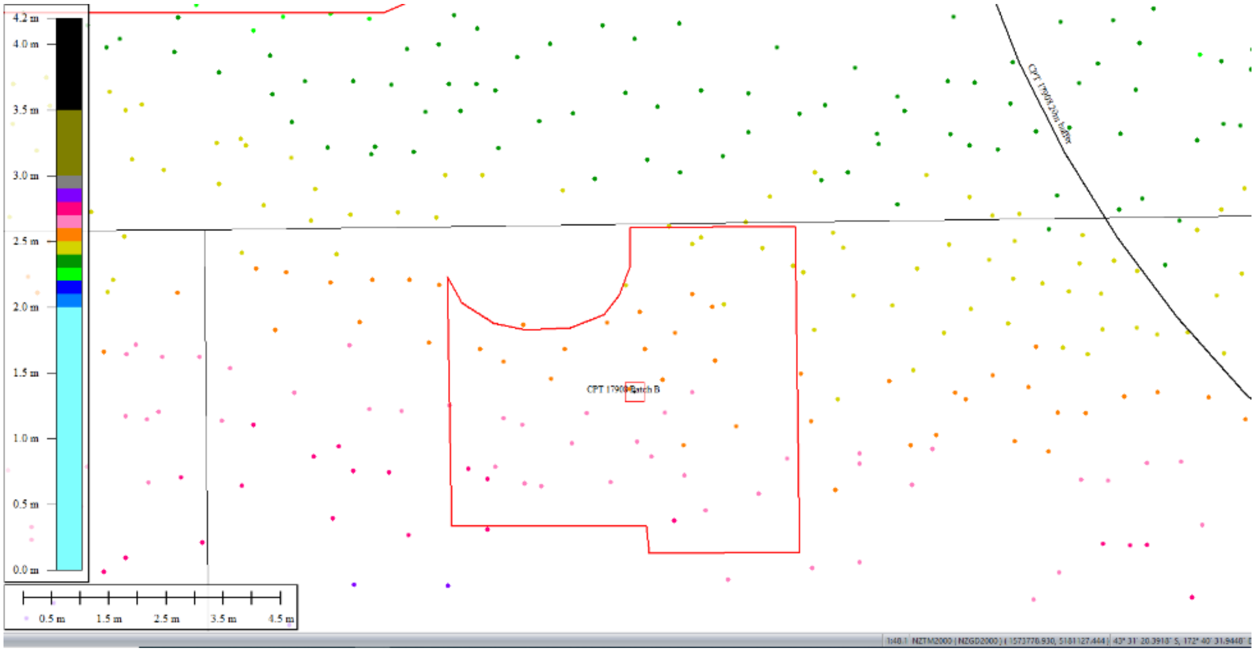

Figure 63: Ground surface elevation averaged over 50-m buffer for Patch B for May 2011 LiDAR survey (el. 2.595m).

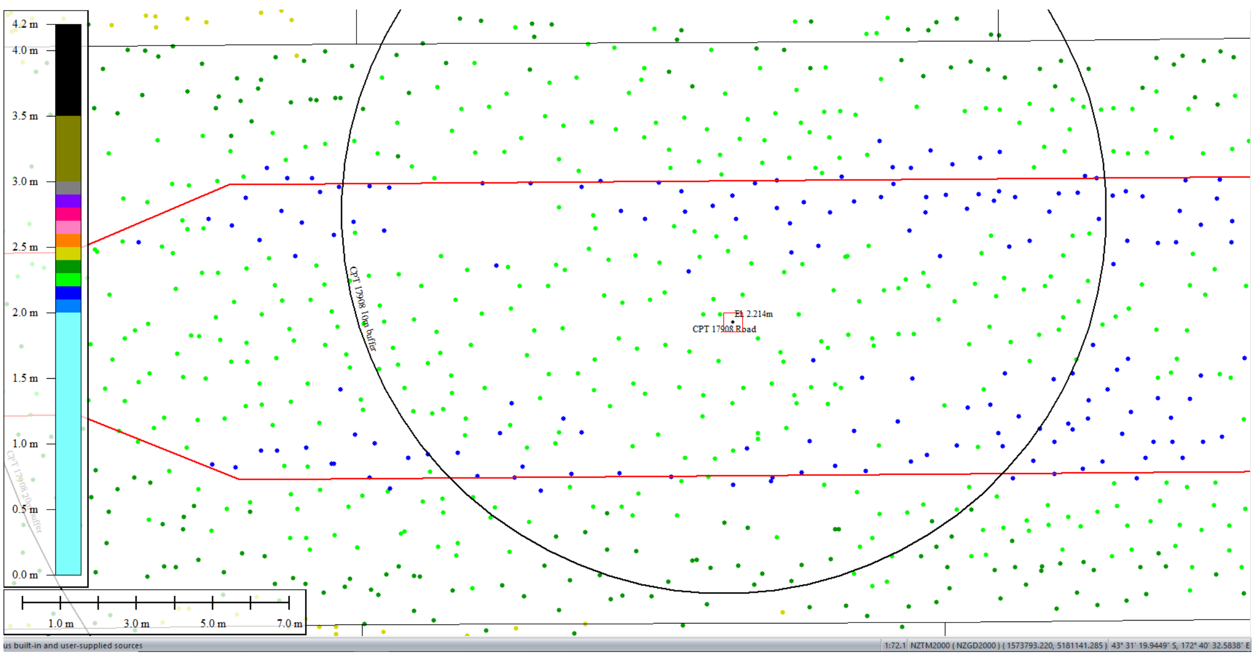

Figure 64: Ground surface elevation averaged over 10-m buffer for Road for May 2011 LiDAR survey.

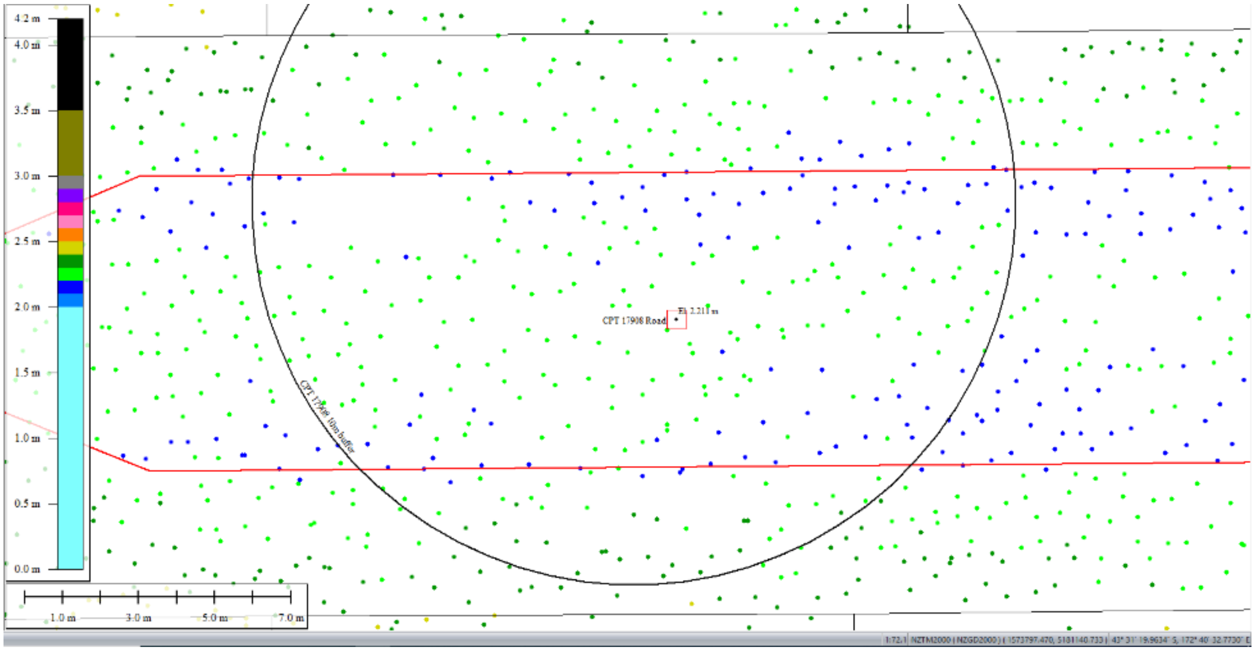

Figure 65: Ground surface elevation averaged over 20-m buffer for Road for May 2011 LiDAR survey.

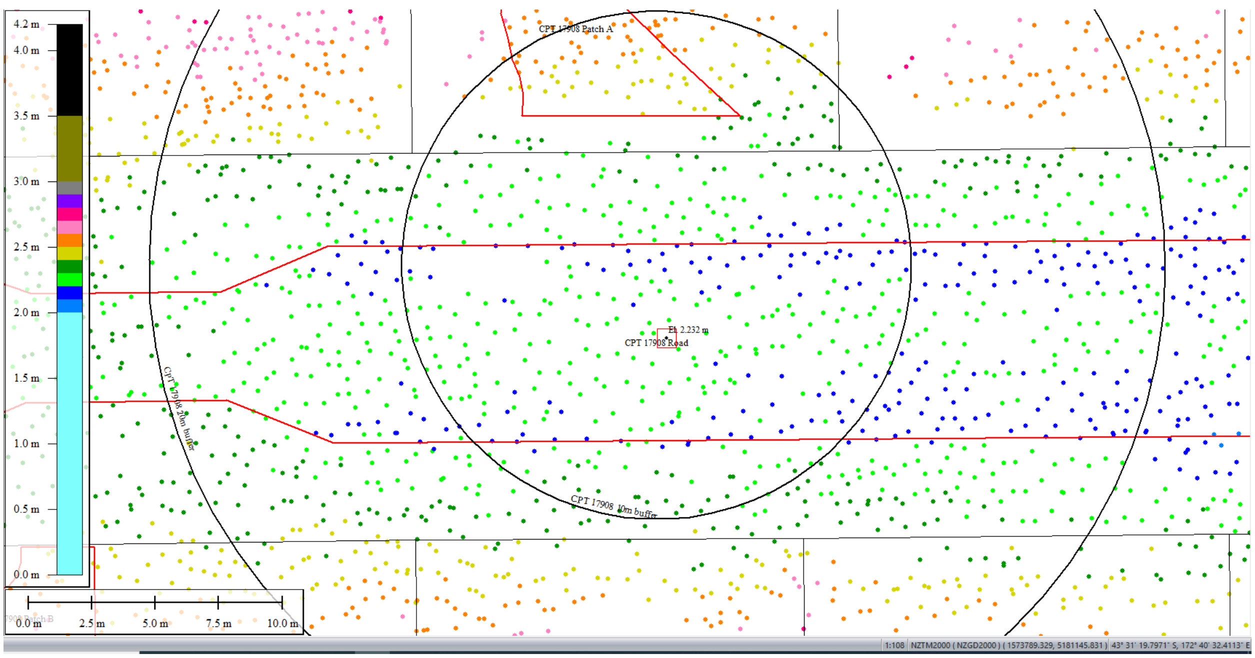

Figure 66: Ground surface elevation averaged over 50-m buffer for Road for May 2011 LiDAR survey.

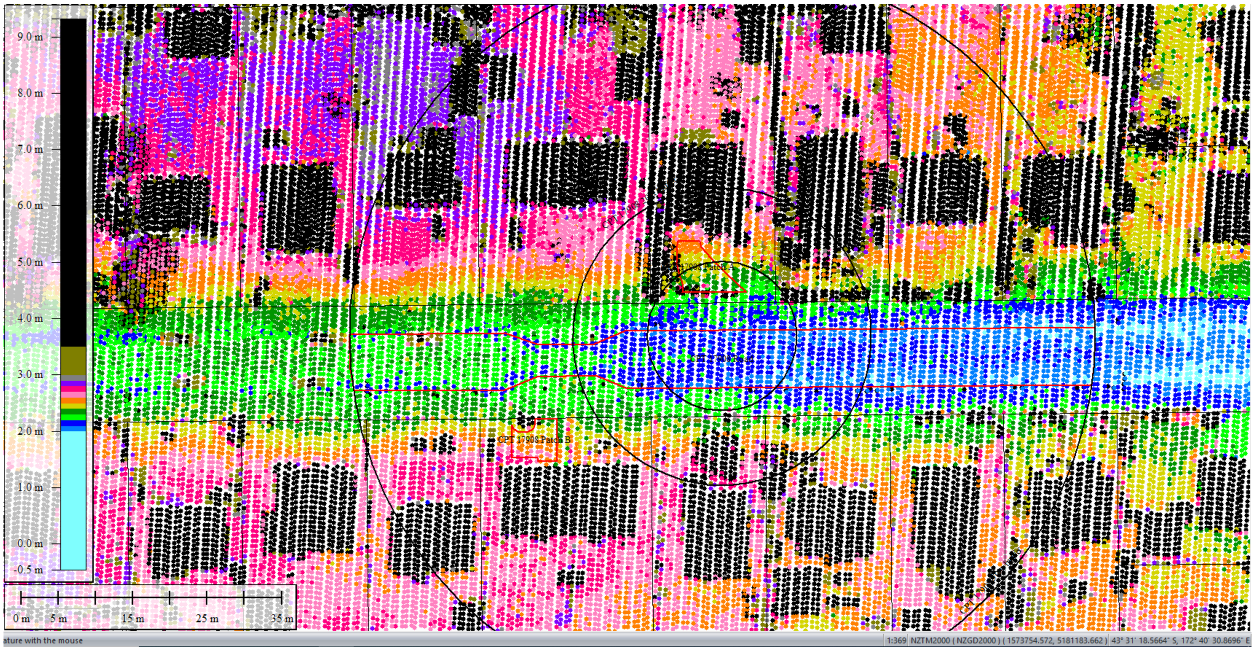

Figure 67: Sep 2011 LiDAR survey.

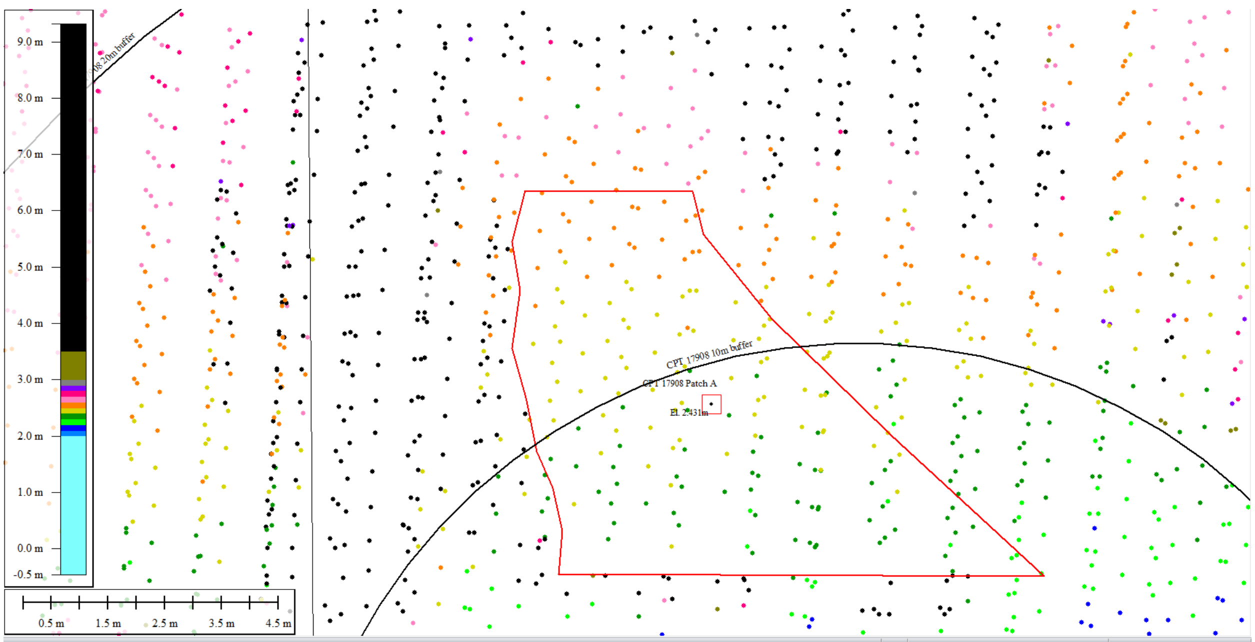

Figure 68: Ground surface elevation averaged over 20-m and 50-m buffers for Patch A for Sep 2011 LiDAR survey.

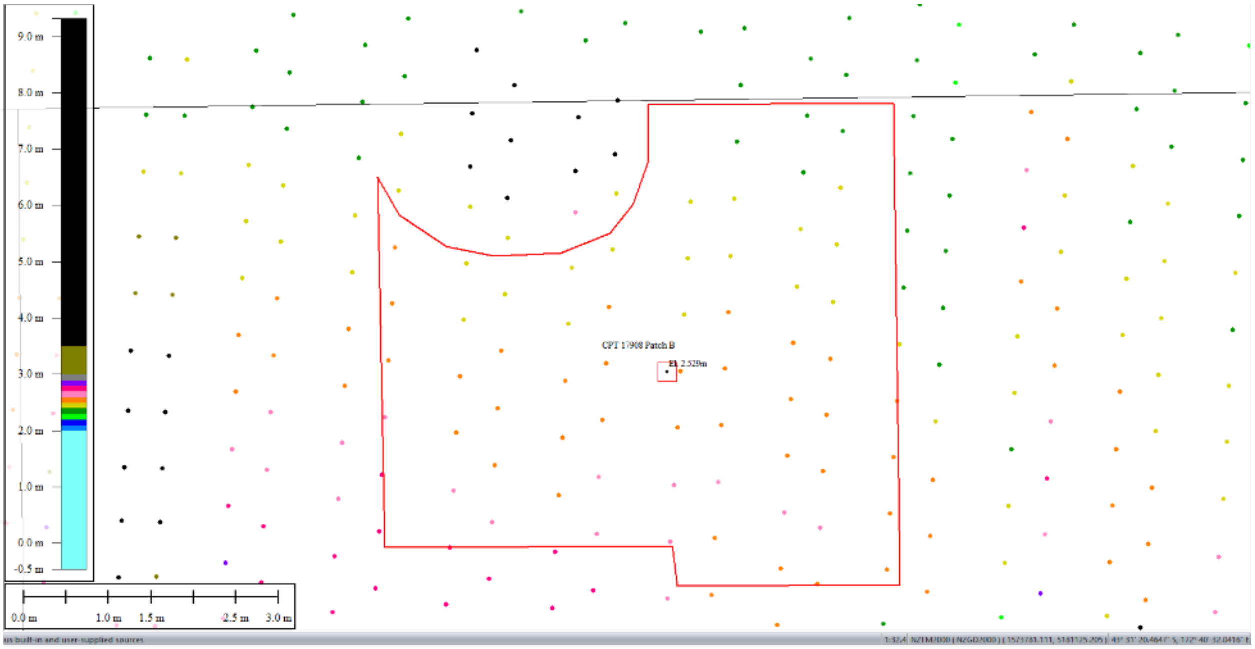

Figure 69: Ground surface elevation averaged over 50-m buffer for Patch B for Sep 2011 LiDAR survey.

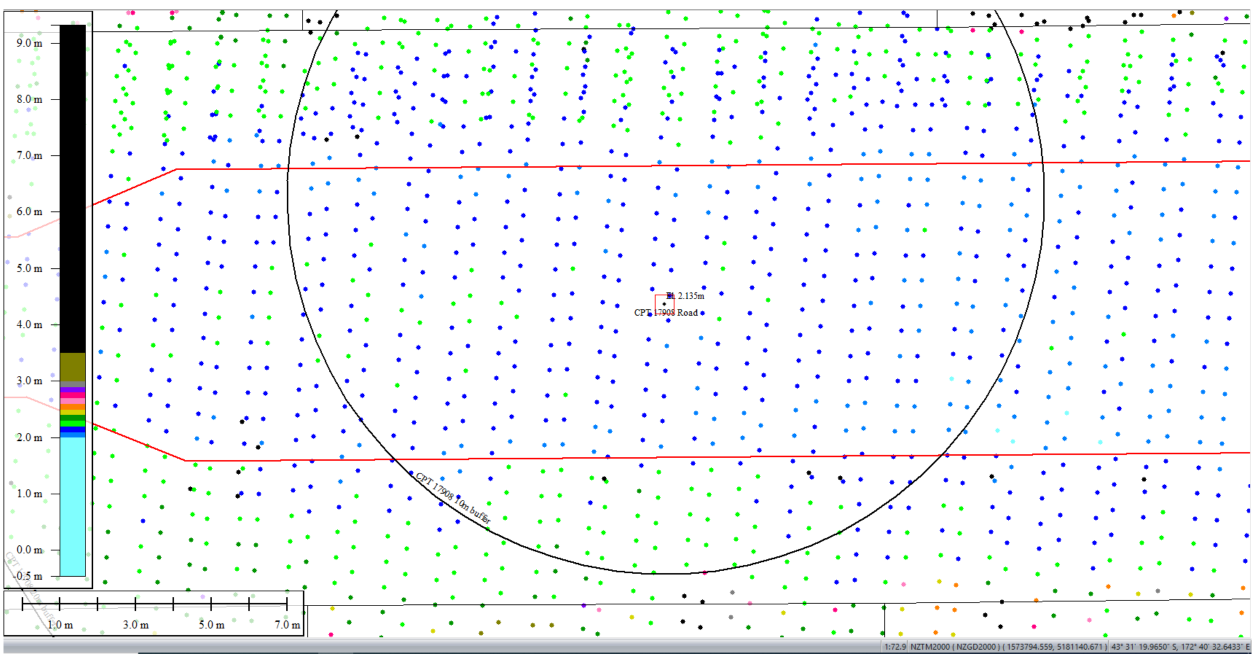

Figure 70: Ground surface elevation averaged over 10-m buffer for Road for Sep 2011 LiDAR survey.

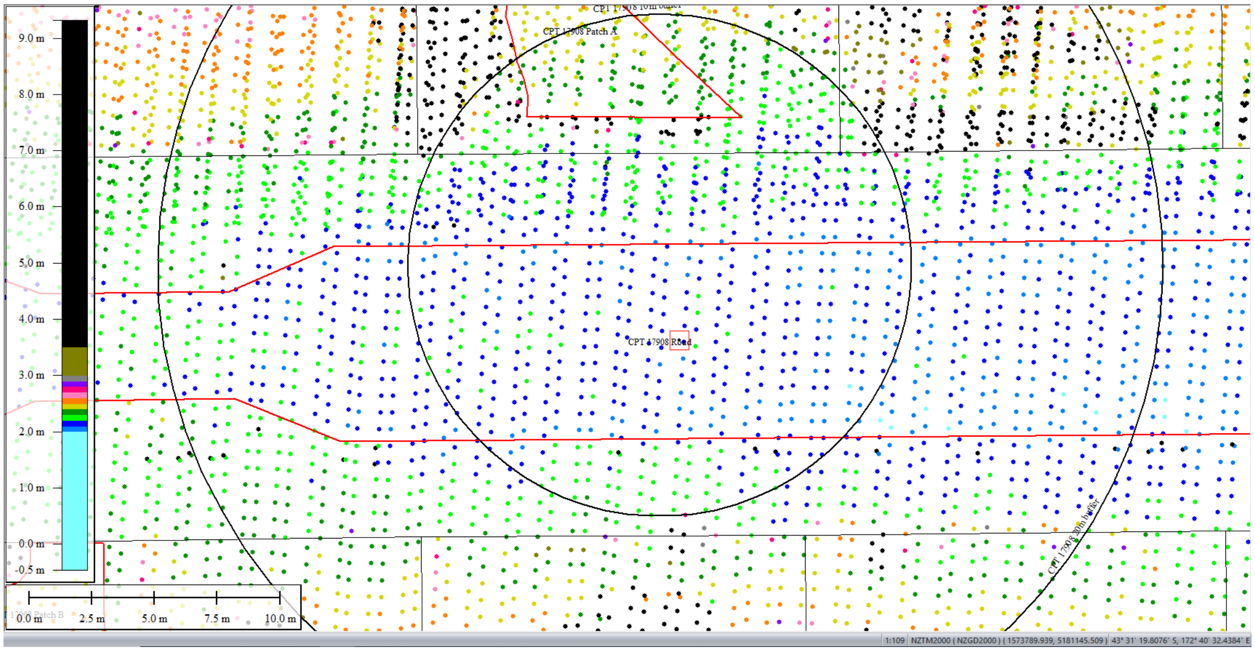

Figure 71: Ground surface elevation averaged over 20-m buffer for Road for Sep 2011 LiDAR survey (el. 2.134m).

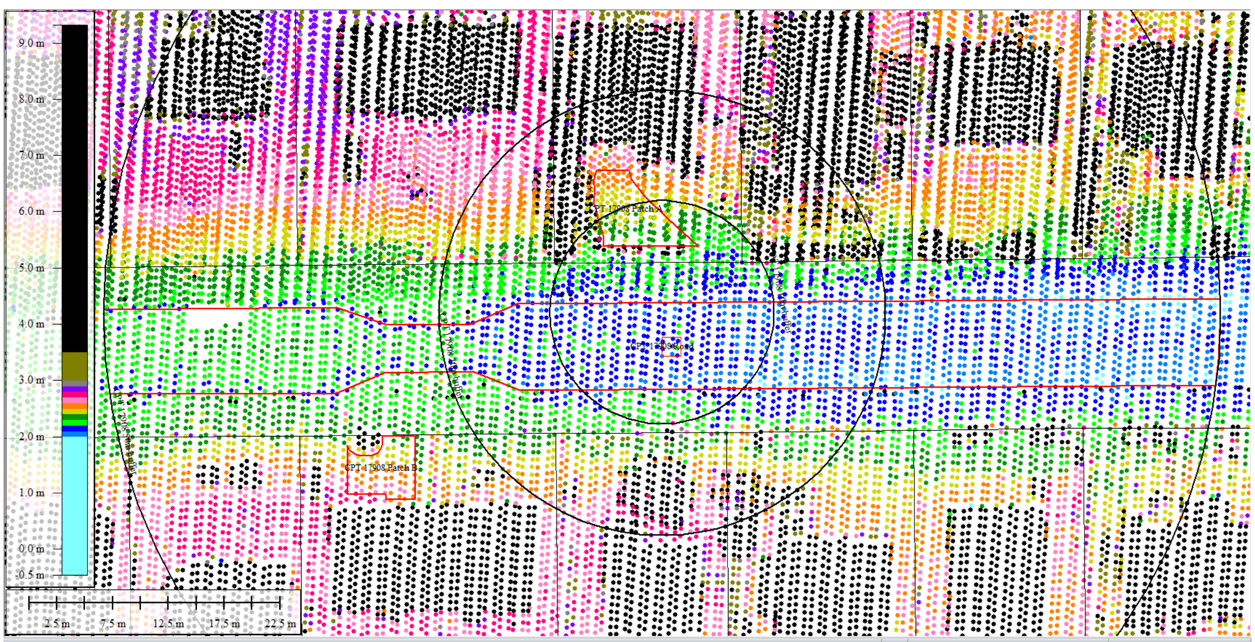

Figure 72: Ground surface elevation averaged over 50-m buffer for Road for Sep 2011 LiDAR survey (el. 2.152m).

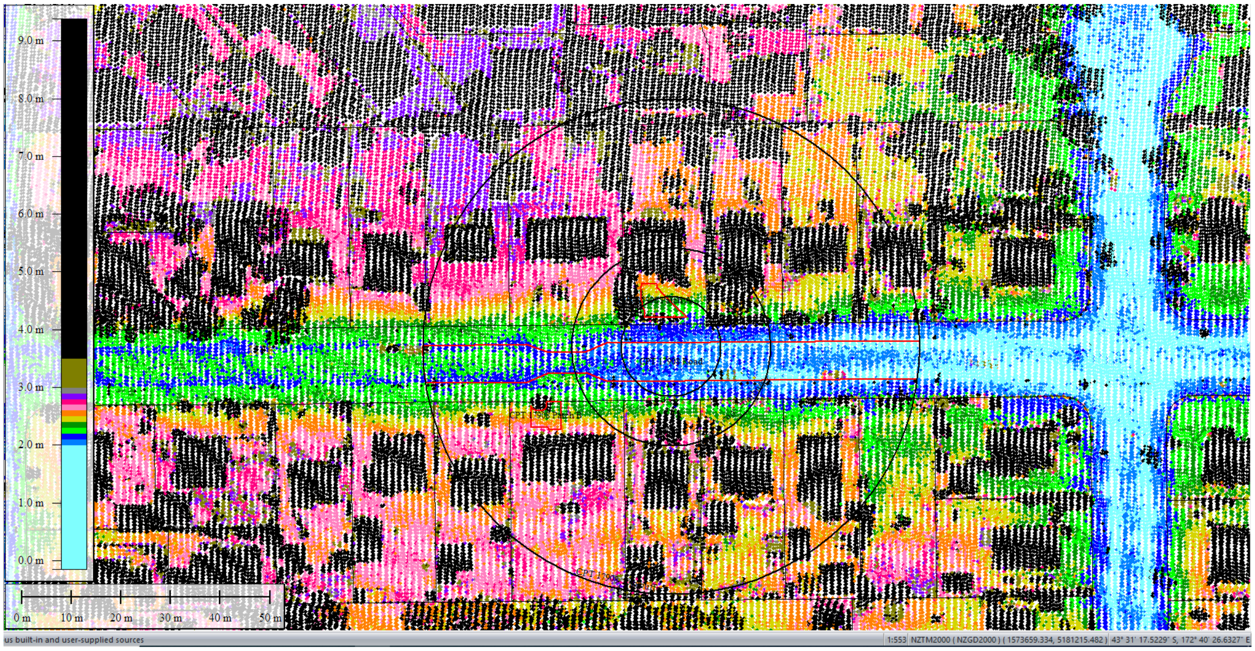

Figure 73: Feb 2012 LiDAR survey.

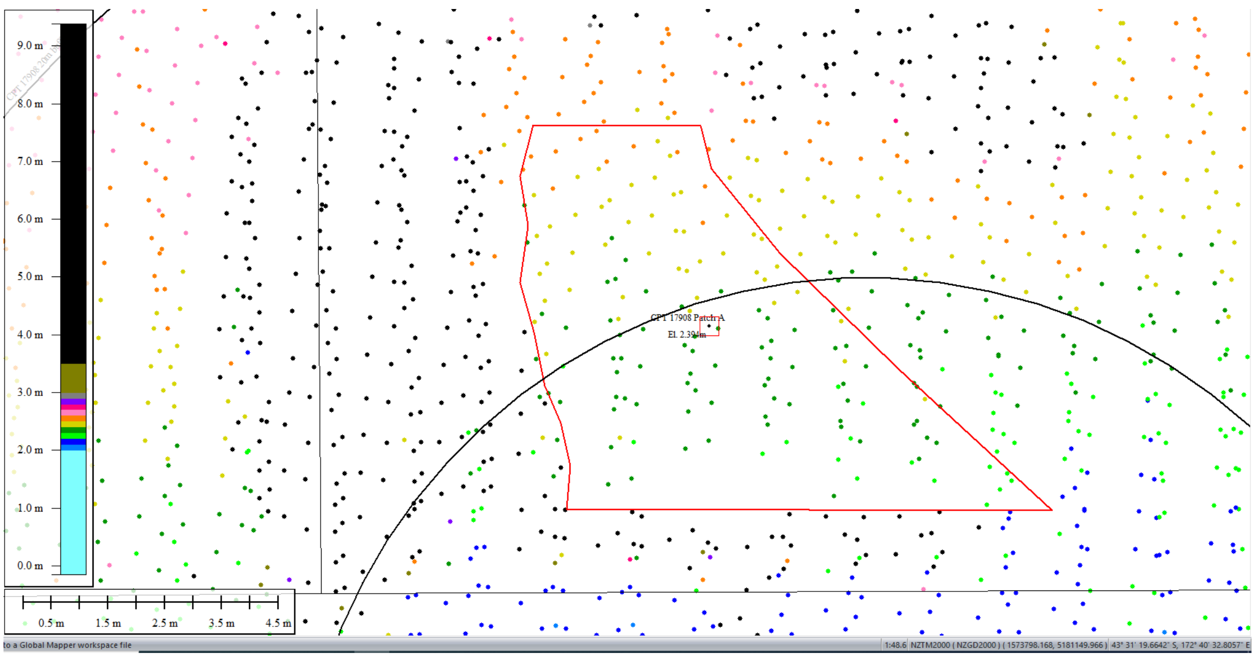

Figure 74: Ground surface elevation averaged over 20-m and 50-m buffers for Patch A for Feb 2012 LiDAR survey.

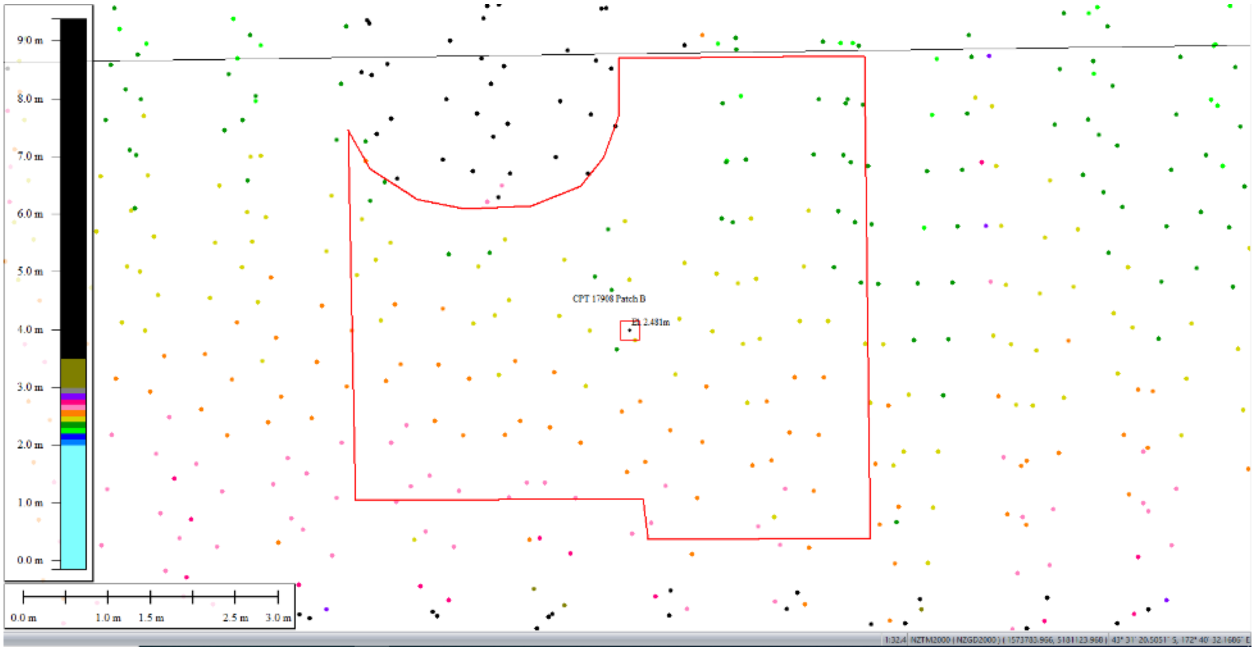

Figure 75: Ground surface elevation averaged over 50-m buffer for Patch B for Feb 2012 LiDAR survey.

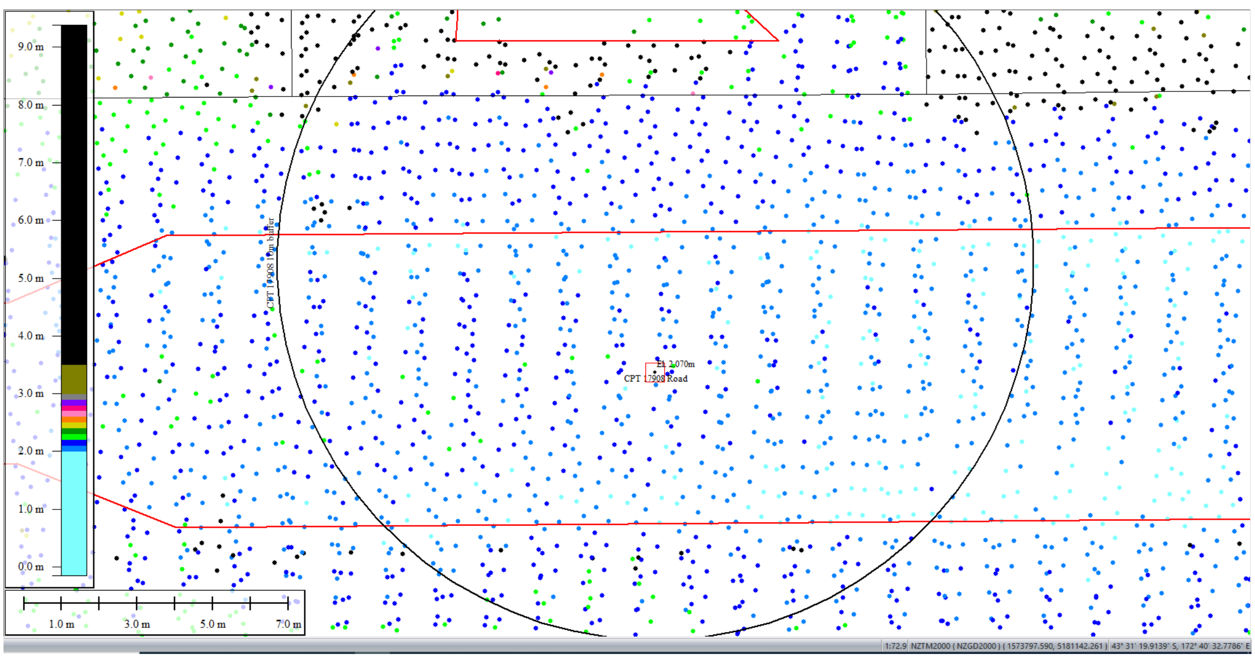

Figure 76: Ground surface elevation averaged over 10-m buffer for Road for Feb 2012 LiDAR survey.

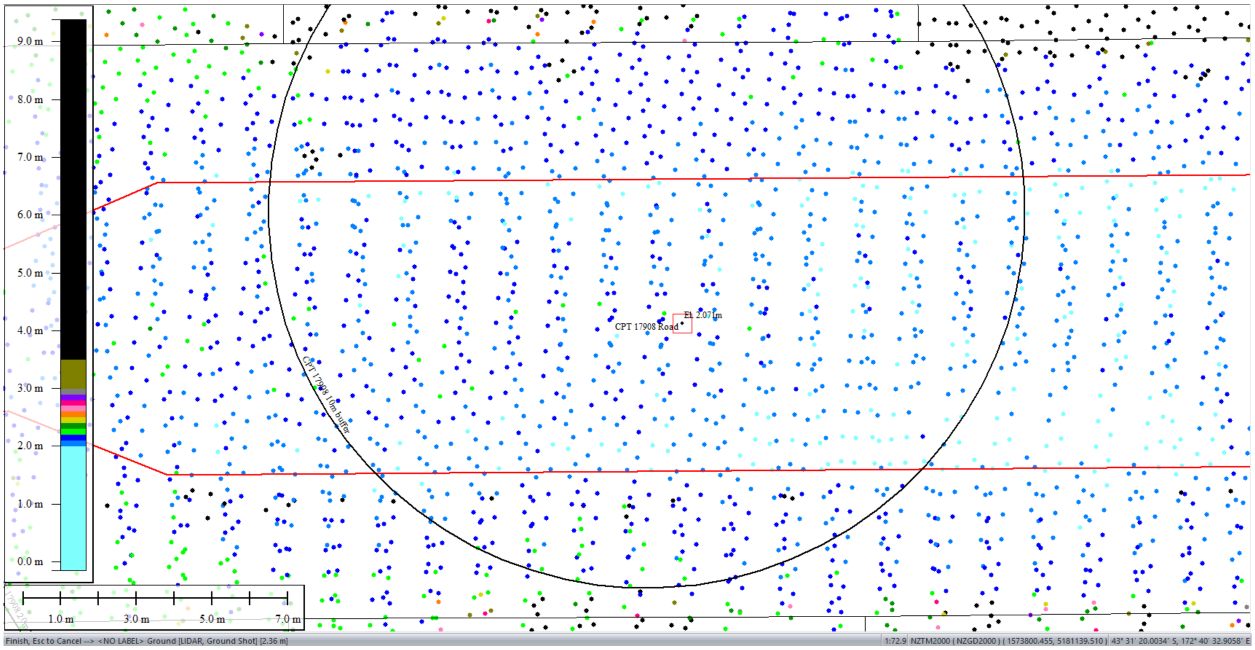

Figure 77: Ground surface elevation averaged over 20-m buffer for Road for Feb 2012 LiDAR survey.

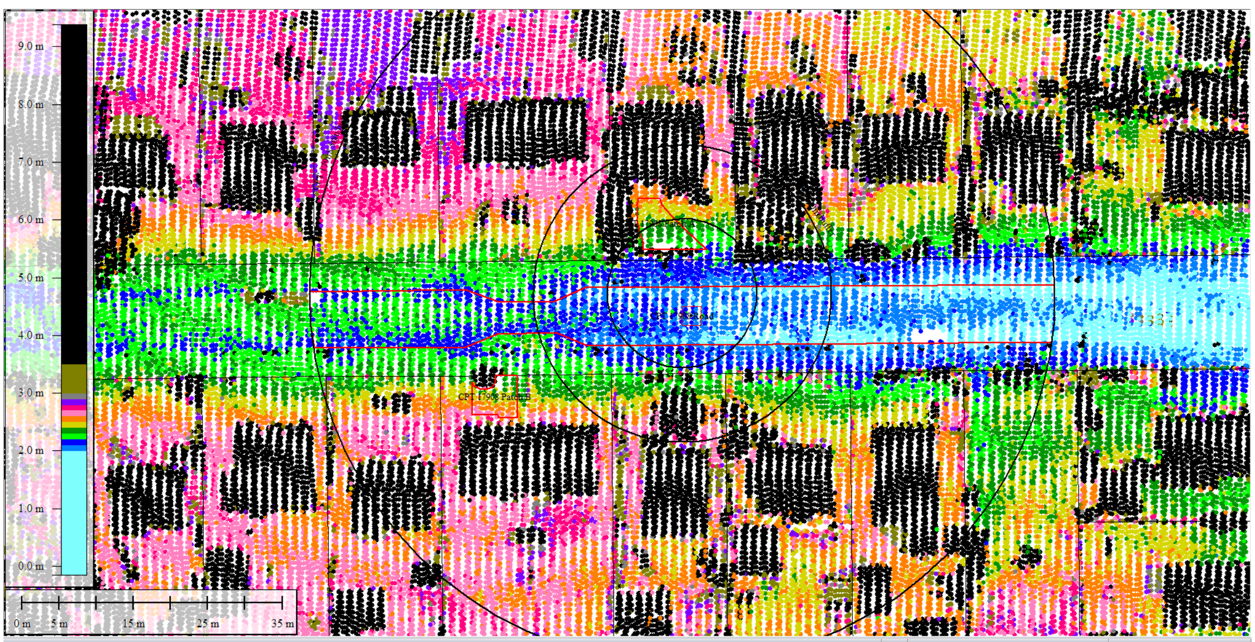

Figure 78: Ground surface elevation averaged over 50-m buffer for Road for Feb 2012 LiDAR survey (el. 2.087m).

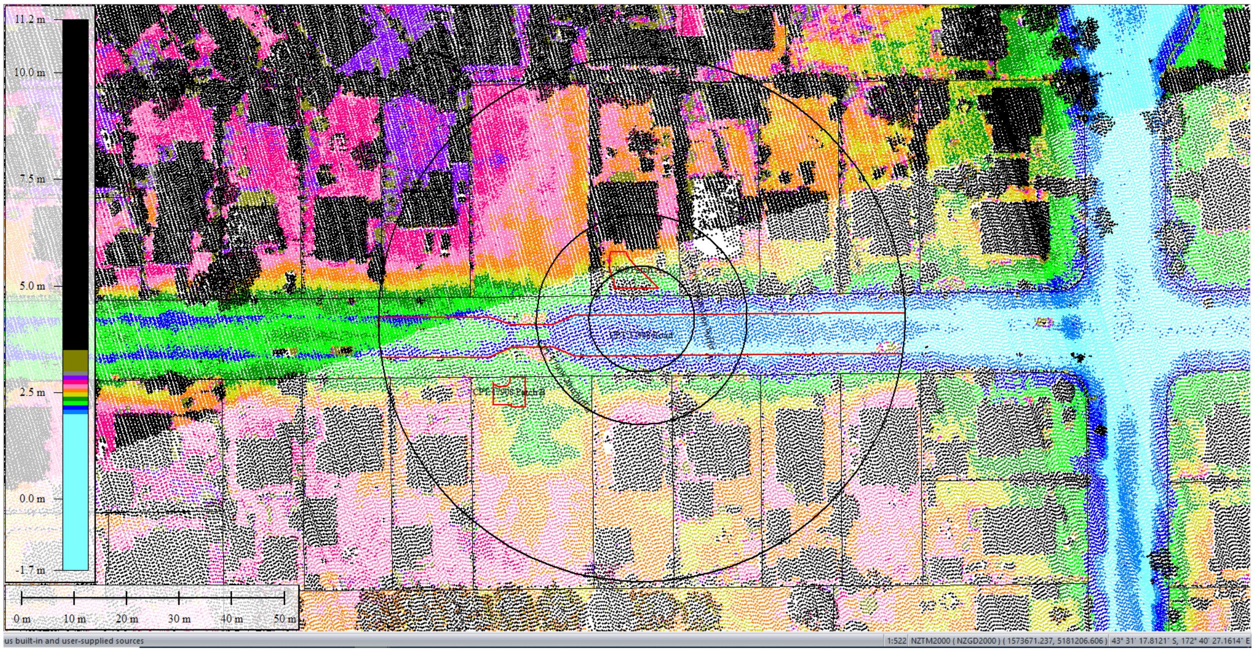

Figure 79: Oct 2015 LiDAR survey.

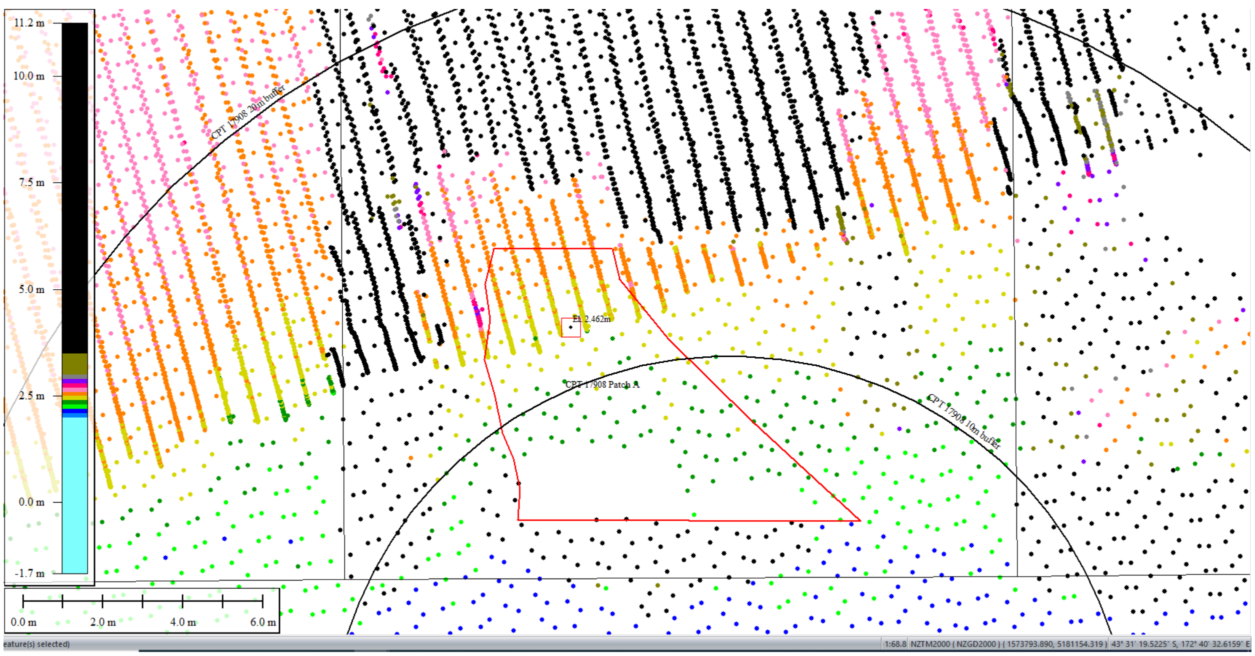

Figure 80: Ground surface elevation averaged over 20-m and 50-m buffers for Patch A for Oct 2015 LiDAR survey.

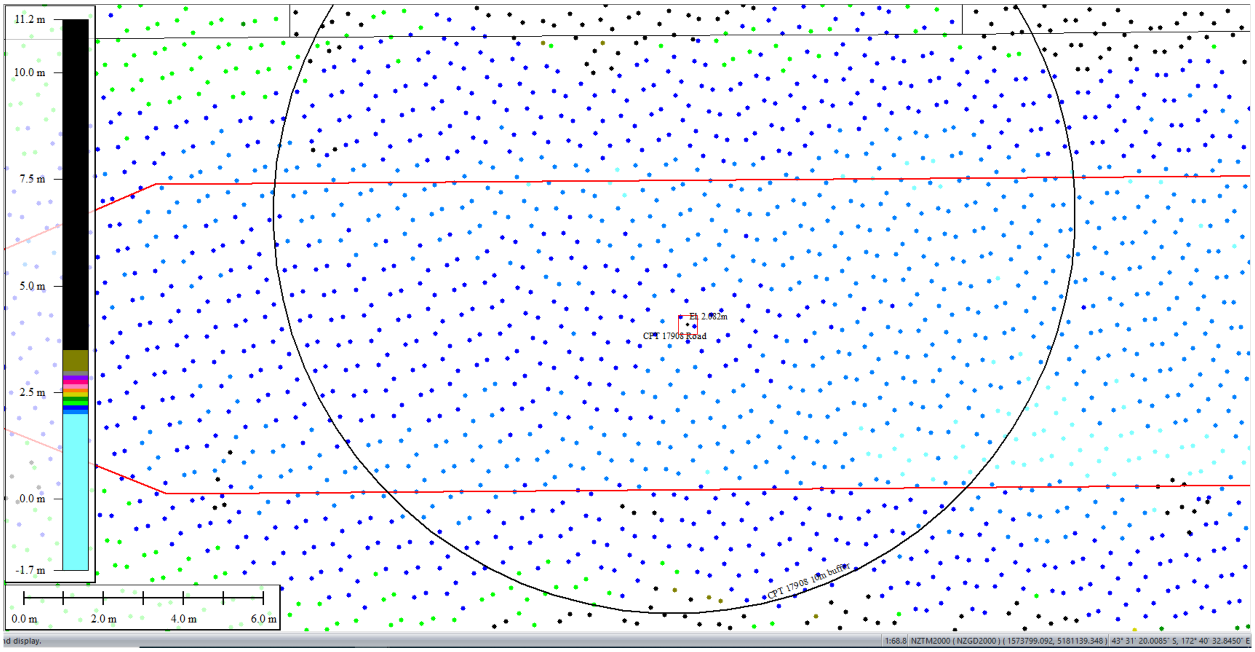

Figure 81: Ground surface elevation averaged over 10-m buffer for Road for Oct 2015 LiDAR survey.

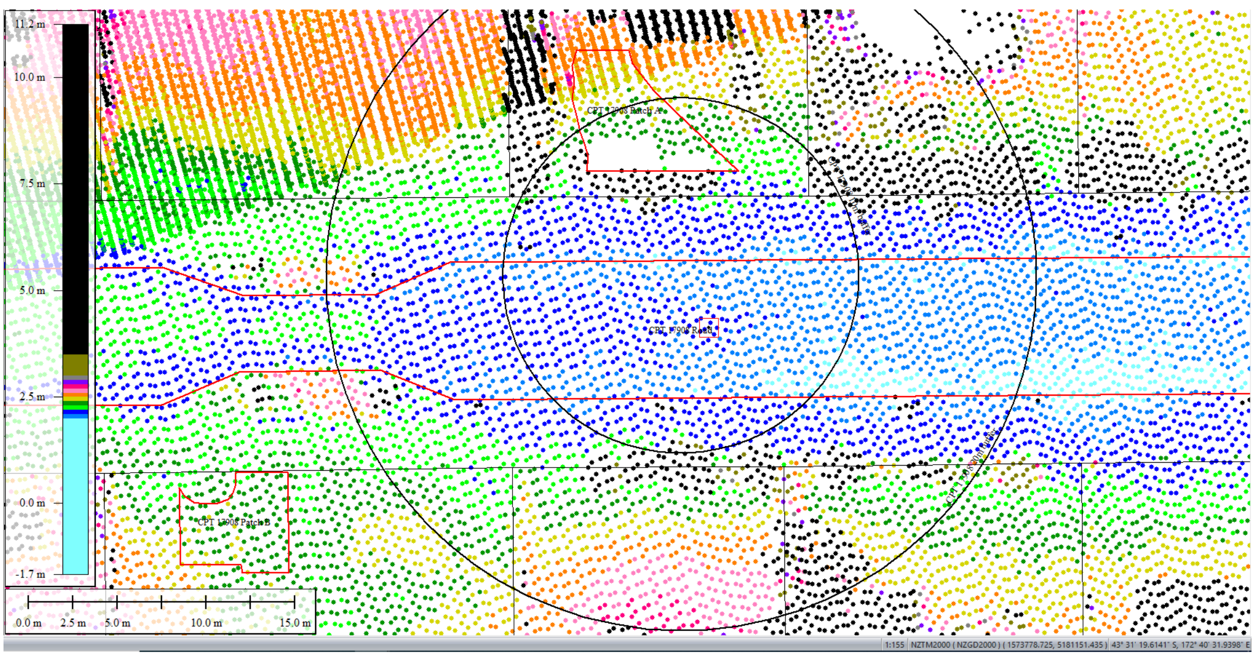

Figure 82: Ground surface elevation averaged over 20-m buffer for Road for Oct 2015 LiDAR survey (el. 2.080m).

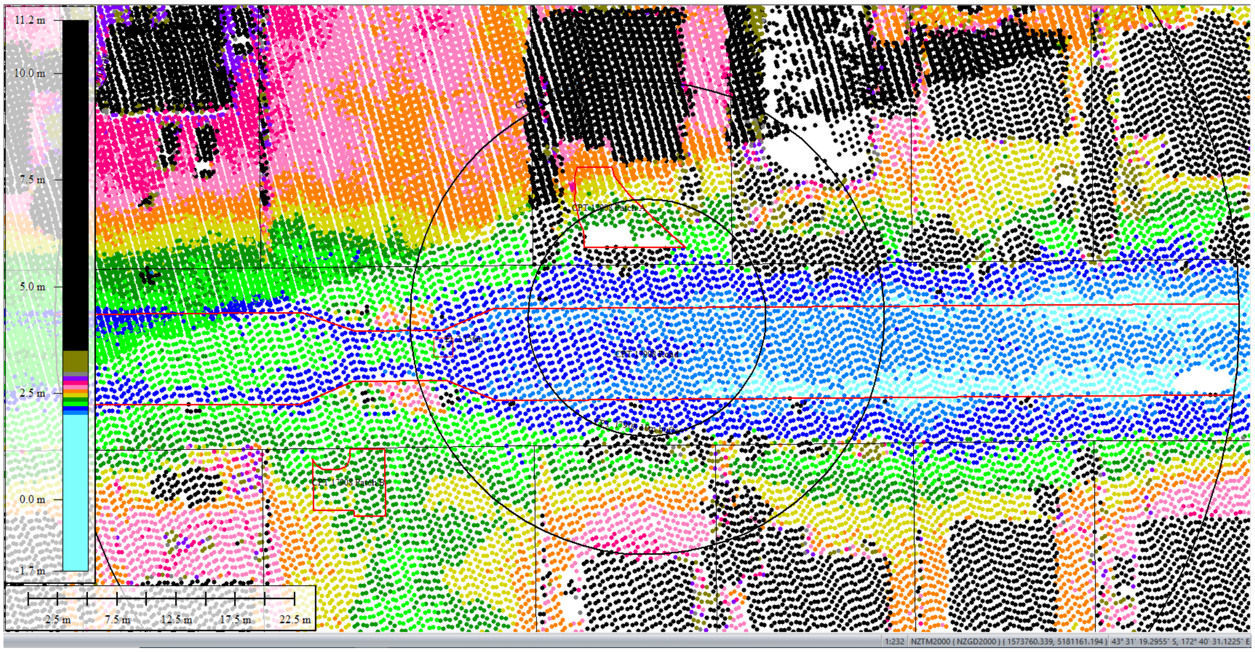

Figure 83: Ground surface elevation averaged over 50-m buffer for Road for Oct 2015 LiDAR survey.

Figure 84: Aerial photograph showing the ejecta outline at the site for Feb-11 EQ.

Figure 85: Aerial photograph acquired on 16 Jun 2011 showing the ejecta outline at the site for Jun-11 EQ.

Figure 86: Aerial photograph showing the ejecta outline at the site for Dec-11 EQ.

Figure 87: Ground photograph showing ejecta at nearby properties (photograph date: Sep 2011).

Figure 88: PGA for Sep-10 EQ (st. dev. = 0.250-0.300 ln units).

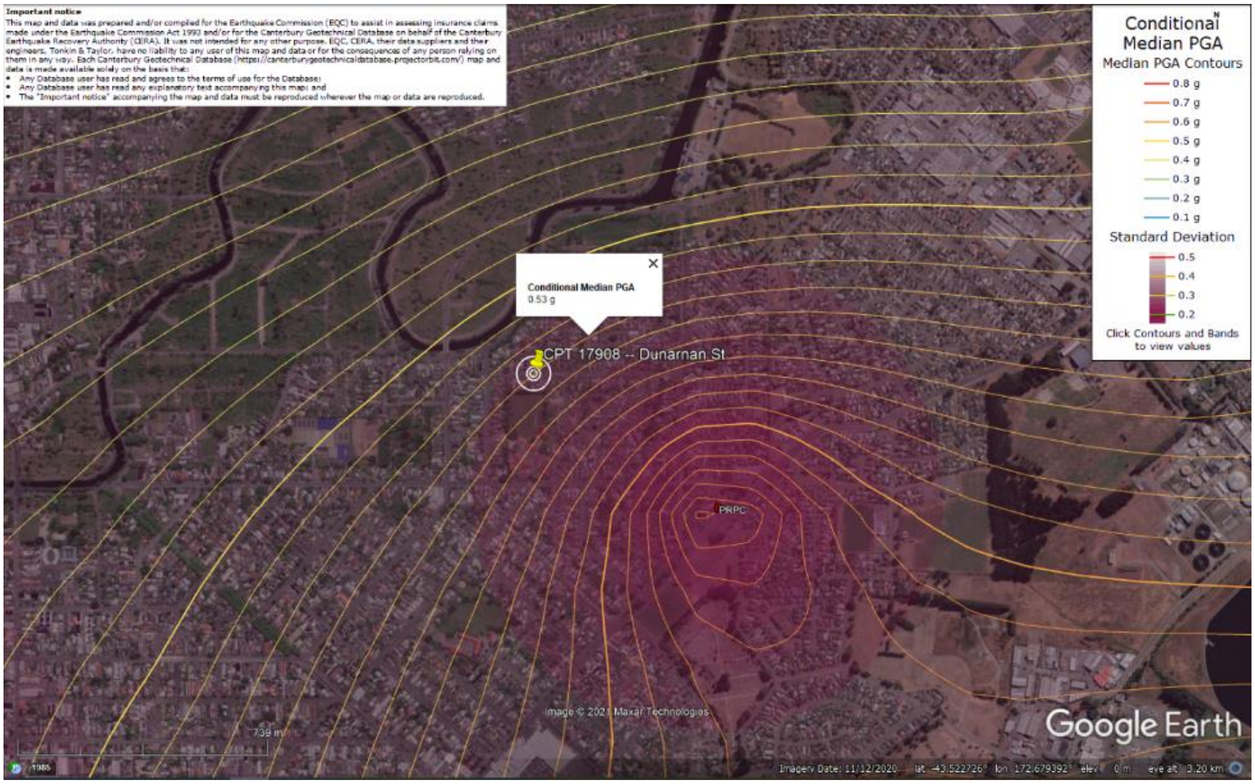

Figure 89: PGA for Feb-11 EQ (st. dev. = 0.275-0.300 ln units).

Figure 90: PGA for Jun-11 EQ (st. dev. = 0.300-0.325 ln units).

Figure 91: PGA for Dec-11 EQ (st. dev. = 0.375-0.400 ln units).

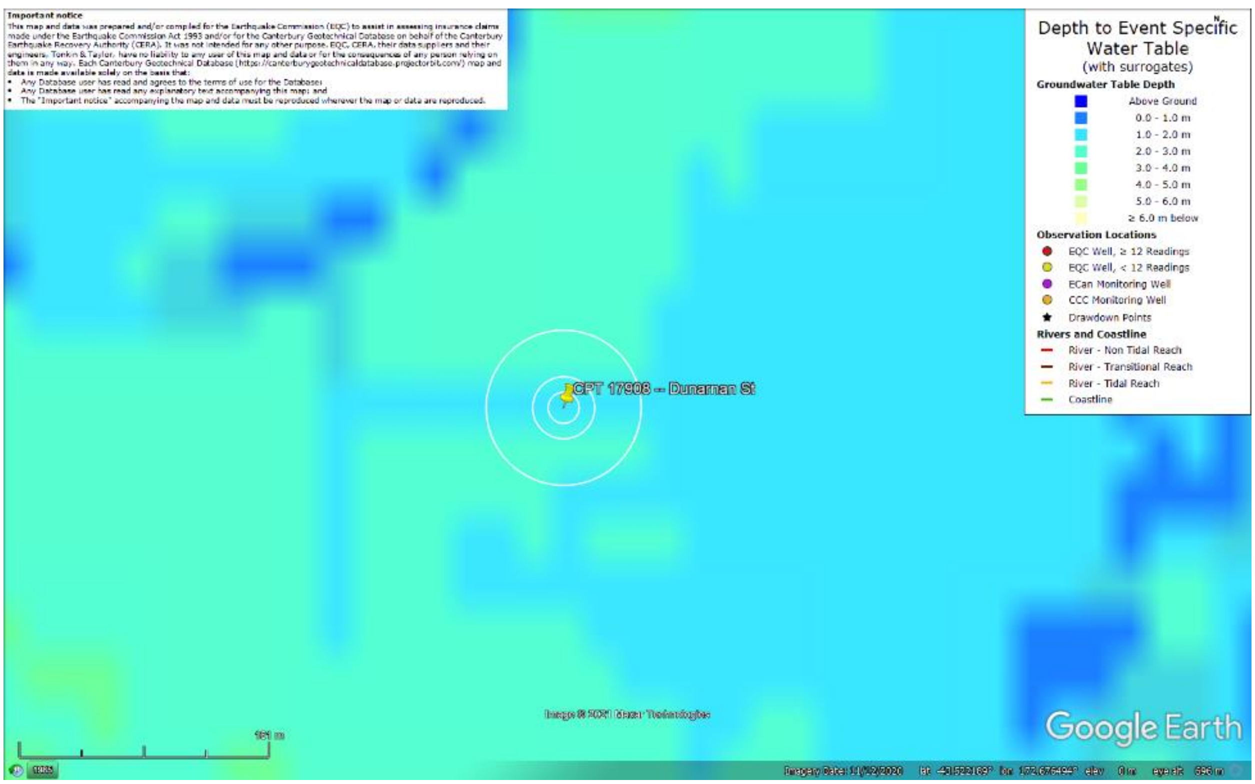

Figure 92: Depth to groundwater table for Sep-10 EQ.

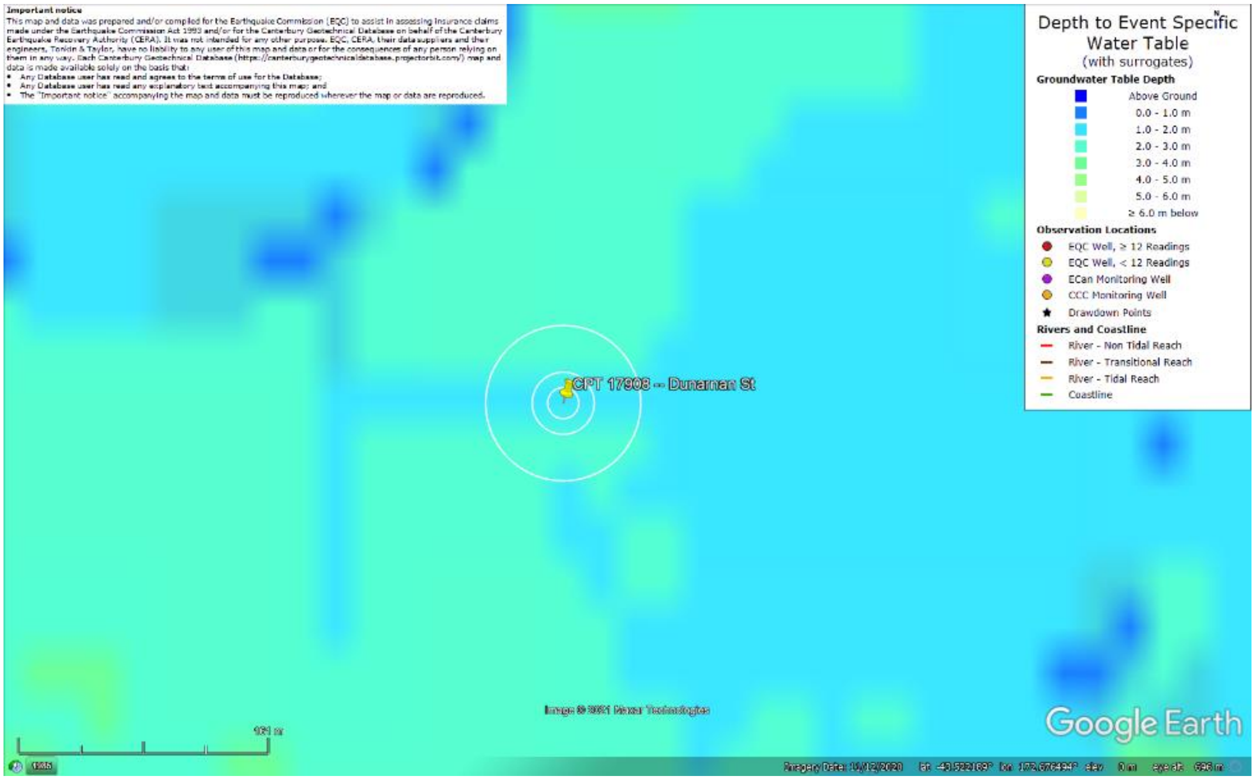

Figure 93: Depth to groundwater table for Feb-11 EQ.

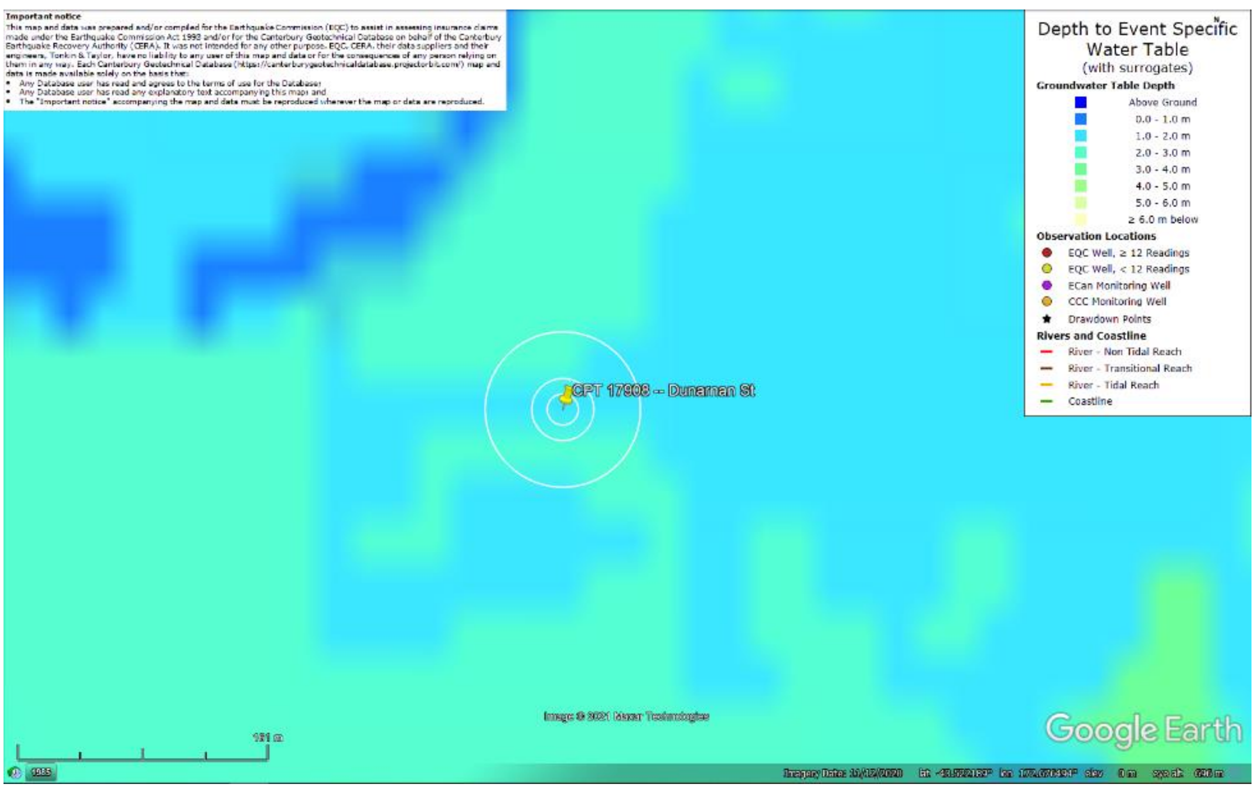

Figure 94: Depth to groundwater table for Jun-11 EQ.

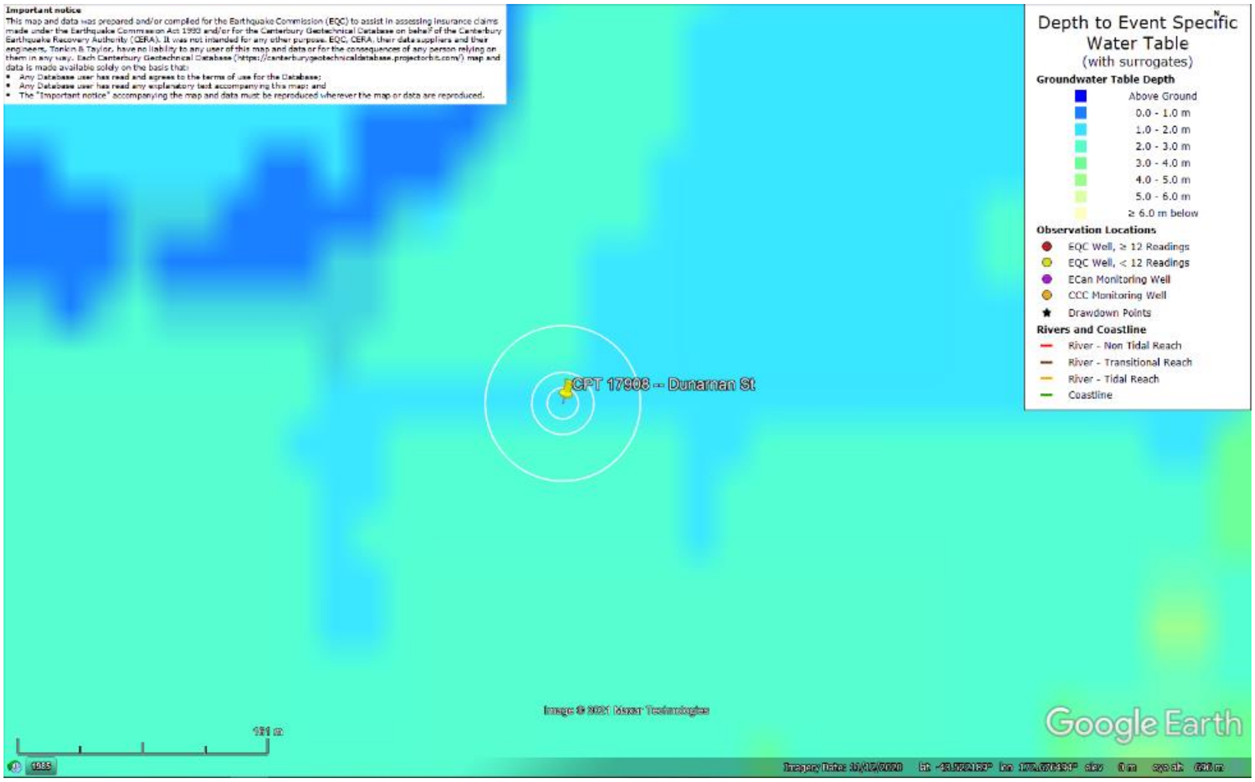

Figure 95: Depth to groundwater table for Dec-11 EQ.

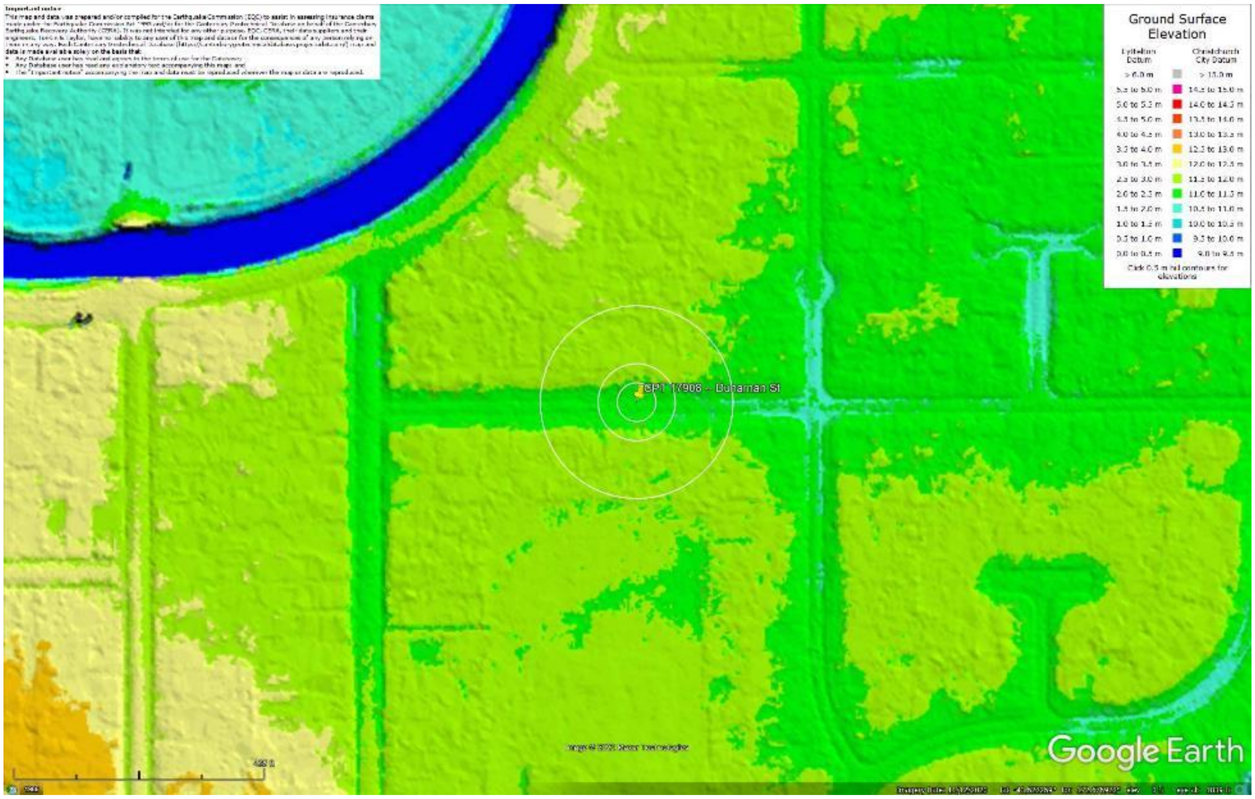

Figure 96: Ground surface elevation (Sep-11 LiDAR survey).

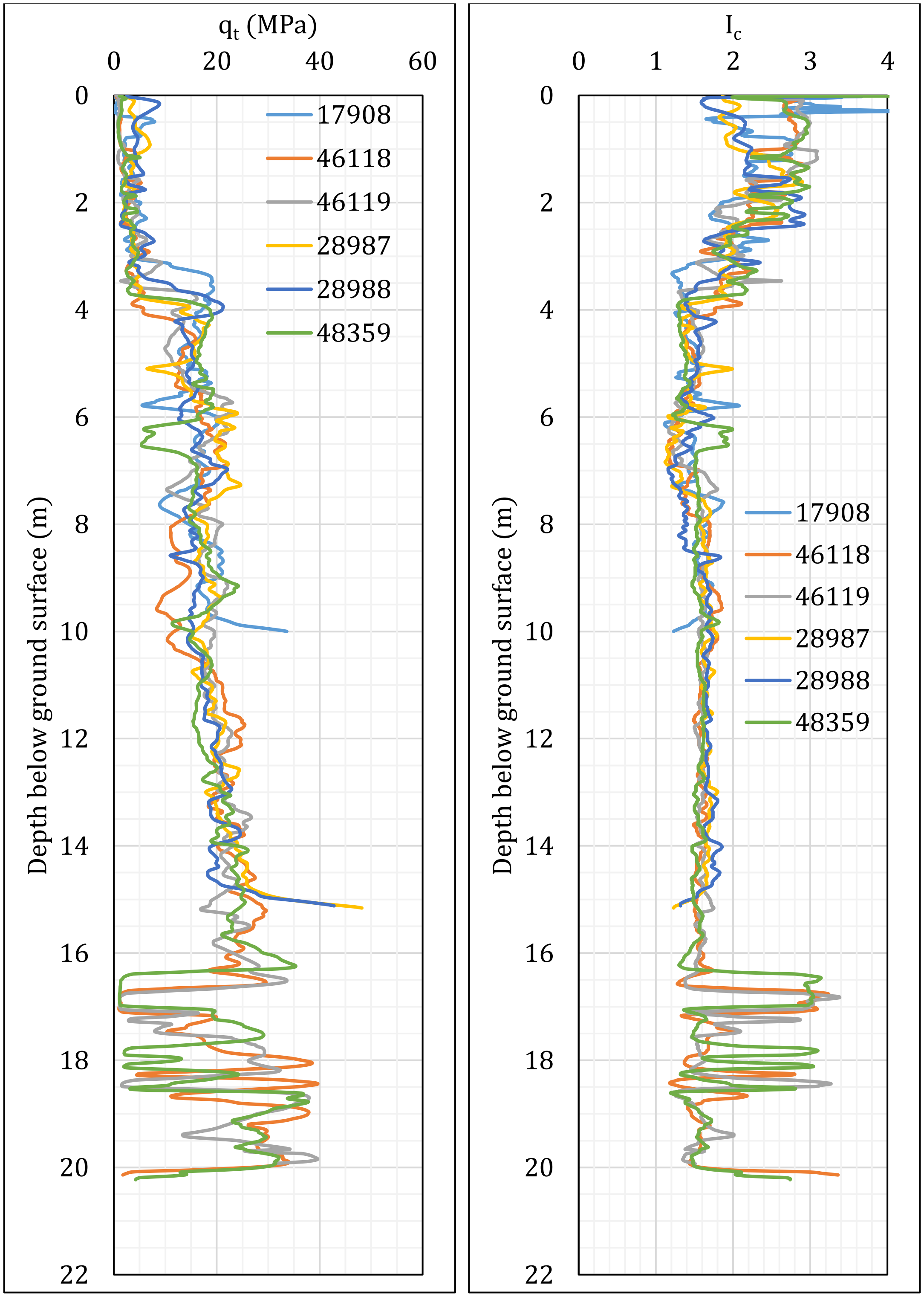

Figure 97: q_t and I_c profiles.

Note 7: The selection of CPTs for the area considered for settlement assessment (Figure 1) is based on the proximity of the CPTs to the considered areas. In accordance with that, the following table shows CPTs that were used for the volumetric settlement analysis in *Cliq v.3.0.3.2*, a CPT soil liquefaction software developed by GeoLogismiki. (The average volumetric settlements were reported in Table 8.)

Table 12: CPT profiles used in volumetric settlement analysis for areas selected for settlement assessment.

CPT ID No.	Patch A	Patch B	Road (10- and 20-m buffers)	Road (50-m buffer)
24039	✓	✓	✓	✓
46118		✓		
46119				
28987 (17648)				
28988 (17651)				
48359		✓		✓

Note: CPT 46118 was used to estimate the volumetric settlement for CPTs 24039, 28987, and 28988 for the respective depth ranges: 10-20 m, 15-20 m, and 15-20 m.

Table 13: CPT-based results.

		CPT ID							
EQ Event	Parameter	24039	46118	46119	28987	28988	48359	$\Delta_{10m\text{-}20m}$	$\Delta_{15m\text{-}20m}$
Sep-10	S_{V1D} (mm)	2	16	8	7	2	15	2	2
	LSN	1	3	1	2	1	2	0	0
	LPI	0	0	0	0	0	0	0	0
	LPI_{ish}	0	0	0	0	0	0	--	--
	$D_{FS<1}$ (m)	undet.	undet.	undet.	undet.	undet.	undet.	--	--
Feb-11	S_{V1D} (mm)	36	102	56	46	36	71	18	9
	LSN	11	22	15	16	9	15	1	1
	LPI	5	13	6	8	4	8	1	0
	LPI_{ish}	5	11	6	8	3	7	--	--
	$D_{FS<1}$ (m)	2.01	2.01	2.01	2.02	2.46	2.32	--	--
Jun-11	S_{V1D} (mm)	14	51	23	32	9	38	4	2
	LSN	5	13	6	11	3	9	0	0
	LPI	1	3	1	2	0	2	0	0
	LPI_{ish}	1	0	1	0	0	0	--	--
	$D_{FS<1}$ (m)	undet.	2.06	17.28	1.96	undet.	2.64	--	--
Dec-11	S_{V1D} (mm)	5	24	11	12	4	22	2	2
	LSN	2	6	2	4	1	5	0	0
	LPI	0	0	0	0	0	0	0	0
	LPI_{ish}	0	0	0	0	0	0	--	--
	$D_{FS<1}$ (m)	undet.	3.16	undet.	undet.	undet.	3.52	--	--

Notes: $D_{FS<1}$ = Depth to the first liquefiable layer (FS_L<1) that is at least 200-mm thick, as determined by the Boulanger and Idriss (2016) liquefaction-triggering procedure (P_L=50%, C_{FC}=0.13, and $I_{c,cutoff}$ =2.6), and exported from *Cliq v.3.0.3.2*; undet. = the specified soil layer was not detected.

Note 8: Based on the borehole log (BH 17908, Figure 1), the groundwater table is at a depth of 1.5 m below the ground surface. The soil profile consists of the (1) gravelly, GW, fill to a depth of 1.5 m, (2) sandy silt, ML, the Yaldhurst member of the Springston formation, to a depth of 2.6 m, (3) fine to coarse sand, SP, the Yaldhurst member of the Springston formation, to a depth of 4.9 m, (4) sandy fine to medium gravel, GW, the Yaldhurst member of the Springston formation, to a depth of 5.5 m, (5) silty fine to medium sand, SM, the Yaldhurst member of the Springston formation, to a depth of 5.7 m, (6) gravelly fine to coarse sand, SW, the Yaldhurst member of the Springston formation, to a depth of 6.2 m, (7) fine to medium sand, SP, the Yaldhurst member of the Springston formation to a depth of 7.1 m, (8) sandy fine to coarse gravel, GW, the Yaldhurst member of the Springston formation, to a depth of 7.6 m, (9) fine to medium sand, SP, of the Christchurch formation to a depth of 10.5 m (the end of the borehole). The log for a borehole, BH 1701, that is ~100 m to the NE from the center of the site, suggests the SP layer predominates to a depth of 20 m.

Note 9: The ejecta-induced free-field settlement provided in Table 11 is an areal average settlement due to ejecta, which is based on the total settlement assessment area, A_T (provided in Table 9 and repeated in Table 14). However, the considered area was not always covered completely with ejecta; thus, it is important to provide the localized ejecta-induced settlement, too. The localized settlement due to ejecta is estimated using photographic evidence only as

$$S_{E,P\_localized} = \frac{V_E}{A_E}$$

where V_E is the total volume of ejecta within A_T and A_E is the total coverage area of ejecta within A_T. Please note that the areal ejecta-induced settlement provided in Table 14 as S_{E,P_areal} is the same as $S_{E,P}$ in Table 11, which was estimated as

$$S_{E,P\_areal} = S_{E,P} = \frac{V_E}{A_T}$$

where V_E is the total volume of ejecta within A_T and A_T is the total settlement assessment area.

Table 14a: Areal and localized ejecta-induced settlement estimates for Patch A (20-m and 50-m buffers) based on photographic evidence.

Earthquake Event	A_T (m^2)	A_E (m^2)	V_E (m^3)	S_{E,P_areal} (mm)	$S_{E,P\_localized}$ (mm)
Sep-10	37.5	0	0	0	0
Feb-11	35.1	18.7	0.8-1.2	30±5	55±10
Jun-11	37.5	NA	NA	NA	NA
Dec-11	37.5	6.7	0.2-0.3	10±5	40±10

Notes: S_{E,P_areal} = $S_{E,P}$ reported in Table 11 = areal ejecta-induced settlement; $S_{E,P\_localized}$ = localized ejecta-induced settlement; A_T = total settlement assessment area; V_E = total volume of ejecta within A_T; A_E = total area of ejecta within A_T; The estimates of both areal and localized ejecta-induced settlement are rounded to the nearest 5; Final plus/minus values are also rounded to the nearest 5.

Table 14b: Areal and localized ejecta-induced settlement estimates for Patch B (50-m buffer) based on photographic evidence.

Earthquake Event	A_T (m^2)	A_E (m^2)	V_E (m^3)	S_{E,P_areal} (mm)	$S_{E,P\_localized}$ (mm)
Sep-10	27.9	0	0	0	0
Feb-11	27.9	26.9	1.8-2.7	80±15	80±15
Jun-11	27.9	14.2	0.4-0.7	20±5	40±10
Dec-11	27.9	4.3	0.1-0.2	5±5	40±10

Notes: S_{E,P_areal} = $S_{E,P}$ reported in Table 11 = areal ejecta-induced settlement; $S_{E,P\_localized}$ = localized ejecta-induced settlement; A_T = total settlement assessment area; V_E = total volume of ejecta within A_T; A_E = total area of ejecta within A_T; The estimates of both areal and localized ejecta-induced settlement are rounded to the nearest 5; Final plus/minus values are also rounded to the nearest 5.

Table 14c: Areal and localized ejecta-induced settlement estimates for Road (10-m buffer) based on photographic evidence.

Earthquake Event	A_T (m^2)	A_E (m^2)	V_E (m^3)	S_{E,P_areal} (mm)	$S_{E,P\_localized}$ (mm)
Sep-10	149	0	0	0	0
Feb-11	149	92.2	0.6-1.1	5±5	10±5
Jun-11	149	102	2.5-5.0	25±10	35±15
Dec-11	148	13.9	0.07-0.1	<5	10±5

Notes: S_{E,P_areal} = $S_{E,P}$ reported in Table 11 = areal ejecta-induced settlement; $S_{E,P\_localized}$ = localized ejecta-induced settlement; A_T = total settlement assessment area; V_E = total volume of ejecta within A_T; A_E = total area of ejecta within A_T; The estimates of both areal and localized ejecta-induced settlement are rounded to the nearest 5; Final plus/minus values are also rounded to the nearest 5.

Table 14d: Areal and localized ejecta-induced settlement estimates for Road (20-m buffer) based on photographic evidence.

Earthquake Event	A_T (m^2)	A_E (m^2)	V_E (m^3)	S_{E,P_areal} (mm)	$S_{E,P\_localized}$ (mm)
Sep-10	298	0	0	0	0
Feb-11	298	209	1.4-2.7	5±5	10±5
Jun-11	297	211	5.9-11.6	30±10	40±15
Dec-11	297	34.8	0.2-0.4	<5	10±5

Notes: S_{E,P_areal} = $S_{E,P}$ reported in Table 11 = areal ejecta-induced settlement; $S_{E,P\_localized}$ = localized ejecta-induced settlement; A_T = total settlement assessment area; V_E = total volume of ejecta within A_T; A_E = total area of ejecta within A_T; The estimates of both areal and localized ejecta-induced settlement are rounded to the nearest 5; Final plus/minus values are also rounded to the nearest 5.

Table 14e: Areal and localized ejecta-induced settlement estimates for Road (50-m buffer) based on photographic evidence.

Earthquake Event	A_T (m^2)	A_E (m^2)	V_E (m^3)	S_{E,P_areal} (mm)	$S_{E,P\_localized}$ (mm)
Sep-10	750	0	0	0	0
Feb-11	750	498	5.4-9.9	10±5	15±5
Jun-11	750	427	10.6-21.0	20±5	35±10
Dec-11	750	103	0.7-1.3	<5	10±5

Notes: S_{E,P_areal} = $S_{E,P}$ reported in Table 11 = areal ejecta-induced settlement; $S_{E,P\_localized}$ = localized ejecta-induced settlement; A_T = total settlement assessment area; V_E = total volume of ejecta within A_T; A_E = total area of ejecta within A_T; The estimates of both areal and localized ejecta-induced settlement are rounded to the nearest 5; Final plus/minus values are also rounded to the nearest 5.

<u>Summary 2:</u>

- **The best estimate of the <u>localized</u> ejecta-induced free-field ground settlement at the Dunarnan St site for the SEP 2010, FEB 2011, JUN 2011, and DEC 2011 earthquake is 0 mm, 55±10 mm, 40±10 mm, and 40±10 mm, respectively.**
- **The best estimate of the <u>localized</u> ejecta-induced settlement of the road at the Dunarnan St site for the SEP 2010, FEB 2011, JUN 2011, and DEC 2011 earthquake is 0 mm, 10±5 mm, 40±15 mm, and 10±5 mm, respectively.**